



THÈSE / UNIVERSITÉ DE RENNES 1
sous le sceau de l'Université Européenne de Bretagne

pour le grade de

DOCTEUR DE L'UNIVERSITÉ DE RENNES 1

Mention : Mathématiques et Applications

Ecole doctorale Matisse

présentée par

Vincent NOËL

préparée à l'unité de recherche 6625 du CNRS : IRMAR

Institut de Recherche Mathématique de Rennes

UFR de Mathématiques

**Modèles réduits et
hybrides de réseaux de
réactions biochimiques**

**Applications à la
modélisation du
cycle cellulaire**

Thèse soutenue à Rennes
le 20 Décembre 2012

devant le jury composé de :

Jean-Pierre FRANÇOISE

Professeur / Université de Paris 6 / rapporteur

Jérôme FERET

Chercheur INRIA / ENS Paris / rapporteur

Alexander GUTERMAN

Professeur / Université d'Etat de Moscou / rapporteur

Dimitri PETRITIS

Professeur / Université de Rennes 1 / examinateur

Ovidiu RADULESCU

Professeur / l'Université de Montpellier 2 / directeur de thèse

Nathalie THERET

Directeur de recherche INSERM / Université de Rennes 1 / co-directrice de thèse

Remerciements

Je voudrais tout d'abord remercier Ovidiu Radulescu pour m'avoir encadré durant ces années et pour m'avoir tant appris.

Je tiens également à remercier Nathalie Theret pour sa co-direction.

Je remercie Jean-Pierre Françoise, Jérôme Feret et Alexander Guterman pour avoir accepté d'évaluer ce travail, ainsi que Dimitri Petritis pour avoir accepté de présider le jury.

Je remercie plus spécialement Jeremy Gruel pour m'avoir fait découvrir la bioinformatique il y a déjà 6 ans, et tous les rennais, Kevin, Simon, Guillaume, Aurelien, David, Damien, Clément, etc...

Je tiens également à remercier tous les membres de l'équipe DIMNP de l'Université de Montpellier 2 pour leur accueil, Andrea, Adelaide, Daniel, Partho, Olivier, Mickael, Sylvain, Thomas, ...

Je remercie également Axelle, Hélène, Nathalie, Andres, Damien, et les autres pour m'avoir soutenu et changé les idées pendant les 3 dernières années.

Enfin je tiens à remercier ma famille pour m'avoir aidé pendant mes études, et en particulier mes parents.

Table des matières

Résumé en français	5
0.1 Introduction	5
0.2 Modèles hybrides pour les réseaux de réactions biochimiques	7
0.3 Réduction de modèles pour les modèles de biologie computationnelle	9
0.4 Principe d'équilibration tropicale pour les cinétiques chimiques	12
0.5 Deux modèles paradigmatisques du cycle cellulaire et leurs tropicalisations .	13
Introduction	17
1 Hybrid models for networks of biochemical reactions	19
1.1 Introduction	19
1.2 Hybrid models	20
1.3 Regulated reaction graphs and hybrid reaction schemes	22
1.4 Identification of piecewise smooth models	22
1.5 Parallel simulated annealing.	24
1.6 Examples	27
1.7 Conclusion	35
2 Model reduction for computational biology models	39
2.1 Introduction	39
2.2 Deterministic dynamical networks	42
2.3 Multi-scale reduction of monomolecular reaction networks	42
2.4 Separation, dominance, and tropical geometry	44
2.5 Quasi-steady state and Quasi-equilibrium, revisited	48
2.6 Graph rewriting for large nonlinear, deterministic, dynamical networks . .	52
2.7 Model reduction and model identification	55
2.8 Conclusion	58
2.9 Algorithms	58
2.9.1 Algorithm 1 : reduction of monomolecular networks with separation	58
2.9.2 Algorithm 2 : reduction of nonlinear networks with separation . .	60
3 Tropical equilibration principle for chemical kinetics.	63
3.1 Introduction.	63
3.2 General settings	64
3.3 Justification of the tropicalization and some estimates	65
3.4 Geometry of tropical equilibrations	71
3.5 Tropical approach to the permanency problem	72
3.6 Appendix : Theorems on invariant manifolds	73

4 Two paradigmatic cell cycle models and their tropicalization	77
4.1 Description of the models	77
4.2 Tropical equilibrations and model reduction of model 1	79
4.3 A priori estimates and permanency for the two component version of the cell cycle model 1	82
4.4 Singular limit cycle and hybrid dynamics of model 1	84
4.5 Checking condition (4.2.8)	90
4.6 Tropical equilibrations and reduction of model 2	92
4.7 Tropical approach for excitable systems. Two component case.	95
4.8 Generalized two component cell cycle model	99
4.9 Conclusion	100
Bibliographie	103

Résumé en français

0.1 Introduction

La biologie est aujourd’hui confrontée à une situation sans précédents. Les nouvelles techniques expérimentales en biologie moléculaire, biophysique, biochimie, produisent une avalanche de données qui ont besoin d’être traitées, analysées, et comprises. La modélisation devient une partie du raisonnement biologique. Cependant, dans le but d’être détaillée, la taille des modèles doit pouvoir augmenter sans limites. Par exemple, pour pouvoir représenter les processus d’une seule voie de signalisation, un modélisateur peut utiliser des centaines, voire des milliers de réactions biochimiques, produisant un nombre équivalent d’équations différentielles. Une cellule utilise des centaines de voies de signalisation qui interagissent entre elles. Des systèmes aussi larges ne sont pas seulement difficiles à analyser, mais également pratiquement impossible à identifier à partir des données expérimentales. Une stratégie pour surmonter une telle complexité est d’utiliser des abstractions, c’est à dire des versions réduites des modèles qui peuvent reproduire avec suffisamment de précision le comportement du modèle initial. Ces modèles simplifiés peuvent être de différents types. Si le modèle initial est un système d’équations différentielles ordinaires (EDOs), l’abstraction peut être un plus petit système d’EDOs, ou un modèle hybride combinant des variables continues et discrètes, ou un modèle totalement discret (comme par exemple un réseau booléen). Toutes ces descriptions sont actuellement utilisées en biologie computationnelle. Cependant, il nous manque des méthodes générales nous permettant de réduire ou de convertir un type de modèle en un autre type, automatiquement. Comme les paramètres des modèles sont rarement disponibles avec une précision suffisante, nous avons besoin de méthodes permettant de gérer des paramètres incertains.

Le travail présenté dans cette thèse a été motivé par cette situation en biologie computationnelle.

Nous discutons une classe de méthodes semi-formelles permettant de réduire des grands réseaux de réactions biochimiques. Dans le but de surmonter l’incertitude des paramètres, nous avons basé les méthodes de réduction sur les relations de dominance entre les paramètres et/ou les taux de réactions. Ces méthodes exploitent le caractère multi-échelles des réseaux biochimiques, c’est à dire leur propriété d’avoir de nombreuses échelles de concentration et de temps bien séparées. Dans les réseaux multi-échelles, les paramètres peuvent être remplacés par des ordres de grandeur, qui sont beaucoup plus simples à obtenir que les valeurs précises de paramètres. De plus, la dynamique dissipative des réseaux de réactions avec de nombreuses échelles de temps bien séparées peut être décrite comme une séquence d’équilibrations successives de différents sous-ensembles de variables du système. Les systèmes polynomiaux avec échelles séparées sont équilibrés quand au moins deux termes, de signes opposés, ont le même ordre de grandeur et dominent les autres. Ces

équilibrations et les systèmes dynamiques tronqués correspondants, obtenues en éliminant les termes dominés, trouvent une formulation naturelle dans l'analyse tropicale et peuvent être utilisées pour la réduction de modèles.

Grâce à la réduction de modèles nous transformons des systèmes d'équations différentielles en des systèmes d'équations différentielles avec moins de variables et de paramètres. Ces simplifications nous apportent des approximations précises globalement, c'est à dire pour des grands domaines de valeurs de paramètres et pour tous temps. Localement, c'est à dire pour des domaines restreints de valeurs de paramètres et pour intervalles de temps finis, des modèles plus simples que le modèle simplifié global peuvent être trouvés. Cette situation conduit à une description hybride régulière par morceaux de la dynamique du système, dans laquelle une trajectoire régulière générée par un modèle complexe est approximée par une séquence de morceaux réguliers générés par des EDOs simplifiés, mais changeantes. Il y a des manières simples d'hybridiser un réseau de réactions biochimiques, consistant à remplacer les fonctions sigmoïdes apparaissant dans la définition des taux de réactions par des fonctions de type "marche d'escalier", ou par des fonctions linéaires par morceaux. Une autre solution pour hybridiser est fournie par l'analyse tropicale sous la forme du principe de correspondance de Litvinov-Maslov. Cette idée peut être appliquée à des systèmes d'équations différentielles polynomiaux ou rationnels (résultant en biochimie de la loi d'action de masse) et consiste à approximer les fonctions polynomiales par des polynômes max-plus.

La réduction de modèles et l'hybridisation trouvent des applications dans le contexte des modèles du cycle cellulaire en biologie computationnelle. Le cycle cellulaire régule la prolifération cellulaire par l'activité cyclique de protéines appelées cyclines. Les modifications de ces protéines peuvent intervenir de manière abrupte, entraînant des changements de régime dynamique qui sont bien décrits par des changements de modes dans des modèles hybrides réguliers par morceaux. D'un point de vue dynamique, les modèles du cycle cellulaire prédisent des oscillations singulières, alternant entre parties rapides et lentes. En réduisant ces modèles, nous pouvons mettre en valeur les variables essentielles et les paramètres des modèles du cycle cellulaire et, dans certains cas, calculer les attracteurs périodiques de manière analytique.

La structure de ce manuscrit est la suivante :

Dans le chapitre 1, nous proposons des méthodes numériques permettant d'identifier un modèle hybride à partir de séries temporelles. Nous utilisons cette méthode pour obtenir des approximations hybrides de modèles réguliers existants du cycle cellulaire.

Dans le chapitre 2, nous passons en revue les méthodes de réduction de modèle. Ces nouveaux résultats consistent à utiliser l'analyse et la géométrie tropicale dans le but d'unifier les approches qui sont appliquées aux modèles de réactions biochimiques avec séparation d'échelles.

Dans le chapitre 3, nous discutons la méthode de tropicalisation et trouvons des estimations justifiant son applicabilité.

Dans le chapitre 4, nous discutons la dynamique d'oscillateurs singuliers du cycle cellulaire, justifiant rigoureusement leur réduction en système de dimension moindres et leur hybridation.

0.2 Modèles hybrides pour les réseaux de réactions biochimiques

Les systèmes hybrides sont beaucoup utilisés en théorie de contrôle automatique pour gérer des situations où des machines à nombre d'états finis sont couplées avec des mécanismes qui peuvent être modélisés par des équations différentielles [92]. Dans le cas des robots, contrôleurs de centrales, disques durs d'ordinateurs, systèmes automatiques routiers, systèmes de contrôle de vol en aéronautique, etc. Le comportement général de tels systèmes est de passer d'un type de dynamique régulière (mode) décrite par un système d'équations différentielles à une autre dynamique régulière (mode) décrite par un autre système d'équations différentielles. La commande de ces modes peut être accomplie en changeant une ou plusieurs variables discrètes. Le changement de mode peut être accompagné ou non par des sauts (discontinuités) des trajectoires. Suivant comment les variables discrètes sont modifiées, il peut y avoir plusieurs types de systèmes hybrides : systèmes commutés [124], automates différentiels multivalués [137], systèmes réguliers par morceaux [40]. Notons que dans le dernier cas, le changement de mode intervient quand la trajectoire atteint des variétés régulières. Dans ces exemples, le changement de variables discrètes et l'évolution des variables continues sont déterministes. La classe des systèmes hybrides peut être étendue en considérant des dynamiques stochastiques pour les variables discrètes ou pour les variables continues, produisant des processus déterministes par morceaux, des diffusions commutées, ou des diffusions avec sauts [114, 27, 26, 125, 16]. Des réseaux de Petri hybrides, différentiels ou stochastiques apportent des descriptions dynamiques équivalentes et ont aussi été utilisés dans ce contexte. [32]

L'utilité des modèles hybrides en biologie peut être justifiée par le caractère multi-échelle temporel et spatial des processus biologiques, et par le besoin de combiner des approches qualitatives et quantitatives pour étudier la dynamique des réseaux de régulation cellulaire. De plus, la modélisation hybride offre un bon compromis entre une description réaliste des mécanismes de régulation et la possibilité de tester le modèle en termes d'atteignabilité d'états et de logique temporelle [85, 96]. La dynamique par seuils des réseaux de régulation génétique [10, 115] ou des systèmes de signalisation [149] a été auparavant décrite par des modèles linéaires par morceaux ou affines par morceaux. Ces modèles ont une structure relativement simple et peuvent, dans certains cas, être identifiés à partir des données [108, 35]. Des méthodes ont été proposées pour calculer les ensembles d'états atteignables pour les modèles affines par morceaux [12].

Parmi les applications de la modélisation hybride, une des plus importantes est la régulation du cycle cellulaire. La machinerie du cycle cellulaire, entraînant la division et la prolifération cellulaire, combine une croissance lente, une réorganisation spatio-temporelle de la cellule, et des changements rapides des concentrations de protéines régulatrices induits par des modifications post-translationnelles. La progression dans le cycle cellulaire est une séquence bien définie d'étapes, séparées par des points de contrôles des transitions. Ceci justifie l'approche de modélisation hybride, comme le modèle hybride du cycle cellulaire de Tyson et collab. [126]. Ce modèle est basé sur un automate booléen dont les transitions discrètes déclenchent des changements dans les paramètres cinétiques d'un ensemble d'équations différentielles. Le modèle hybride proposé par Tyson et collab. a été

utilisé pour reproduire des données de flux cytométriques.

Bien que suffisants pour certaines applications comme les réseaux de gènes, les modèles affines par morceaux sont moins adaptés pour décrire les phénomènes où la dynamique entre deux événements discrets successifs est fortement non-linéaire. Un exemple typique d'un tel phénomène est la machinerie du cycle cellulaire. La dégradation protéolytique des cyclines est activée rapidement par les complexes kinases cyclines-dépendants mais entre deux commutations successives les complexes ont une dynamique non-linéaire impliquant plusieurs rétroactions positives (processus-auto catalytiques) et négatives. Ces processus non-linéaires contribuent à la robustesse du mécanisme. L'idée des systèmes réguliers par morceaux survient naturellement dans le contexte de systèmes biochimiques avec de multiples échelles de temps séparées. La dynamique dissipative d'un grand modèle multi-échelles peut être réduite à celle d'un modèle plus simple, appelé le sous système dominant [112, 58, 57]. Pour les modèles non linéaires, le sous système dominant (qui peut être assimilé à un mode) est seulement constant par morceaux et peut changer plusieurs fois pendant la dynamique. Les méthodes de réduction de modèle proposées dans [57, 112] génèrent des sous-systèmes dominants pour monômes multivariés des concentrations de variables, comme les bien connus S-Systèmes [120]. En effet, quand on les applique à des modèles utilisant la loi d'action de masse, les quasi-états stables et les approximations des quasi-équilibres [58] nous amènent à regrouper plusieurs réactions et espèces effectives dont les taux résultent de la résolution de systèmes d'équations polynomiales. En général, ces polynômes contiennent peu des termes (fewnomials). Les solutions de tels systèmes sont très simplifiées dans le cas d'une séparation totale des termes non constants dans les fewnomials et produisent des taux monomiaux. Les taux d'une même réaction peuvent être représentés par différents monômes dans différents sous systèmes dominants (modes). Par exemple, le taux d'un mécanisme de Michaelis-Menten dépend linéairement de la concentration du substrat pour des faibles concentrations et est constant à la saturation. Nous nous attendons à ce que des taux de lois plus générales [84] puissent être traités similairement par notre approche.

Dans ce chapitre nous nous proposons une heuristique pour construire des modes appropriés des modèles réguliers par morceaux adéquats en utilisant une approche descendante. Puis, nous montrons comment les paramètres du modèle hybride peuvent être identifiés à partir des données ou des trajectoires produites par des modèles réguliers existants, mais plus complexes. Les détails de ce travail sont présentés dans le chapitre 1.

Les résultats que nous présentons ici sont une preuve de principe que les modèles hybrides réguliers par morceaux peuvent être construits avec une heuristique simple à partir d'informations basique sur les interactions biochimiques. Utiliser cette classe de modèles hybrides au lieu d'approximations linéaires par morceaux nous permet, dans beaucoup de situations, d'obtenir un meilleur équilibre entre interactions discrètes et régulières. L'algorithme d'identification proposé dans ce travail combine la localisation statique des événements, l'identification des modes par une méthode de recuit simulé, et l'identification des paramètres de contrôle des modes par localisation dynamique. L'étape la plus difficile de cet algorithme est le recuit simulé. De plus, pour des grands modèles, nous nous attendons à obtenir plusieurs solutions pour les paramètres de contrôle des modes. Nous améliorons actuellement cet algorithme de manière à résoudre ces situations. Un meilleur choix des modes dicté par les techniques de réduction de modèles pourrait réduire le temps du recuit simulé. Egalement, nous étudions l'utilisation des fonctions de locali-

sation d'événements qui sont linéaires dans le logarithme des variables continues. D'après les idées de l'introduction, ces fonctions de localisation non linéaires pourront indiquer les changements des monômes dominants dans les fonctions de taux de manière plus précises que les fonctions de localisation linéaires. De plus, ils peuvent être obtenus directement à partir du modèle régulier initial sans le besoin de résoudre des fonctions de localisation dynamiques (possiblement non déterminées). Des techniques de segmentations améliorées sont nécessaires pour de futures applications de cet algorithme directement à partir de données.

Dans le futur nous appliquerons cette heuristique et l'algorithme d'ajustement (fitting) pour modéliser des situations complexes où des voies de signalisation interagissent avec le cycle cellulaire eucaryote. Les modèles hybrides obtenus seront aussi utilisé pour rechercher les propriétés émergentes des réseaux de régulations comme la viabilité et la robustesse.

0.3 Réduction de modèles pour les modèles de biologie computationnelle

Pendant les dernières décennies, les biologistes ont identifié un grand nombre de composants moléculaires et de mécanismes régulateurs sous-jacents au contrôle des fonctions cellulaires. Les cellules intègrent des signaux externes via les mécanismes sophistiqués des voies de transduction, affectant in fine la régulation de l'expression des gènes, y compris ceux codant pour des composants de la signalisation. Les fonctions métaboliques sont soutenues et contrôlées par des systèmes biochimiques complexes, impliquant des gènes, des enzymes et des métabolites. Les régulations génétiques résultent des effets coordonnés de beaucoup de gènes interagissant mutuellement. Ces interactions impliquent beaucoup d'acteurs moléculaires, incluant des protéines et des ARNs régulateurs, et définissent des grands réseaux de régulation.

Les modèles dynamiques actuels des processus moléculaires cellulaires sont des réseaux de petite taille. Ces petits modèles ne prennent pas en compte les spécificités des mécanismes régulateurs. Des nouvelles méthodes sont nécessaires, permettant de réconcilier les petits modèles dynamiques avec des grandes, mais statiques, architectures de réseaux. L'obstacle principal pour augmenter la taille des réseaux dynamiques est l'information incomplète sur les paramètres et sur les détails mécanistiques des interactions. Les mesures biochimiques fournissent des valeurs de paramètres “in vitro”. Les valeurs “in vivo” des paramètres dépendent de l'encombrement et de l'hétérogénéité du milieu intracellulaire, et peuvent être plusieurs ordres de magnitude différents de ce qui est mesuré *in vitro*. De plus, construire des modèles à partir de données pose des problèmes de non-identifiabilité et de sur-ajustement (overfitting) des paramètres. La réduction de modèle est donc une étape inévitable dans l'étude des grands réseaux, permettant d'extraire les fonctionnalités principales du modèle, qui peuvent être identifiés à partir des données. La réduction de modèle en biologie computationnelle doit avoir quelques caractéristiques spécifiques.

Premièrement, la réduction de modèles doit permettre de répondre au problème des paramètres incomplets ou imprécis. Une certaine classe de méthodes de réduction n'utilise pas les valeurs des paramètres et respecte automatiquement cette propriété. Dans les réseaux biochimiques, le nombre d'espèces chimiques nécessaires pour préciser un mécanisme de réaction peut croître de manière exponentielle, due à de nombreuses pos-

sibilités d’interactions entre molécules et à la possibilité de sites d’interaction multiples. Les méthodes de réduction par aggregation (lumping) [15, 25] diminuent le nombre de micro-états et évitent l’explosion combinatoire dans la description et l’analyse de grands modèles de signalisation. Une technique similaire appelée modélisation à base de règles est utilisée pour organiser rationnellement les complexes supramoléculaires et leurs interactions. D’autres techniques, indépendantes des valeurs des paramètres sont des méthodes graphiques formalisant la suppression de noeuds et les opérations d’aggrégation dans les réseaux biochimiques [42], regroupant des métabolites en des réseaux métaboliques de grande taille [106, 72], parfois basées sur recherches extensives dans l’ensemble de tous les regroupements possibles [34]. Enfin, des méthodes de réduction qualitative ont été utilisées pour simplifier des grands réseaux de régulation booléens, supprimant de manière adéquate des noeuds et définissant des sous-approximations de la dynamique [99, 100].

Deuxièmement, les processus biochimiques gouvernant la dynamique des réseaux impliquent des nombreuses échelles de temps. Par exemple, le changement d’expression des gènes peut prendre des heures, alors que la formation des complexes de protéines est de l’ordre de la seconde et que les modifications post-translationnelles prennent des minutes. La demi-vie des protéines peut varier de plusieurs minutes à plusieurs jours. La réduction de modèles peut bénéficier fortement du caractère multi-échelle des réseaux. La dynamique asymptotique des réseaux avec des processus rapides et lents peut être fortement simplifiée en utilisant des idées comme les variétés invariantes (IM) ou les approximations par moyen-nisation.

Les méthodes de calcul numériques de variétés invariantes visent à trouver une IM de faible dimension, contenant la dynamique asymptotique [51, 52, 116]. La méthode de calcul de perturbations singulières (CSP) [80, 19] vise à trouver l’IM ainsi que la géométrie de la fibration définie par les directions. Les variétés invariantes peuvent être calculées par de nombreuses autres méthodes [53, 55, 116, 74, 77].

Les méthodes pour le calcul des “premières approximations” des IM lentes sont très populaires. L’approximation classique des états quasi-stationnaires (QSS) a été proposée par [13] et a été élaborée comme un outil important pour l’analyse des mécanismes cinétiques des réactions chimiques [123, 20, 66]. L’approximation QSS classique est justifiée pour les concentrations relativement faibles de certains réactifs (radicaux, concentrations d’enzymes et de complexes substrats-enzymes, ou les quantités de centres actifs sur la surface catalysatrice) [6, 122, 148]. L’approximation par quasi-équilibre (QE) a deux formulations basiques : l’approche thermodynamique, basée sur le maximum d’entropie conditionnelle (ou le minimum d’énergie libre conditionnelle), ou la formulation cinétique, basée sur l’équilibration de réactions réversibles rapides. Le premier usage du principe de maximum d’entropie remonte à Gibbs [43]. Des corrections à l’approximation par quasi-équilibre avec comme applications la cinétique physique ou chimique ont été développées par [54, 53]. Un problème important, toujours non résolu, de ces deux approximations est la détection d’espèces QSS et de réactions en QE sans appliquer toute la machinerie de l’IM ou des méthodes CSP. En effet, toutes les réactions avec des grandes constantes ne sont pas en quasi-équilibre, et il n’y a pas de méthode simple pour trouver les espèces quasi-stationnaires s’il n’y a pas d’indices comme l’existence d’invariants à faible valeur (comme la concentration totale d’une enzyme). La méthode de la variété intrinsèque de faible dimension (ILDM, [89, 18]) fournit une approximation de la variété invariante de faible dimension et peut être considérée comme une première étape de la méthode CSP [73].

Une autre méthode permettant de simplifier des dynamiques multi-échelles est la moyennisation. Cette idée remonte au traitement perturbatif du problème des trois corps de Poincaré pour la mécanique céleste [107], développé davantage en mécanique classique par d'autres auteurs [7, 88], et aussi connu comme approximation adiabatique ou approximation Born-Oppenheimer en mécanique quantique [94]. De manière générale, la moyennisation peut être appliquée quand certaines variables d'échelles fines (fine-scales) oscillent rapidement. Alors, la dynamique des variables lentes, grossières (coarse-scale), peut être obtenue en moyennisant sur une échelle de temps bien plus grande que la période des oscillations rapides. La façon d'effectuer la moyennisation dépend de la structure du système, principalement de la définition des variables fines et grossières [14, 8, 3, 121, 2, 47, 127].

Enfin, le caractère multi-échelle ne s'applique pas uniquement aux échelles de temps, mais de manière équivalente à l'abondance des différentes espèces dans ces réseaux. Le nombre de copies d'ARNs messagers peut varier de quelques copies à des dizaines de milliers, et l'éventail des concentrations dynamiques des protéines biologiques peut varier jusqu'à cinq ordres de magnitude. De plus, la molécule d'ADN peut avoir une seule ou plusieurs copies. Des petits nombres conduisent, directement ou indirectement, à l'expression stochastique des gènes (une espèce peut être stochastique même avec un grand nombre de copies). En biologie computationnelle, la réduction de modèles doit donc s'appliquer non seulement à des modèles déterministes, mais aussi à des modèles stochastiques et hybrides. Le besoin de réduire des grands modèles stochastiques est crucial. En effet, les algorithmes de simulation stochastiques (SSA [44, 45]) peuvent être très gourmands en temps de calcul quand on les appliquent à grands modèles non réduits, même en excluant l'analyse des trajectoires et l'identification des paramètres. Pour cette raison, un effort intensif a été dédié à l'adaptation des idées principales utilisées pour la réduction de modèles déterministes, à savoir le regroupement exact, les variétés invariantes, la quasistationnarité, le quasi-équilibre, la moyennisation, au cas des modèles stochastiques.

La réduction des modèles stochastiques à base de règles, basée sur une version affaiblie du critère d'aggregation exacte, a été proposée par [38] pour définir des espèces abstraites ou des fragments stochastiques qui peuvent être utilisés pour des calculs simplifiés. De manière plus générale, les modèles à base de règles permettent de surmonter la complexité combinatoire dans les simulations stochastiques [30]. La performance des simulateurs stochastiques de modèles à base de règles comme Nfsim [130] est indépendante de la taille du réseau. La réduction approximative du nombres d'états de chaînes de Markov décrivant les réseaux stochastiques a été proposés par [98].

A l'exception des méthodes paramètres-indépendantes, toutes les méthodes de réduction de modèles décrites ci-dessus ont besoin d'une paramétrisation complète du modèle. C'est un besoin rigoureux, et ne peut pas être simplement contourné. En effet, la réduction a une validité locale. Les éléments définissant un modèle réduit, comme les variétés invariantes, les espèces quasistationnaires et les réactions en quasi-équilibre dépendent des paramètres locaux et aussi de la position dans l'espace des phases le long de la trajectoire. On s'attend à ce que la réduction de modèles soit robuste, c'est à dire qu'un modèle réduit donné fournisse une bonne approximation de la dynamique du modèle initial pour un large ensemble de paramètres et de valeurs des variables. On peut constater que cette propriété est satisfaite par les réseaux biochimiques avec des constantes bien séparées, car dans ce cas les réseaux simplifiés dépendent des relations d'ordre parmi les modèles de paramètres et non des valeurs précises de ces paramètres [56, 112, 103].

Dans ce chapitre, nous allons revisiter les concepts fondamentaux de la réduction de modèles à la lumière d'un nouveau cadre, qui devrait ammener, sur le long terme, à une nouvelle génération d'outils de réduction satisfaisant tous les besoins spécifiques de la biologie computationnelle. Ce cadre est basé sur des idées d'analyse tropicale. Les détails de cette partie sont présentés dans le chapitre 2.

Les techniques mathématiques décrites dans ce travail définissent les stratégies pour l'étude de grands réseaux dynamiques en biologie computationnelle. Ces grands réseaux sont nécessaires pour comprendre la dépendance du contexte, la spécialisation, ainsi que les variations d'un individu à l'autre du comportement des cellules. L'accumulation des base de données sur les interactions moléculaires soutient l'idée que la cellule biologique est un puzzle de réseaux et de voies, et qu'une fois ces voies regroupées dans une carte cohérente, la physiologie de la cellule pourrait être révélée par une simulation numérique. En réalité, confronter les réseaux biochimiques avec la vie réelle n'est pas un défi aisés. Les techniques de réduction de modèles sont nécessaires pour nous rapprocher de cet objectif, et ces méthodes peuvent révéler des fonctionnalités importantes de ces organisations complexes.

Nos résultats sont basés sur les notions de limitation et de dominance entre les éléments du système. Ces notions sont importantes pour comprendre les modèles dynamiques en biologie computationnelle. Les fonctionnalités essentielles, critiques des systèmes avec de nombreuses échelles de temps bien séparées peuvent être résumées par un sous-système dominant réduit. Ce sous-système dominant dépend des relations d'ordre entre les paramètres du modèle et des combinaisons des paramètres du modèle. Nous avons montré comment calculer un tel sous-système dominant pour des réseaux linéaires et non-linéaires. L'interprétation géométrique de ces concepts en terme de tropicalisation fournit un cadre mathématique puissant, permettant d'identifier les variétés invariantes, les espèces quasi-stationnaires et les réactions en quasi-équilibre. Nous avons aussi discuté comment la réduction de modèles peut être appliquée pour les stratégies d'apprentissage de paramètres.

Des efforts supplémentaires sont nécessaires pour étendre la validité des idées mathématiques et pour améliorer les algorithmes de réduction de modèles, et pour les implémenter dans des outils de biologie computationnelle.

0.4 Principe d'équilibration tropicale pour les cinétiques chimiques

La biologie systémique développe des modèles biochimiques dynamiques de nombreux processus cellulaires comme la signalisation, le métabolisme, et la régulation génétique. Ces modèles peuvent reproduire les comportements spatio-temporels dynamiques complexes observés dans les expériences de biologie moléculaire. Malgré leur comportement complexe, les modèles dynamiques disponibles actuellement sont des approximations de taille relativement petite, contenant uniquement des dizaines de paramètres et de variables. Cette taille modeste résulte d'une part du manque d'informations précises sur les paramètres cinétiques des réactions biochimiques, et d'autre part des limitations dans les méthodes d'identification de paramètres. D'autres limitations peuvent provenir de l'explosion combinatoire des interactions entre molécules avec des modifications et des sites d'in-

teraction multiples [29]. Ces petits modèles peuvent également être justifiés par le fait qu'il faut trouver le niveau de complexité optimal pour capturer les fonctionnalités essentielles du phénomène à étudier. La capacité de choisir les détails importants et d'omettre ceux moins importants est une propriété importante de l'art de modéliser. Au delà de l'art du modélisateur, le succès des modèles simples provient d'une propriété importante des grands systèmes dynamiques. La dynamique de grands modèles dissipatifs multi-échelles peut être réduite à celle de modèles plus simples, appelés sous-systèmes dominants [112, 58, 57]. Les sous-systèmes dominants contiennent moins de paramètres et sont plus faciles à analyser. Le choix du sous-système dominant est dicté par la comparaison entre les échelles de temps du grand modèle. Parmi les conditions amenant à la dominance et permettant de générer des modèles réduits, les plus importantes sont les approximations de quasi-équilibre (QE) et de quasistationnarité (QSS) [58]. Dans les systèmes non-linéaires, les échelles de temps et avec elles les sous-systèmes dominants, peuvent changer durant la dynamique et subir des transitions plus ou moins brusques. L'existence de ces transitions suggère qu'un cadre hybride, discret/continu est bien adapté pour la description de la dynamique de grands systèmes non-linéaires multi-échelles de temps [27, 102, 103].

La notion de dominance peut être exploitée pour obtenir des modèles plus simples à partir de grand modèles avec des échelles de temps multiples et séparées, et pour assembler ces modèles dans des modèles hybrides. Cette notion est asymptotique, et un cadre mathématique naturel pour capturer les multiples relations asymptotiques est la géométrie tropicale. Motivée par des applications en physique mathématique [87], des systèmes d'équations polynomiales [133], etc., la géométrie tropicale utilise un changement d'échelle pour transformer des systèmes non-linéaires en des systèmes discontinus linéaires par morceaux. Plus précisément, la tropicalisation consiste à remplacer une fonction polynomiale par le polynôme max-plus correspondant. La tropicalisation est une propriété robuste du système, qui reste constante pour un grand domaine de valeurs des paramètres. Elle peut révéler des fonctionnalités qualitatives stables de la dynamique du système, comme certains types d'attracteurs. L'utilisation de la tropicalisation pour analyser des modèles de grands systèmes pourrait donc être une solution pleine de promesses pour le problème du manque d'information sur les paramètres cinétiques. Dans le chapitre 3, nous fournissons des justifications mathématiques rigoureuses pour l'idée de tropicalisation.

0.5 Deux modèles paradigmatisques du cycle cellulaire et leurs tropicalisations

Les deux modèles paradigmatisques du cycle cellulaire présentés datent tous les deux du début des années 1990.

Le premier est le modèle du cycle cellulaire proposé par Tyson et collab. [140]. Ce modèle reproduit l'interaction entre la cycline et la kinase cycline-dépendante Cdc2 (formant un complexe appelé facteur promoteur de maturation, MPF) durant la progression du cycle cellulaire. Ce modèle démontre que ce système biochimique peut fonctionner comme un oscillateur, ou converger vers un état stable avec des grandes concentrations de MPF, ou fonctionner comme un commutateur excitable qui atteint des grandes concentrations transitoires de MPF avant de revenir à un état basal non-excité. Les trois régimes peuvent être

associés à la division rapide des jeunes embryons, l'arrêt en métaphase des œufs non fertilisés, et la division contrôlée par la croissance des cellules somatiques, respectivement. Ce modèle prend en compte l'activité auto-catalytique du facteur MPF (rétrocontrôle positif).

Le second modèle, proposé par Goldbeter et collab. [48], reproduit également un oscillateur mitotique minimal. Cet oscillateur est basé sur une cascade de modifications post-transcriptionnelles qui modulent l'activité de la kinase Cdc2. Au fur et à mesure que la cycline augmente, elle active le complexe MPF, qui déclenche la dégradation de la cycline et la mitose. La dégradation de la cycline n'est pas déclenchée directement par MPF, mais par une troisième variable (une protéase de cycline), activée par MPF. Dans le modèle original la cinétique des modifications post-translationnelles est décrite par des équations de Michaelis-Menten. De plus, pour gérer les situations avec une grande quantité d'enzyme, l'auteur représente la dépendance du paramètre V_{Max} sur la concentration de l'enzyme par une autre fonction de Michaelis-Menten. Le travail sur ces modèles est présenté dans le chapitre 4.

Nous montrons que les idées tropicales peuvent être utilisées pour réduire et hybridiser des systèmes dynamiques polynomiaux ou rationnels résultant de la modélisation de la machinerie moléculaire du cycle cellulaire. L'idée principale consiste à garder seulement le terme monomial dominant dans la partie droite des équations différentielles ordinaires. Suivant la position dans l'espace des phases, il faut garder un, deux, ou plusieurs de ces termes. L'endroit où deux ou plusieurs termes monomiaux sont égaux définit ce qu'on appelle la variété tropicale. L'approximation à un seul terme est valable loin de la variété tropicale, alors que près de la variété tropicale, plusieurs termes dominants de signe opposés peuvent s'équilibrer entre eux. Ces "équilibrations tropicales" des termes dominants ralentissent la dynamique et produisent des variétés invariantes attractives.

Les applications possibles de ces méthodes sont multiples. En général, cette méthode peut être utilisée pour obtenir des modèles simplifiés. Dans le cas du modèle de Tyson, nous sommes partis d'un modèle à cinq variables, qui a été réduit à deux variables et hybridisé. Les modes du modèle hybride ont la structure simple d'équations différentielles monomiales ou sont définies par des équations différentielles algébriques. Deux méthodes générales, que nous appelons tropicalisation complète et tropicalisation à deux termes, fournissent les descriptions des modes et des changements de modes. Cependant, ces procédures générales peuvent amener à des mauvaises approximations quand le modèle complet ne satisfait pas globalement la propriété de permanence, utilisée auparavant en écologie (modèle Lotka-Volterra) ou en théories de la co-évolution (réplicateurs d'Eigen et Schuster). Dans de tels cas, une analyse plus poussée est nécessaire. Nous avons montré que le modèle de cycle cellulaire embryonnaire de Tyson a essentiellement trois modes avec des échelles de temps différentes, à savoir l'accumulation de cycline, l'activation rapide de MPF et de manière intermédiaire la dégradation rapide de la cycline et la désactivation de MPF. Le mode le plus rapide est décrit par des équations différentielles ordinaires monomiales, alors que les modes moins rapides correspondent à des équilibrations tropicales et sont décrits par des équations différentielles algébriques.

Plusieurs améliorations et développements sont nécessaires afin d'appliquer ces méthodes à grande échelle. Le calcul des équilibrations tropicales subit une explosion combinatoire. Cependant, pour le réseau biochimique utilisé comme exemple, le nombre de solutions semble très petit comparé à la grande combinatoire des termes monomiaux. On peut

espérer que, une fois formulés en programmation logique par contraintes, le problème d'équilibrations peut être efficacement calculé en pratique comme un problème de satisfaction de contraintes. Des méthodes efficaces sont également nécessaires pour calculer les transitions entre les modes. La principale difficulté ici est liée au passage à travers les murs (les segments de la variété tropicale). A proximité des murs, deux termes ou plus dominent. Quand ces termes sont équilibrés, les orbites restent proches de ces murs et sont contenues dans des variétés invariantes. La tropicalisation, complète ou à deux termes, fournit une heuristique générale pour les transitions entre modes. Cette heuristique pourrait échouer à proximité des murs. Par exemple, comme montré en [101] (Voir Chapitre 2), la tropicalisation complète prédit des modes glissants qui évoluent le long des murs et restent proches des orbites du système complet. Cependant, ces modes glissants peuvent être trop longs, quittant le mur quand les orbites du système complet sont déjà très éloignées. Dans le but d'avoir une description précise du comportement à proximité des murs, il nous faut calculer les variétés invariantes. Bien que cela soit généralement plus simple qu'intégrer l'ensemble complet des équations, ce calcul peut devenir difficile pour les équilibrations tropicales impliquant plus de deux termes. Des travaux futurs seront dédiés au développement de méthodes générales pour ce problème.

Introduction

Biology faces today an unprecedented situation. New experimental techniques in molecular biology, biophysics, biochemistry, produce avalanches of data that need to be processed, analysed, and understood. Modeling becomes part of biological reasoning, but in order to be comprehensive, models increase their size practically without limits. For instance, in order to represent the processes in a single signaling pathway a computational biologist could use hundreds or thousands of biochemical reactions, leading to an equivalent number of differential equations. A biological cell uses tens to hundreds of signaling pathways that interact with one another. Such large systems are not only difficult to analyse, but also practically impossible to identify from the available data. A strategy to cope with such a tremendous complexity is to use abstractions, ie reduced versions of the models that can reproduce with sufficient accuracy the behavior of the initial model. These simplified models can be of various types. If the initial model is a system of ordinary differential equations (ODEs), the abstraction can be a smaller system of ODEs, or a hybrid model combining discrete and continuous variables or a purely discrete model (for instance a Boolean network). All such descriptions are currently used in computational biology. However, we lack general methods allowing to reduce or convert one type of model into another, automatically. As model parameters are rarely known with precision, we need methods to cope with uncertain parameters.

The work presented in this thesis was motivated by the above described situation in computational biology.

We discuss a class of semi-formal methods allowing to reduce large networks of biochemical reactions. In order to cope with parameter uncertainty we have based the reduction methods on dominance relations among parameters and/or reaction rates. These methods exploit the multi-scaleness of biochemical networks, ie their property to have many, well separated time and concentration scales. In multiscale networks parameters can be replaced by orders of magnitude, that are much easier to obtain than the precise values. Furthermore, the dynamics of dissipative reaction networks with many well separated time scales can be described as a sequence of successive equilibrations of different subsets of variables of the system. Polynomial systems with separation are equilibrated when at least two monomial terms, of opposite signs, have the same order of magnitude and dominate the others. These equilibrations and the corresponding truncated dynamics, obtained by eliminating the dominated terms, find a natural formulation in tropical analysis and can be used for model reduction.

By model reduction we transform systems of ODEs into systems of ODEs having less variables and parameters. These simplifications can provide accurate approximations globally, ie for large domains of values of parameters and for all positive times. Locally, ie for restricted domains of values of parameters and intervals of times, reduced models that are simpler than the global simplification can be found. This situation leads to a piecewise-smooth hybrid description of the dynamics of the system, in which a smooth

trajectory generated by the complex model is approximated by a sequence of smooth pieces generated by simpler, but changing, ODEs. There are simple ways to hybridize a network of biochemical reactions, consisting in replacing the sigmoidal functions occurring in the definition of the reaction rates, by step functions, or by piecewise linear functions. Another solution to perform hybridization is offered by tropical analysis under the form of the Litvinov-Maslov correspondence principle. This idea can be applied to polynomial or rational systems of ODEs (resulting in biochemistry from the mass action law) and consists in approximating the polynomial functions by max-plus polynomials.

Both model reduction and hybridization are meaningful in the context of cell cycle models in computational biology. Cell cycle regulates cell proliferation by the cyclic activity of special proteins named cyclins. The modifications of these proteins can occur abruptly, leading to changes of dynamical regime that are well described by mode changes in piecewise smooth hybrid models. From a dynamical point of view, cell cycle models have singular oscillations, alternating slow and fast intervals. By model reduction one can emphasize the essential variables and parameters of the cell cycle models, and, in certain cases, calculate the attractors analytically.

The structure of the manuscript is the following.

In Chapter 1 we propose numerical methods allowing to identify a hybrid model from time series. We use this method to obtain hybrid approximations to existing smooth cell cycle models.

In Chapter 2 we give a review of model reduction methods. The new results consist in using tropical analysis and geometry in order to unify various approaches that apply to networks with separation.

In Chapter 3 we discuss the tropicalization method and find some estimates justifying its applicability.

In Chapter 4 we discuss the dynamics of singular cell cycle oscillators, justify rigorously their reduction to lower dimensional systems and their hybridization.

Chapitre 1

Hybrid models for networks of biochemical reactions

1.1 Introduction

Hybrid systems are widely used in automatic control theory to cope with situations arising when a finite-state machine is coupled to mechanisms that can be modeled by differential equations [92]. It is the case of robots, plant controllers, computer disk drives, automated highway systems, flight control, etc. The general behavior of such systems is to pass from one type of smooth dynamics (mode) described by one set of differential equations to another smooth dynamics (mode) described by another set of differential equations. The command of the modes can be performed by changing one or several discrete variables. The mode change can be accompanied or not by jumps (discontinuities) of the trajectories. Depending on how the discrete variables are changed, there may be several types of hybrid systems : switched systems [124], multivalued differential automata [137], piecewise smooth systems [40]. Notice that in the last case, the mode changes when the trajectory attains some smooth manifolds. In these examples, the changes of discrete variables and the evolution of continuous variables are deterministic. The class of hybrid systems can be extended by considering stochastic dynamics of both continuous and discrete variables, leading to piece-wise deterministic processes, switched diffusions or diffusions with jumps [114, 27, 26, 125, 16]. Hybrid, differential, or stochastic Petri nets provide equivalent descriptions of the dynamics and were also used in this context [32].

The use of hybrid models in systems biology can be justified by the temporal and spatial multi-scaleness of biological processes, and by the need to combine qualitative and quantitative approaches to study dynamics of cell regulatory networks. Furthermore, hybrid modelling offers a good compromise between realistic description of mechanisms of regulation and possibility of testing the model in terms of state reachability and temporal logics [85, 96]. Threshold dynamics of gene regulatory networks [10, 115] or of excitable signaling systems [149] has been modelled by piecewise-linear and piecewise-affine models. These models have relatively simple structure and can, in certain cases, be identified from data [108, 35]. Some methods were proposed for computing the set of reachable states of piecewise affine models [12].

Among the applications of hybrid modeling, one of the most important is the cell cycle regulation. The machinery of the cell cycle, leading to cell division and proliferation, combines slow growth, spatio-temporal re-organisation of the cell, and rapid changes of regulatory proteins concentrations induced by post-translational modifications. The advancement through the cell cycle is a well defined sequence of stages, separated by check-

point transitions. This justifies hybrid modelling approaches, such as Tyson's hybrid model of the mammalian cell cycle [126]. This model is based on a Boolean automaton whose discrete transitions trigger changes of kinetic parameters in a set of ODEs. The model has been used to reproduce flow cytometry data.

Although sufficient for certain applications like gene networks, piecewise affine models are less adapted to describe phenomena where the dynamics between two successive discrete events is strongly nonlinear. A typical example of such phenomena is the machinery of the cell cycle. Proteolytic degradation of the cyclins is switched on rapidly by the cyclin dependent kinase complexes but between two successive switchings the complexes have non-linear dynamics implying several positive (autocatalytic processes) and negative feed-back loops. These non-linear processes contribute to the robustness of the mechanism.

The idea of piecewise smooth systems arises naturally in the context of biochemical systems with multiple separated timescales. The dynamics of a multiscale, dissipative, large model, can be reduced to the one of a simpler model, called dominant subsystem [112, 58, 57]. The dominant subsystem depends on the comparison among the time scales of the large model. For nonlinear models, the dominant subsystem (which can be assimilated to a mode) is only piecewise constant and can change several times during the dynamics. The model reduction methods proposed in [57, 112] generate dominant subsystems whose reactions rates are multivariate monomials of the concentration variables, like in the well-known S-systems [120]. Indeed, when applied to models using mass action kinetics, quasi-steady state and quasi-equilibrium approximations [58] lead to lumped models in which the reactions rates result from solving systems of polynomial equations. In general, these polynomials contain only a few terms (fewnomials). The solutions of such systems are much simplified in the case of total separation of the nonconstant terms in the fewnomials and lead to monomial rates. The rate of the same reaction can be represented by different monomials in different dominant subsystems (modes). For instance, the rate of a Michaelis-Menten mechanism depends linearly on the concentration of the substrate for small concentrations and is constant at saturation. We expect that more general rate laws [84] can be treated similarly in our approach.

In this chapter we propose a heuristic to construct appropriate modes and adequate piecewise smooth models by using a top-down approach. Then, we show how the parameters of the hybrid model can be identified from data or from trajectories produced by existing smooth, but more complex models.

1.2 Hybrid models

We consider the so-called hybrid dynamical systems (HDS) consisting of two components : a continuous part, u , satisfying the equations

$$\frac{du_i}{dt} = f_i(u(t), s(t)), \quad t > 0, \quad (1.2.1)$$

where $u(t) = (u_1(t), u_2(t), \dots, u_n(t)) \in \mathbf{R}^n$, and a discrete part $s(t) \in S$, where S is a finite set of states. We consider that there is an increasing series $\tau_0 = 0 < \tau_1 < \dots < \tau_k < \dots$ such that the discrete variables are piecewise constant on the intervals $[\tau_i, \tau_{i+1}[$ and that they change values at $t = \tau_k$. The continuous variables can also have discrete jumps at $t = \tau_k$.

Typically, in molecular networks, the continuous variables are protein concentrations and the discrete states may be gene or protein activities described by boolean variables $s(t) = (s_1(t), s_2(t), \dots, s_m(t))$, where $s_j(t) \in \{0, 1\}$.

There are several possible ways to define the evolution of the s variables. Rather generally, this can be done by a time continuous Markov chain with transition probabilities $p(s, s', u)$ from the state s to the state s' (per unit time) depending on current state $u(t)$. However, in many molecular regulatory networks, transition probabilities dependence on u is not smooth. For instance, the probability for s to jump is close to one if u goes above some threshold value, and close to zero if u is smaller than the threshold. We can, in certain cases, neglect the transition time with respect to the time needed for u variables to change. In this situation, we can consider that discrete variables are simply deterministic functions of the continuous variables. Further assuming that some of the discrete variables contribute to production of u and that other contribute to the degradation of u we obtain a general model of hybrid piece-wise smooth dynamical system

$$\begin{aligned} \frac{du_i}{dt} &= \sum_{k=1}^N s_k P_{ik}(u) + P_i^0(u) - \sum_{l=1}^M \tilde{s}_l Q_{il}(u) - Q_i^0(u), \\ s_j &= H\left(\sum_{k=1}^n w_{jk} u_k - h_j\right), \quad \tilde{s}_l = H\left(\sum_{k=1}^M \tilde{w}_{lk} u_k - \tilde{h}_l\right), \end{aligned} \quad (1.2.2)$$

where H is the unit step function $H(y) = 1$, $y \geq 0$, and $H(y) = 0$, $y < 0$, $P_{ik}, P_i^0, Q_{il}, Q_i^0$ are positive, smooth functions of u representing production, basal production, consumption, and basal consumption, respectively. Here w, \tilde{w} are matrices describing the interactions between the u variables, $i = 1, 2, \dots, n$, $j = 1, 2, \dots, N$, $l = 1, \dots, M$ and h, \tilde{h} are thresholds.

One will usually look for solutions of the piecewise-smooth dynamics (1.2.2) such that trajectories of \mathbf{u} are continuous. However, we can easily extend the above definitions in order to cope with jumps of the continuous variables. Similarly to impact systems occurring in mechanics [33], the jumps of the continuous variables can be commanded by the following rule : \mathbf{u} instantly changes to $\mathbf{p}_j^\pm(\mathbf{u})$ whenever a discrete variable $\hat{s}_j = H(\sum_{k=1}^n \hat{w}_{jk} u_k - \hat{h}_j)$ changes. The \pm superscripts correspond to changes of \hat{s}_j from 0 to 1 and from 1 to 0, respectively. We can consider reversible jumps in which case the functions $\mathbf{p}_j^\pm(\mathbf{u})$ satisfy $\mathbf{p}^+ \circ \mathbf{p}^- = Id$. The typical example in molecular biology is the cell cycle. In this case, the command to divide at the end of mitosis is irreversible and corresponds to $\mathbf{p}_j^+(\mathbf{u}) = \mathbf{u}/2$. No return is possible, $\mathbf{p}_j^-(\mathbf{u}) = \mathbf{u}$.

The class of models (1.2.2) is too general. We will restrict ourselves to a subclass of piecewise smooth systems where smooth production and degradation terms are assumed multivariate monomials in u , plus some basal terms that we try to make as simple as possible. A system with constant basal production and linear consumption is the following :

$$\begin{aligned} P_{ik}(\mathbf{u}) &= a_{ik} u_1^{\alpha_1^{ik}} \dots u_n^{\alpha_n^{ik}}, \\ P_i^0(\mathbf{u}) &= a_i^0, \\ Q_{il}(\mathbf{u}) &= \tilde{a}_{il} u_1^{\tilde{\alpha}_1^{il}} \dots u_n^{\tilde{\alpha}_n^{il}}, \\ Q_i^0(\mathbf{u}) &= \tilde{a}_i^0 u_i, \end{aligned} \quad (1.2.3)$$

which will be chosen according to an heuristic presented in the next sections.

This restriction does not reduce the power of the method. As argued in the introduction, the monomial rates represent good approximations for nonlinear networks of biochemical reactions with multiple separated timescales [112, 57]. More generally, rational functions are good candidates for general rate laws [84]. However, when concentrations are very large or very small the monomial laws are recovered. For instance, Michaelis Menten, Hill, or

Goldbeter-Koshland reactions switch from a saturated regime where rates are constant to a small concentration regime where rates follow power laws. Finally, by methods described in [141, 142] one can show that the above subclass of models can approximate with arbitrary precision any structurally stable dynamics.

These models have several advantages with respect to standard models in molecular biology and neuroscience based on differential equations. They allow us to simulate, in a fairly simple manner, discontinuous transitions occurring in such systems (see a typical graph describing time evolution of protein concentration within cellular cell cycle, Fig.4.1). The discontinuous transitions result either from fast processes or from strongly non-linear (thresholding) phenomena. This class of models is also scalable in the sense that more and more details can be introduced at relatively low cost, by increasing the number of discrete variables and the size of the interaction matrices.

The definition of the rates slightly extends the one used in S-systems, introduced by Savageau [120]. Our choice was motivated by the fact that S-systems proved their utility as models for metabolic networks whose dynamics we want to encompass by considering the modes. The introduction of basal terms avoids spurious long living states when some products have zero concentrations.

1.3 Regulated reaction graphs and hybrid reaction schemes

Interaction mechanisms in molecular biology can be schematized as regulated reaction graphs.

A regulated reaction graph is a quadruple (V, R, E, E_r) . The triplet (V, R, E) , where $E \subset V \times R \cup R \times V$, defines a reaction bipartite graph, ie $(x, y) \in E$ iff $x \in V, y \in R$ and x is a substrate of R , or $x \in R, y \in V$ and y is a product of x . $E_r \subset V \times R$ is the set that defines regulations, $(x, z) \in E_r$ if the rate of the reaction $z \in R$ depends on $x \in V$ and x is not a substrate of R .

Similar structures of regulated reactions were proposed elsewhere for non-hybrid models [84].

In order to define a hybrid model we first need a *hybrid reaction scheme*. This consists in saying, for each given species, whether its production/degradation can be switched on and off and by which species, also which species modulate the production/degradation of a given species in a smooth way. This means specifying a partition of the regulations $E_r = E_r^d \cup E_r^c$. A regulation $(x, r) \in E_r^d$ is discrete if the decision to switch on and off the reaction r depends (among others) on x . Discrete interactions manifest themselves punctually as a consequence of thresholding and/or of rapid phenomena. The continuous regulations guide the dynamics of the modes. Similarly, there is a partition of the reactions $R = R^s \cup R^c$. A reaction r belongs to the switched reactions $r \in R^s$ if $(x, r) \in E_r^d$, for some $x \in V$. The role of the regulators (continuous if they modulate the reaction rate, discrete if they contribute to switching it on and off) should be indicated on the graph together with the signs of the regulations.

1.4 Identification of piecewise smooth models

We would like to develop methods allowing to find the parameters of a model from the class introduced above that best describes the observed trajectories of a biological system. These trajectories can come from experiments or can be produced by non-hybrid models. In both situations we obtain a model whose parameters can be easily interpreted

in biological terms. The hybrid model can be further analyzed or used to model more complex situations.

In the following we present a reverse engineering algorithm that works well for systems with sharp transitions.

Data. n trajectories (time series) $u_1(t), \dots, u_n(t)$ given at time moments t_0, t_1, \dots, t_N . A regulated reaction graph (the smooth/discrete partition of the regulations can be unspecified).

Output. A model of the type (1.2.2), (1.2.3) with values of the parameters that fit well the data.

The algorithm has several steps, some of them involving several alternative numerical solutions. For some of the steps the choice of the numerical solution was adapted to the application presented in the paper, which is the reconstruction of a hybrid cell cycle oscillator.

I. Choice of hybrid reaction scheme and of monomials giving the smooth part of the rates.

The reaction rates have the forms given by (1.2.3). The monomial exponents α_{ij} , $\tilde{\alpha}_j^i$, the rate functions defining the modes, the mode switching and the jumps can be obtained from the following heuristic rules :

- i) If a reaction j is activated then $\alpha_j^i = 1$ for all activators i and $\alpha_j^i = -1$ for all inhibitors i in the absence of cooperativity. By cooperativity we design generically, situations when the reaction rates depend on powers of the concentrations of regulators instead of just being proportional to them (this includes the case of regulator complexes, synergetic binding of molecules on a substrate, as well as allosteric) These phenomena can be taken into account by considering $|\alpha_j^i| > 1$.
- ii) Basal rates are constant for reactions without substrates and proportional to the concentration of the substrate otherwise.
- iii) If activated reactions are present with intermittence, their non-basal rates are multiplied by discrete variables s_i ; this defines the mode switching.
- iv) If a continuous variable u_i is known to induce a jump decision (for instance cell division), it should appear in the definition of the jump discrete variables \hat{s} . The functions $p(\mathbf{u})$ follow from biological observations.

Once the hybrid reaction scheme chosen, we want to fit the remaining model parameters in order to reproduce the observed dynamics.

II. Detection of the events locations.

We look for K time intervals I_1, I_2, \dots, I_K . The dynamics on each of the intervals is smooth, it is given by (1.2.2) with the s variables fixed. Mode transitions (change of the variables) occur at the borders of these intervals. We denote the switching times as τ_1, \dots, τ_K .

Finding τ_k is a problem of singularity detection. This could be done by various methods, for example by wavelet analysis [139]. Here we decided to use the derivatives of the reaction rates to locate the mode switching events. The peaks of these derivatives indicate the positions of switching events, whereas the sign of the derivatives indicate the sign of the change (activation if positive, inactivation if negative). With this simple criterion we are able to reconstruct the sequence of modes which is defined

by the values of the boolean variables $s(t)$.

III. Determining the mode internal parameters.

The previous steps define a set of modes and the static event location. Given a choice of the modes internal parameters the hybrid trajectories can be integrated without knowing the discrete regulations (this will allow the dynamic event location at the next step) : the values of s between two successive events are enough. Modes internal parameters are obtained by optimization. Let $u_i^{modes}(t)$ be the continuous hybrid trajectories obtained by integrating the modes between the calculated transition times. We use a parallel version of Lam's simulated annealing algorithm [22] to minimize the following objective function :

$$F = \sum_{i,k} C_k (u_i^{modes}(t_k) - u_i(t_k))^2,$$

where C_k are positive weights. The choice of the weights depends on the dynamical features one wants to reproduce. For instance, for the cell cycle application we choose weights that increase with time. We thus penalize large time deviations that can arise from the loss of synchronicity among variables u_i and avoid the period misfit that could arise between the hybrid and the smooth dynamics after dynamic event location.

IV. Determining the mode control parameters and dynamic event location.

Let $s_m = H(\sum_{(m,j) \in E^r} w_{mj} u_j - h_j)$ be the discrete variables determined above. Let s_k^m be the constant values of s_m on I_k . Consider now the optimal trajectories $u_i^{modes*}(t_l)$ obtained before.

Then, one should have

$$\left(\sum_{(m,j) \in E^r} w_{mj} u_j^{modes*}(t_l) - h_j \right) s_k^m > 0, \text{ for all } t_l \in I_k, \quad (1.4.1)$$

which is a linear programming problem for w_{mj} that can be resolved (if it has a solution) in polynomial time. This complexity result is well known since Khachiyan's proof of polynomial runtime for the ellipsoid method.

Remark. This algorithm hybridizes switched biochemical reactions whose rates should be modelled by complicated functions (for instance Goldbeter-Koshland) in smooth models. In our hybrid modeling these rates are multivariate monomials piecewisely.

1.5 Parallel simulated annealing.

Solving combinatorial optimization problems is a NP-hard problem, a known bottleneck for parameter identification. One of the main method used to solve this issue is a generalisation of the Metropolis algorithm [138], known as Simulated Annealing (SA), which comes from the analogy with annealing in metallurgy.

In order to reach an optimal crystalline structure, metallurgists use heating and controlled cooling of the material. Heating allow the atoms to escape local energy minima configurations and reach thermal equilibrium. Then, a slow cooling gives them a higher probability of reaching an optimal lower energy configuration, if cooling is quasi-static, i.e. if it preserves thermal equilibrium.

This algorithm has been introduced by Kirkpatrick et al. [76]. The analogy with metallurgy is that the system is allowed to accept cost increase during the optimization, and by this process the probability to get stuck in a local optimum is decreased. To achieve this, a variable called temperature (by analogy to the material temperature) is slowly decreased during the optimisation. A higher temperature increases the probability to accept higher costs, whereas at low temperatures this happens only rarely. The temperature should be kept constant sufficiently long for the system to reach equilibrium. Then, it will finally reach a point where no increase in cost is accepted and the result is a global optimum.

One of the difficulties with this algorithm is to schedule the decrease in temperature. The faster it is decreased, the bigger the chance to get stuck in a local optimum. Only a infinitely slow decrease guarantees convergence to the global optimum with probability one. Thus, there need to be a cut-off value for the rate of temperature decrease. Different methods have been proposed to schedule the decrease of the value of this variable [97, 1].

Another difficulty is the move generation strategy, which ideally must be adaptable.

Lam and Delosme developed in 1988 [78, 79] a schedule which adaptively controls the temperature decrease, with the constraint of maintaining quasi-equilibrium. A key difference from other adaptive schedules is that it takes into account the move generation strategies, and provides an adaptive recipe for their control.

The Lam schedule is an adaptive exponential schedule given by :

$$s_{k+1} = s_k + \lambda \left(\frac{1}{\sigma(s_k)} \right) \left(\frac{1}{s_k^2 \rho^2(s_k)} \right) \left(\frac{4\rho_0(s_k)(1 - \rho_0(s_k))^2}{(2 - \rho_0(s_k))^2} \right), \quad (1.5.1)$$

where $s_k = 1/T_k$, and T_k is the temperature at the k th evaluation of the cost function E . $\rho(s_k)$ is the standard deviation of E at this step, and $\rho_0(s_k)$ is the ratio of accepted to attempted moves, called acceptance ratio. The four factors of this equation play the following roles :

1. λ is a quality factor. With a smaller λ , the quality of the answer increases, but so is the computation time.
2. $\frac{1}{\rho(s_k)}$ is the distance of the system from quasi-equilibrium
3. $\frac{1}{s_k^2 \rho^2(s_k)}$ is the inverse of the statistical specific heat which depends on the variance, see [76].
4. $\frac{4\rho_0(s_k)(1 - \rho_0(s_k))^2}{(2 - \rho_0(s_k))^2}$ is equal to $\rho_2/2$, where ρ_2 is the variance of the average energy change during a move. It is a measure of how effectively the state space is sampled and was found to be at a maximum value when $\rho_0 \simeq 0.44$.

In our particular problem of fitting parameters of ODEs, one of the issues is that the state variables for the optimization have widely different characteristic scales.

In the Metropolis Algorithm [138], a new state always depends on one or more previous states and one or more random variables. The serial nature of this algorithm makes it difficult to parallelize, especially in our particular case. Asynchronous parallelization can lead to acceptable speed-up, but only for cost functions that are separated or loosely coupled. Without such properties, the algorithm can show catastrophic divergences [90]. In the case of fitting parameters of ODEs from time series data, the cost function is completely inseparable, and asynchronous simulated annealing fails to converge.

The essential idea to achieve it is to make all processors work on an independent Markov chain. From time to time, these processors must communicate to pool statistics, and select the best states of energy. The most successful method has been proposed by Chu et al. [21], and can lead to nearly 100% parallel efficiency.

The implementation we choose for the optimization is the method proposed by Chu et al. [21], and a basic implementation has been provided by John Reinitz from the University of Chicago. It is coded in C, and uses MPI for the parallel implementation. For our particular problem, we have to deal with stiff transitions within the hybrid model, and we needed to use an appropriate solver. Our choice has been to use the CVODE solver [24]. It is part of the SUNDIALS collection of solvers [68] developed by the Center for Applied Scientific Computing at Lawrence Livermore National Laboratory.

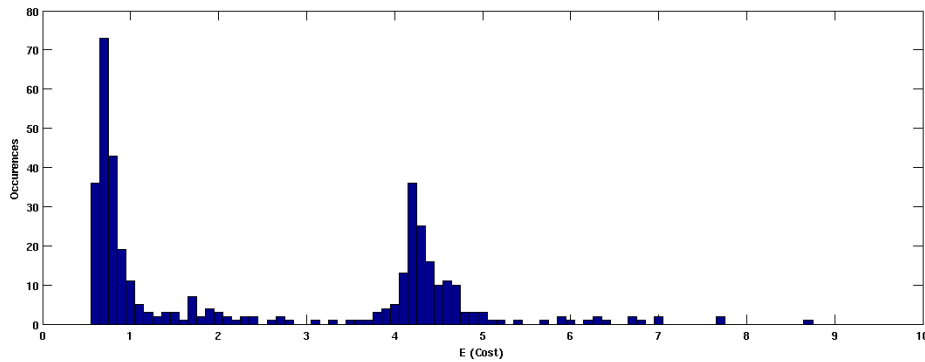


FIGURE 1.1 – Bimodal behaviour in the final solution E_f . Solutions superior to three belong to the quenched attractor.

We tried to reproduce the results from Chu et al. with a simple model, involving only 2 variable and 4 parameters. We first needed to find an appropriate λ for our problem. For large value of λ , the optimization exhibit a bimodal behaviour in the final solution E_f (see Fig. 1.1). The first attractor is a local optimum, referred to as the quenched attractor. The second attractor is the global optimum. The comprise chosen is to allow approximately 50% if the solution in the quenched attractor. Implementation shows a maximum speedup of 70% with 8 processors, and a reach a plateau at 50% for 32 processors (see Fig. 1.2).

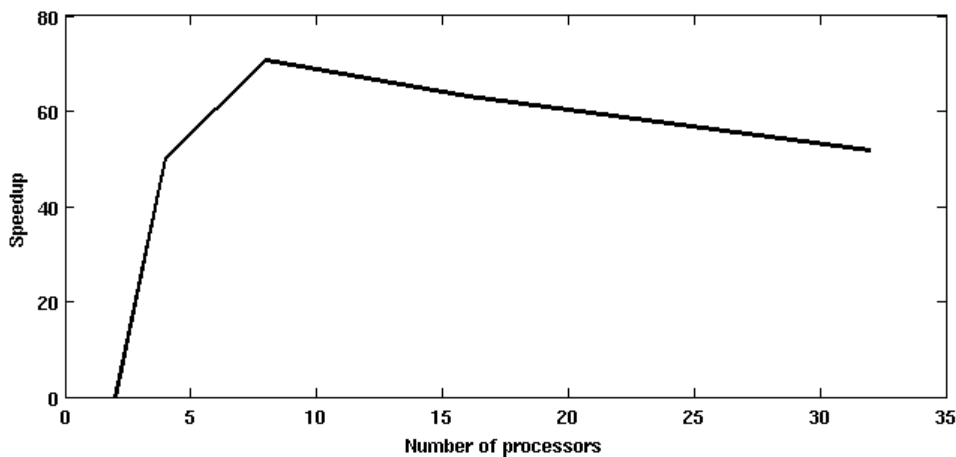


FIGURE 1.2 – Speedup of the parallel implementation according the the number of processors

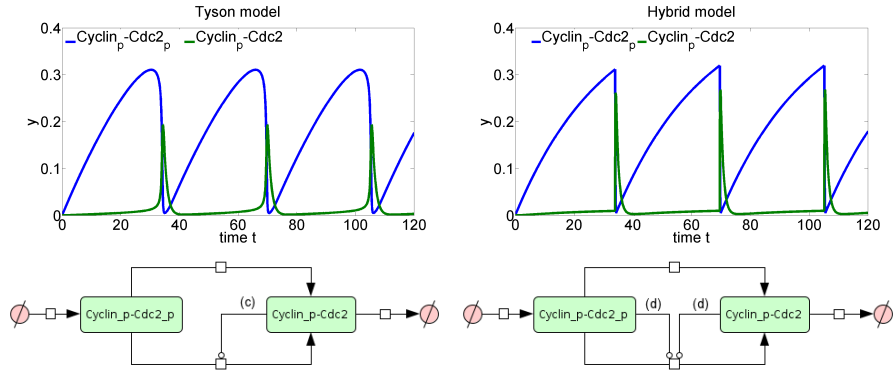


FIGURE 1.3 – (Top Left) Trajectories of the non-hybrid model by Tyson [140]. (Top Right) Trajectories of the hybrid model. (Bottom Left) Reaction graph of the non-hybrid model. (Bottom Right) Reaction graph of the hybrid model.

1.6 Examples

A simple cell cycle model As a simple example let us consider the minimal model proposed by Tyson for Cdc2 and Cyclin interactions [140]. This model, which contains initially 6 species and 9 reactions, can be reduced to only 2 species and 4 reactions (details of the reduction will be given elsewhere), while keeping the same dynamics. The two species left are Cyclin-Cdk complexes, with two phosphorylation states : phosphorylation of both monomers ($C_{pp} := Cyclin_p.Cdc2_p$), or only Cyclin phosphorylated ($C_p := Cyclin_p.Cdc2$).

$$\begin{aligned} \frac{d[C_{pp}]}{dt} &= k_1 - k'_4[C_{pp}] - k_4[C_{pp}][C_p]^2, \\ \frac{d[C_p]}{dt} &= -k_6[C_p] + k'_4[C_{pp}] + k_4[C_{pp}][C_p]^2 \end{aligned} \quad (1.6.1)$$

The regulated reaction graph and the hybrid scheme are represented in Fig.4.1. The dynamics of this model is quite simple. The linear dephosphorylation is slower than the production of C_{pp} . This creates an accumulation of C_{pp} . Then at some threshold the C_p produced activates the second, faster, dephosphorylation, which drains the accumulated C_{pp} . Here we model this second, faster reaction as an hybrid reaction, totally controlled by thresholds. This is justified by the observed peaks of the rate derivative (Fig.1.4) and leads to the following hybrid model :

$$\begin{aligned} \frac{d[C_{pp}]}{dt} &= \tilde{k}_1 - \tilde{k}'_4[C_{pp}] - \tilde{k}_4 s[C_{pp}], \\ \frac{d[C_p]}{dt} &= -\tilde{k}_6[C_p] + \tilde{k}'_4[C_{pp}] + \tilde{k}_4 s[C_{pp}], \end{aligned} \quad (1.6.2)$$

where $s = H(w_1[C_{pp}] + w_2[C_p] - h)$ is the boolean variable.

After the parameter fit we find that w_1 and w_2 are both positive.

For this model no jumps of the continuous variables are needed. Indeed, at the end of mitosis, all continuous variables have small values. Bringing their values to half would not change much the behavior of the model.

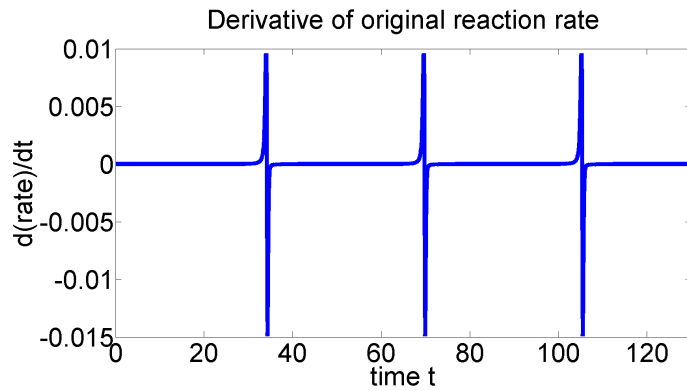


FIGURE 1.4 – Rate derivative for the simple cell cycle model.

Generic mammalian cell cycle model This model has been proposed by the group of Tyson [28] and is designed to be a generic model of the cell cycle for eukaryotes. The cell cycle being an old, but important system that evolved, there have to be homologies, i.e. common mechanisms shared by the cell cycle regulation of all eukaryotes. The goal of this model is to bring to light these mechanisms, while producing models that reproduce experimental results. Four different eukaryotic organisms were modelled : budding yeast, fission yeast, Xenopus embryos, and mammalian cells. For each of these organisms, a set of parameters is provided. By changing parameter sets, one can activate or deactivate some modules, fine tune some mechanisms, in order to reproduce the behaviour of the cell cycle in the chosen organism.

We analyse here only the model describing mammalian cells. This model uses twelve variables (eleven of them being concentrations of proteins, and one being the mass of the cell) and forty reactions. We briefly discuss the steps of the algorithm applied to this model.

Choice of the hybrid scheme. Five of these reactions are typically switch-like, following Goldbeter-Koshland kinetics, defined as follows :

$$GK(v_1, v_2, J_1, J_2) = \frac{2v_1J_2}{B + \sqrt{B^2 - 4(v_2 - v_1)v_1J_2}}, \quad (1.6.3)$$

with $B = v_2 - v_1 + J_1v_2 + J_2v_1$.

These kinetics describe a steady-state solution for a 2-state biological system, meaning that this reaction will have two basic modes : active or inactive. These reactions are replaced by switched reactions whose rates are simplified monomial rates multiplied by a boolean variable.

For instance the reaction that produces Cyclin-B, induced by the cell mass, has the following kinetic rate :

$$R = k_{sb} [Mass] GK(k_{afb} [CycB], k_{ifb}, J_{afb}, J_{ifb}) \quad (1.6.4)$$

In this case we replace the Goldbeter-Koshland (GK) function by a step function and obtain the following simpler rate :

$$R' = k' [Mass] s, \quad (1.6.5)$$

where s is a boolean variable.

We apply the same method for all the five GK reactions of the model. The original and hybridized reaction rates can be find in the Table 2.1 at the end of this chapter.

Another set of reactions we want to modify in this model are Michaelis-Menten (MM) reactions. We want to reproduce the two functioning modes of Michaelis-Menten kinetics, namely the linear and the saturated behaviour. The linear behaviour is observed when the substrate is in low supply. In this case, the flux of the MM reaction will be linear with respect to the substrate supply. The saturated behaviour is observed when the substrate supply is in excess, and produce a constant flux. Our goal is to obtain an hybrid reaction which switches between these two modes, controlled by boolean variables.

There are ten such reactions within this model. A classic MM reaction rate would be the following :

$$MM(X) = \frac{k \cdot X}{X + k_m}, \quad (1.6.6)$$

and we propose to replace it by the following reaction :

$$MM(X) = s \cdot k' + \tilde{s} \cdot k'' \cdot X, \quad (1.6.7)$$

where s is a boolean variable, and \tilde{s} is the complementary of s .

We apply this transformation to all the Michaelis-Menten reactions. The original and hybridized reaction rates can be find in the Table 2.1 at the end of this chapter.

Detection of the transitions. Static event locations follow from the positions of sharp local maxima and minima of the derivatives of the reactions rates with respect to time (these correspond to sharp local maxima and minima of the second derivatives of the species concentrations, with respect to time). We have checked numerically that in the case of GK functions, these positions are close to the solutions of the equation $v_1 = v_2$. This property follows from the sigmoidal shape of the GK regulation functions. It is indeed well known that GK sigmoidal functions have an inflection point defined by the condition $v_1 = v_2$, when the activation and inhibition input rates are equal. If the case of MM functions, these positions are close to the solutions of the equation $X = k_m$.

These findings are illustrated in Figs. 1.5,1.6. We can deduce the value of the boolean variables by checking the inequation $v_1 > v_2$ in the GK case, and $X > k_m$ in the MM case. We can observe that the change of the result of these inequations corresponds to the maximum and minimums of the derivative (Fig. 1.5 and Fig. 1.6).

The structure of the model can be used to reduce the number of boolean control variables. In the case of reactions R11,12 or R13,14,15, we can see looking at reaction rates in the Table 2.1 that the inequations controlling their behavior should be the same. Thus, we can use the same boolean variable to control these reactions. Furthermore, we found out while looking for these transitions that for some MM reactions these transitions do not occur along the limit cycle trajectories. In the case of reactions R7 and R9, the behaviour is always saturated. We chose not to represent these reactions as hybrid (switched) reactions, and represented only their saturated behaviour.

We can use these inequalities and hybrid model description to fit parameters in one of three ways :

- i) Statically, meaning that the discrete variables times series $s(t)$ will be calculated at the previous step of the algorithm and will not change during the fit. In this case one fits only the parameters describing the modes. This has the benefit of simplicity, but comes with problems. The simplification in the representation of the reactions will introduce a difference between the original and the hybrid model, and such a difference should impact on the position of transitions.

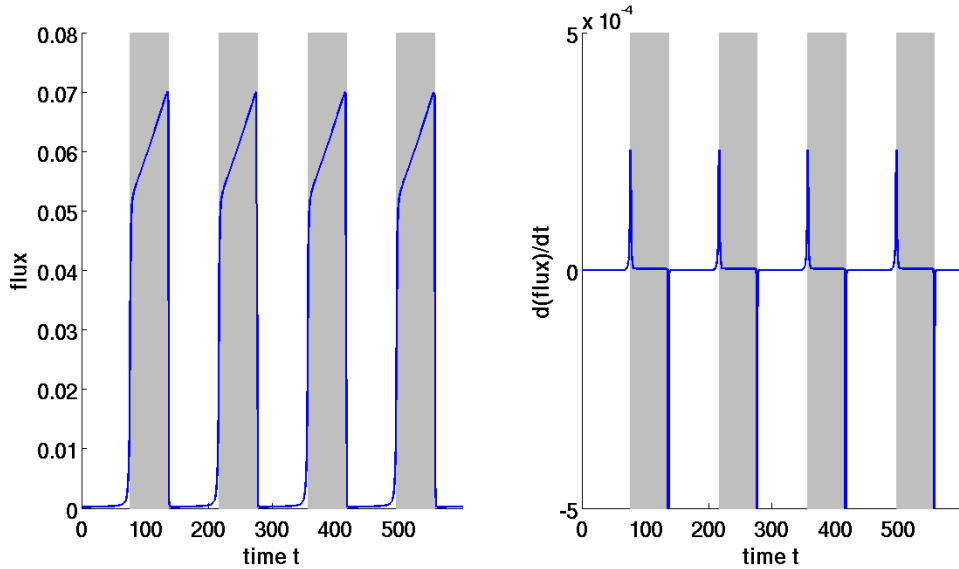


FIGURE 1.5 – Flux and derivative of the flux for the Goldbeter-Koshland reaction R4. The shaded areas correspond to value where the inequation $v_1 > v_2$ is true.

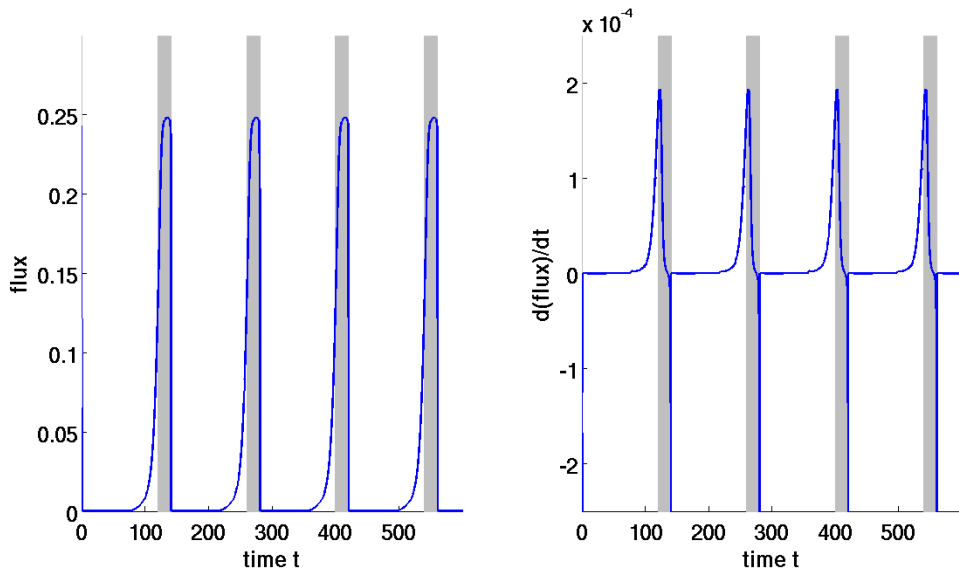


FIGURE 1.6 – Flux and derivative of the flux for the Michaelis-Menten reaction R10. The shaded areas correspond to value where the inequation $X > k_m$ is true.

- ii) Statically, but allow for modifications of the discrete variables time series $s(t)$. We could try to include the positions of these transitions in the fitting parameters, but it would increase the complexity of the cost function. It would notably be a problem to modify all transitions occurring in a single reaction accordingly, which is important for the computation of mode control parameters.
- iii) Dynamically. We could use these inequations dynamically, by evaluating them during the optimization. The transitions positions will be determined according to original model conditions applied on hybrid model trajectories. This solves the problem of adapting transitions positions of a single reaction according to each other. The problem is that the conditions from the original model must be adapted to the hybrid model, therefore all inequality parameters should be added to the fitted parameters. The problem with this addition is that these parameters are more sensitive, thus increasing the optimization difficulty.

Fitting the hybrid model parameters. Once defining the model structure and the parameters to be fitted we can apply the simulated annealing algorithm described previously. We limit the parameters search space to those involved in the hybridized reactions (a more extensive search is nevertheless possible). For the cost function, we have decided to test both species trajectories and reaction fluxes. When we limit ourselves to species trajectories, since some reactions have transitions that are close in time, there is a risk that some hybridized reaction will compensate for others. We wanted each hybridized reaction to be as much as possible a replica of the original reaction.

When using the definition with static discrete variables $s(t)$ and fitting only the mode parameters (cases i) above), we were not able to obtain even an imperfect fit of the model (in this case the trajectories of the hybrid model are very different from the ones of the original model and even become instable). We chose to include transition positions to the parameters of the fitting (case ii)), and were able to obtain a reasonable fit. However, the imperfections in the localisation of these new transition positions made difficult to find good control parameters (see next step) for all the hybridized reactions. The trajectories of the hybrid model fitted using this method are shown in Fig. 1.7. One can notice important differences between the trajectories of the hybrid and original model, although these differences remain bounded and the stability of the limit cycle oscillations is preserved.

When using the definition with the original model conditions for transitions (case iii)), we were able to obtain a working hybrid model, but the fit can still be improved by modifying slightly the mode control parameters. We can observe on Fig. 1.8 that while the dynamics of the model is preserved, there are differences in the transition positions.

Thus, when we included the parameters of transitions conditions, we obtained a model which fits better the original one. As a control we can see the results of the fitting on both the trajectories of the four main variables (Fig.1.9) and the fluxes of some hybridized reactions (Fig.1.10).

An interesting result of this optimization is that some hybridized reactions stopped having transitions, suggesting that the best fit would be obtained without these transitions. The reaction R6 (Fig. 1.11) is one of these reactions. This could be the result of the sensitivity of transition control parameters and a selection of a more robust solution.

Computing the mode control parameters. If we chose the static method of representing transitions during the fit, we now have to determine a regulation matrix, which will allow a dynamic definition of the events location. This is a problem of linear programming, and is solved using simplex algorithm [31] variation implemented in Matlab.

At this step, it is interesting to note that we have some choice about which variable can control reactions. This potentially leads to multiple solutions of the inequations. The

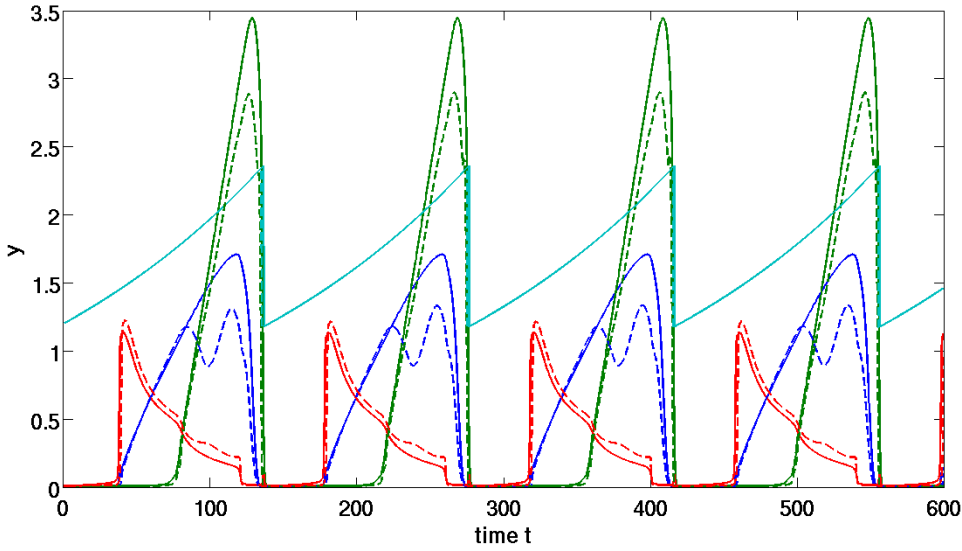


FIGURE 1.7 – Comparison of the trajectories of the four main variables. (blue : Cyclin-A, green : Cyclin-B, red : Cyclin-C, aqua : cell size) (Plain lines) Original model (Dashed lines) Hybrid model without mode control parameters fitting (case ii)).

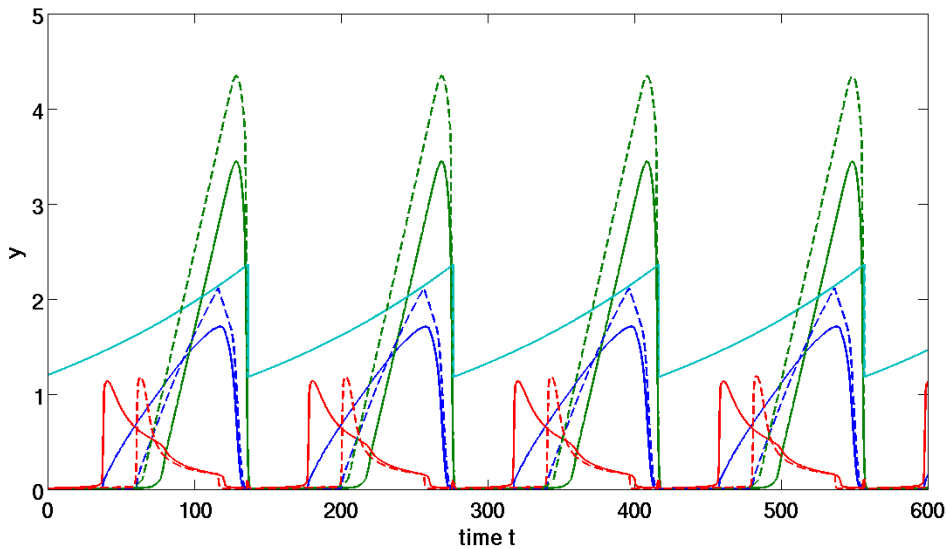


FIGURE 1.8 – Comparison of the trajectories of the four main variables. (blue : Cyclin-A, green : Cyclin-B, red : Cyclin-C, aqua : cell size) (Plain lines) Original model (Dashed lines) Hybrid model without mode control parameters fitting (case iii)).

best choice would be here to use the biological knowledge to choose the species actually involved in the reaction.

The problem with this step is that its success depends on the quality of transition positions used during the fitting of the hybrid model parameters. In order to solve these inequations, all transitions positions must respect the periodicity. The fact that some

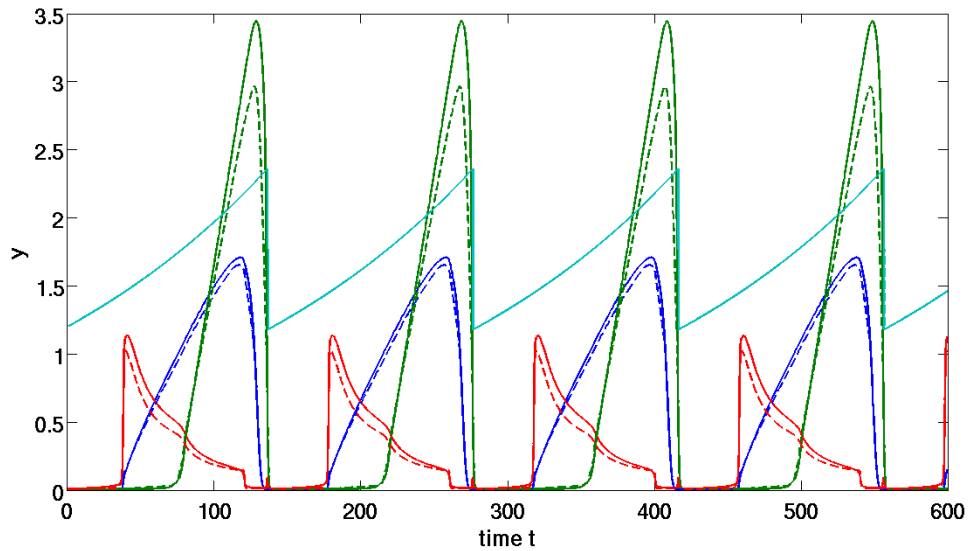


FIGURE 1.9 – Comparison of the trajectories of the four main variables. (blue : Cyclin-A, green : Cyclin-B, red : Cyclin-C, aqua : cell size) (Plain lines) Original model (Dashed lines) Hybrid model with mode control parameters fitting (case iii)W.

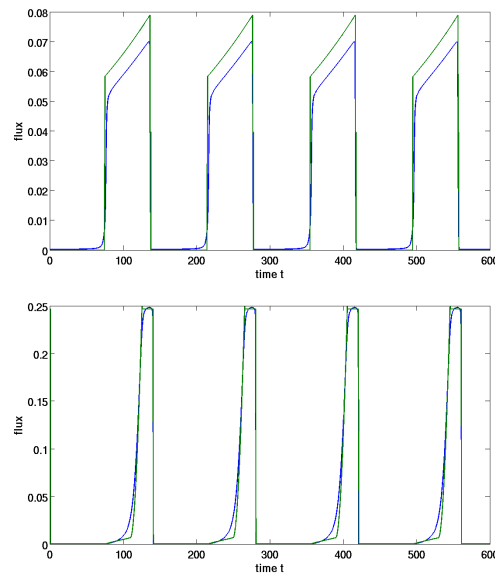


FIGURE 1.10 – Comparison of original and hybridized reaction fluxes. Top : GK Reaction R4. Bottom : MM Reaction R10. Blue : flux of original reaction, Green : flux of hybridised reaction

transitions could occur too soon, and too early in the same timeseries means that solving all these inequations is impossible.

To cope with this issue, we introduced a variable ϵ so that the inequality 1.4.1 is modified to :

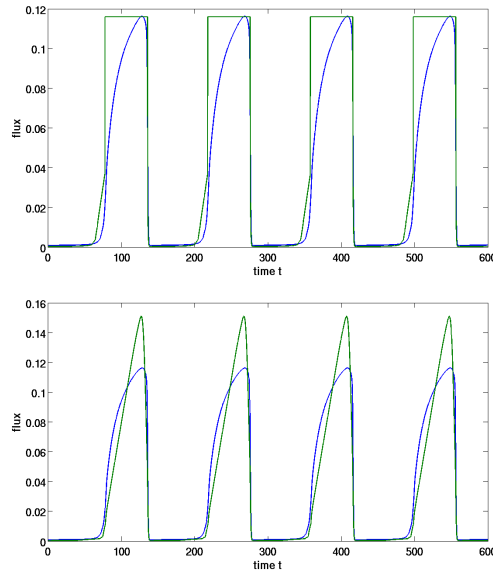


FIGURE 1.11 – Comparison of reaction R6 results without and with the fitting of transition control parameters. Top : Fit without control parameters. Bottom : Fit with control parameters. Blue : flux of original reaction, Green : flux of hybridized reaction

$$\sum_{(m,j) \in E^r} w_{mj} u_j^{modes*}(t_l) - h_j s_k^m + \epsilon_m > 0, \text{ for all } t_l \in I_k, \quad (1.6.8)$$

This modification enables us to solve all the inequations, and gives us a good metric to asses the quality of the resolution. Furthermore, the parameter ϵ particularly can be used within the simplex algorithm to be minimized. The ideal case is when ϵ is negative or zero, which means that we do not have the periodicity issue. When simulating the hybrid model, we found out that without a null or negative epsilon, the model is most of the time unstable.

Periodicity is not the only difficulty for this step. In our formalism, the threshold to modify the boolean variables controlling a given reaction is the same for an activation or an inactivation. This could also be a problem, as we can not always enforce such a condition during the fitting. There are different solutions to this problem. The first one would be to have different thresholds for reaction activation and inactivation, but this choice misses the simplicity of the method of control which is achievable by other means. More precisely, even activation and inactivation thresholds correspond geometrically to control of the modes by manifold crossing (activation when crossing takes place in one direction, inactivation for crossing in the opposite direction), whereas different thresholds do not allow for such a simple picture.

The other solution would be not to limit ourselves to the biologically relevant variables to control these transitions. As we increase the number of variables, the probability to find a combination which satisfies the inequations increases. The problem with this choice is the large number of possible combinations. We used a genetic algorithm which selects the variables which had the lowest ϵ value and were able to find combinations which satisfy the inequations for some reactions. But for others reaction, especially Michaelis-Menten reactions, even with all variables, we were not able to obtain low enough ϵ . We were able to use this method to build an hybrid model which only hybridized the Goldbeter-Koshland

reactions. The result can be seen in Fig. 1.12.

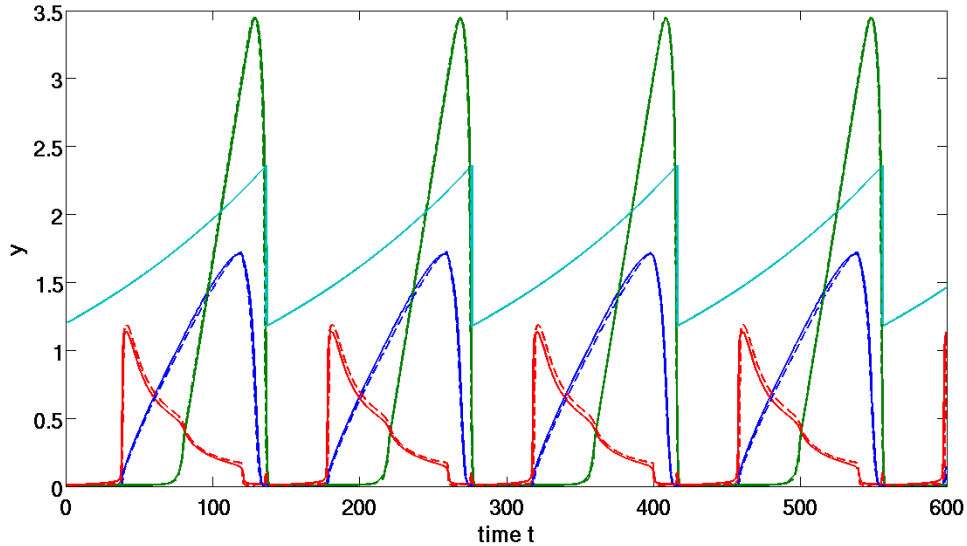


FIGURE 1.12 – Comparison of the trajectories of the four main variables. (blue : Cyclin-A, green : Cyclin-B, red : Cyclin-C, aqua : cell size) (Plain lines) Original model (Dashed lines) Hybrid model with mode control parameters fitting.

1.7 Conclusion

The results that we present are a proof of principle that piecewise smooth hybrid models can be constructed with a simple heuristic from basic information about biochemical interactions. Using this class of hybrid models instead of piecewise-linear approximations provides, in many situations, a better balance between discrete and smooth interactions. The identification algorithm proposed in the paper combines the static location of the events, the identification of the modes by simulated annealing, and the identification of the mode control parameters by dynamic location. The hardest step of this algorithm is the simulated annealing. Furthermore, for large models, we expect several solutions for the mode control parameters. We are currently improving the algorithm to cope with these situations. A better choice of the modes dictated by model reduction techniques could reduce the time for simulated annealing. Also, we are investigating the use of event location functions that are linear in the logarithms of the continuous variables. According to the ideas of the introduction, these nonlinear location functions will indicate changes of the dominant monomials in the rate functions, more accurately than the linear location functions. Moreover, they can be obtained directly from the initial smooth model without the need to solve (eventually undetermined) dynamic location inequations. Improved segmentation techniques are needed for future application of the algorithm directly to data.

In the future we will apply the heuristic and the fitting algorithm to model complex situations when signaling pathways interact with the eucaryotic cell cycle. The resulting hybrid models will also be used to investigate emerging properties of regulatory networks such as viability and robustness.

Tables

Table 2.1 - Definition of reactions in the original and hybridized mammalian cell cycle model. The inequalities controlling the mode switching result directly from the definition of the reaction rates in the original model.

reaction smooth	variables	reaction hybrid	control
$R_1 = ksa_{pp}.[Mass].GK(v_1, v_2, Jatf, Jitf)$	$v_1 = katf_p + katfa_{pp}.[CycA] + katfd_{pp}.CycD0.[Mass]$ $v_2 = kitf_p + kitfa_{pp}.[CycA] + kitfb_{pp}.[CycB]$	$R_{1h} = ksa_{pp}.[Mass].s_1$	$s_1 = v_1 > v_2$
$R_2 = k25_{pp}.[pB].GK(v_1, v_2, Ja25, Ji25)$	$v_1 = ka25_p + ka25_{pp}.[CycE]$ $v_2 = ki25_p + ki25_{pp}.[Cdc20A]$	$R_{2h} = k25_{pp}.[pB].s_2$	$s_2 = v_1 > v_2$
$R_3 = kwhee_{pp}.[CycB].GK(v_1, v_2, Jawee, Jiwee)$	$v_1 = kawee_p + kawee_{pp}.[Cdc20A]$ $v_2 = kiwhee_p + kiwhee_{pp}.[CycB]$	$R_{3h} = kwhee_{pp}.[CycB].s_3$	$s_3 = v_1 > v_2$
$R_4 = ksb_{pp}.[Mass].GK(v_1, v_2, Jafb, Jifb)$	$v_1 = kafb.[CycB]$ $v_2 = kfib$	$R_{4h} = ksb_{pp}.[Mass].s_4$	$s_4 = v_1 > v_2$
$R_5 = kse_{pp}.[Mass].GK(v_1, v_2, Jatf, Jitf)$	$v_1 = katf_p + katfa_{pp}.[CycA] + katfd_{pp}.CycD0.[Mass]$ $v_2 = kitf_p + kitfa_{pp}.[CycA] + kitfb_{pp}.[CycB]$	$R_{5h} = kse_{pp}.[Mass].s_1$	$s_1 = v_1 > v_2$
$R_6 = ks20_{pp}.X/(K_m + X)$	$X = [CycB]$ $K_m = J20$	$R_{6h} = ks20_{pp}.s_5$ $+ks20_{pp2}.\tilde{s}_5.X$	$s_5 = X > K_m$
$R_7 = kiae.[CycB].X/(K_m + X)$	$X = (APCT - [APCP])$ $K_m = Jaie$	$R_{7h} = ks20_{pp}.[CycB]$	
$R_8 = kiie.X/(K_m + X)$	$X = [APCP]$ $K_m = Jiie$	$R_{8h} = kiie.s_6$ $+kiie2 * \tilde{s}_6.X$	$s_6 = X > K_m$
$R_9 = ka20.[APCP].X/(K_m + X)$	$X = [Cdc20i]$ $K_m = Ja20$	$R_{9h} = ka20.[APCP]$	
$R_{10} = ki20.X/(K_m + X)$	$X = [Cdc20A]$ $K_m = Ji20$	$R_{10h} = ki20.s_7$ $+ki202.\tilde{s}_7.X$	$s_7 = X > K_m$
$R_{11} = kah1_p.X/(K_m + X)$	$X = (Cdh1T - [Cdh1])$ $K_m = Jah1$	$R_{11h} = kah1_p.s_8$ $+kah1_{p2}.\tilde{s}_8.X$	$s_8 = X > K_m$
$R_{12} = kah1_{pp}.[Cdc20A].X/(K_m + X)$	$X = (Cdh1T - [Cdh1])$ $K_m = Jah1$	$R_{12h} = kah1_{pp}.[Cdc20A].s_8$ $+kah1_{pp2}.[Cdc20A].\tilde{s}_8.X$	$s_8 = X > K_m$
$R_{13} = kih1a_{pp}.[CycA].X/(K_m + X)$	$X = [Cdh1]$ $K_m = Jih1$	$R_{13h} = kih1a_{pp}.[CycA].s_9$ $+kih1a_{pp2}.[CycA].\tilde{s}_9.X$	$s_9 = X > K_m$
$R_{14} = kih1b_{pp}.[CycB].X/(K_m + X)$	$X = [Cdh1]$ $K_m = Jih1$	$R_{14h} = kih1b_{pp}.[CycB].s_9$ $+kih1b_{pp2}.[CycB].\tilde{s}_9.X$	$s_9 = X > K_m$
$R_{15} = kih1e_{pp}.[CycE].X/(K_m + X)$	$X = [Cdh1]$ $K_m = Jih1$	$R_{15h} = kih1e_{pp}.[CycE].s_9$ $+kih1e_{pp2}.[CycE].\tilde{s}_9.X$	$s_9 = X > K_m$

Table 2.2 - Parameters of the hybridized mammalian cell cycle model described in the table 2.1.

constant	value
ksa_{pp}	0.024635
$katf_p$	0
$katfa_{pp}$	0.00090318
$katfd_{pp}$	2.6897

$katfe_{pp}$	2.1407
$kitf_p$	0.22282
$kitfa_{pp}$	0
$kitfb_{pp}$	0.14253
$k25_{pp}$	3.559
$ka25_p$	0
$ka25_{pp}$	21.93
$ki25_p$	5.425
$ki25_{pp}$	0
$kwee_{pp}$	0.096009
$kawee_p$	3.5714
$kawee_{pp}$	0
$kiwee_p$	0
$kiwee_{pp}$	9.003
ksb_{pp}	0.033299
$kafb$	0.15998
$kifb$	0.0056319
kse_{pp}	0.14842
$ks20_{pp}$	0
$ks20_{pp2}$	0.048074
$J20$	3
$kaie$	0.076693
$kiie$	0.1685
$kiie2$	17.568
$Jiie$	0.0096156
$ka20$	0.4815
$ki20$	0.24271
$ki202$	5.3118
$Ji20$	0.045084
$kah1_p$	0
$kah1_{p2}$	0.15387
$kah1_{pp}$	0
$kah1_{pp2}$	3.9768
$Jah1$	1
$kih1a_{pp}$	0.099851
$kih1a_{pp2}$	2.5689
$kih1b_{pp}$	0
$kih1b_{pp2}$	14.966
$kih1e_{pp}$	0.10502
$kih1e_{pp2}$	1.7755
$Jih1$	0.12035

Table 2.3 - Definition of reactions in the original and hybridized mammalian cell cycle model. The inequalities controlling the mode switching result from the computation of mode control parameters post-fitting.

reaction smooth	variables	reaction hybrid
$R_1 = ksa_{pp} \cdot [Mass].GK(v_1, v_2, Jatf, Jitf)$	$v_1 = katf_p + katfa_{pp} \cdot [CycA] + katfd_{pp} \cdot CycD0 \cdot [Mass]$ $v_2 = kitf_p + kitfa_{pp} \cdot [CycA] + kitfb_{pp} \cdot [CycB]$	$R_{1h} = ksa_{pp} \cdot [Mass].s_1$

$R_2 = k25_{pp} \cdot [pB]$	$v_1 = ka25_p + ka25_{pp} \cdot [CycE]$	$R_{2h} = k25_{pp} \cdot [pB] \cdot s_2$
. $GK(v_1, v_2, Ja25, Ji25)$	$v_2 = ki25_p + ki25_{pp} \cdot [Cdc20A]$	
$R_3 = kw_{ee_{pp}} \cdot [CycB]$	$v_1 = kaw_{ee_p} + kaw_{ee_{pp}} \cdot [Cdc20A]$	$R_{3h} = kw_{ee_{pp}} \cdot [CycB] \cdot s_3$
. $GK(v_1, v_2, Jawee, Jiwee)$	$v_2 = kiw_{ee_p} + kiw_{ee_{pp}} \cdot [CycB]$	
$R_4 = ks_{bp} \cdot [Mass]$	$v_1 = kaf_b \cdot [CycB]$	$R_{4h} = ks_{bp} \cdot [Mass] \cdot s_4$
. $GK(v_1, v_2, Jaf_b, Jif_b)$	$v_2 = kif_b$	
$R_5 = ks_{ep} \cdot [Mass]$	$v_1 = kat_f_p + katfa_{pp} \cdot [CycA] +$	$R_{5h} = ks_{ep} \cdot [Mass] \cdot s_1$
. $GK(v_1, v_2, Jat_f, Jit_f)$	$+ katfd_{pp} \cdot CycD0 \cdot [Mass]$	
	$v_2 = kit_f_p + kitfa_{pp} \cdot$	
	$[CycA] + kitfb_{pp} \cdot [CycB]$	

control	value
s_1	$w_{1,1} \cdot [CycA] + w_{1,2} \cdot [CycB] + w_{1,4} \cdot [APCP] + w_{1,6} \cdot [Cdc20i] + w_{1,7} \cdot [Cdh1] + w_{1,8} \cdot [CKI] + w_{1,9} \cdot [Mass] - 1 > 0$
s_2	$w_{2,3} \cdot [CycE] + w_{2,9} \cdot [Mass] + w_{2,12} \cdot [TriE] - 1 > 0$
s_3	$w_{3,3} \cdot [CycE] + w_{3,9} \cdot [Mass] + w_{3,12} \cdot [TriE] - 1 > 0$
s_4	$w_{2,2} \cdot [CycB] + w_{2,9} \cdot [Mass] + w_{2,10} \cdot [pB] - 1 > 0$

Table 2.4 - Parameters of the hybridized mammalian cell cycle model described in the table 2.3.

constant	value
ksa_{pp}	0.024064
kse_{pp}	0.18569
$kw_{ee_{pp}}$	0.17326
$k25_{pp}$	3.5168
ks_{bp}	0.030148
$w_{1,1}$	1.e+9
$w_{1,2}$	0.4352e+9
$w_{1,4}$	-1.5677e+9
$w_{1,6}$	-4.0592e+9
$w_{1,7}$	1.e+9
$w_{1,8}$	-0.7937e+9
$w_{1,9}$	0.1138e+9
$w_{2,3}$	-2.218e+9
$w_{2,9}$	1.e+9
$w_{2,12}$	-10.027e+9
$w_{3,3}$	0.2278e+9
$w_{3,9}$	-0.1015e+9
$w_{3,12}$	1.e+9
$w_{4,2}$	0.2294e+9
$w_{4,9}$	-0.0294e+9
$w_{4,10}$	1e+9

Chapitre 2

Model reduction for computational biology models

2.1 Introduction

During the last decades, biologists have identified a wealth of molecular components and regulatory mechanisms underlying the control of cell functions. Cells integrate external signals through sophisticated signal transduction pathways, ultimately affecting the regulation of gene expression, including that of the signaling components. Metabolic functions are sustained and controlled by complex machineries involving genes, enzymes and metabolites. The genetic regulations result from the coordinate effect of many, mutually interacting genes. These regulations involve many molecular actors, including proteins and regulatory RNAs, which form large, intricate networks.

Current dynamical models of cellular molecular processes are small size networks. These small scale models, that are subjective simplifications of reality, can not take into account the specificities of regulatory mechanisms. New methods are needed, allowing to reconcile small scale dynamical models and large scale, but static, network architectures. The main obstacle to increasing the size of dynamical networks is the incomplete information, on the parameters and on the mechanistic details of the interactions. *In vivo* values of the parameters depend on crowding and heterogeneity of the intracellular medium, and can be orders of magnitude different from what is measured *in vitro*. Furthermore, learning models from data suffer for non-identifiability and over-fitting problems. Thus, model reduction is an unavoidable step in the study of large networks, allowing to extract the essential features of the model, that can then be identified from data. Model reduction in computational biology should have several features.

First of all, model reduction should cope with parametric incompleteness and/or uncertainty.

A certain class of reduction methods are parameter independent and automatically comply with this specificity. In biochemical networks, the number of possible chemical species grows combinatorially due to numerous possibilities of interactions between molecules with multiple interaction sites. The exact lumping methods [15, 25] reduce the number of microstates and avoid combinatorial explosion in the description and analysis of large models of receptor and scaffold signalling. A similar technique [37] is used to rationally organize supramolecular complexes in rule-based modeling [29] of biochemical networks. Other, parameter independent, coarse-graining techniques are graphical methods formalizing node deletion and merging operations in biochemical networks [42], pooling of metabolites in large scale metabolic networks [106, 72], or extensive searches in the set of

all possible lumps [34]. Finally, qualitative reduction methods were used to simplify large logical regulatory graphs, adequately suppressing nodes and defining sub-approximating dynamics [99, 100].

Secondly, biochemical processes governing network dynamics span over many timescales. For example, changing gene expression programs can take hours and even days while protein complex formation goes on the second scale and post-translational protein modifications take minutes to happen. Protein life half-times can vary from minutes to days. Model reduction can strongly benefit from the network multiscaleness. Asymptotic dynamics of networks with slow and fast processes, can be strongly simplified using various ideas such as inertial and invariant manifolds (IM) and averaging approximations.

The iterative methods of IM aim to find a slow low dimensional IM, containing the asymptotic dynamics [51, 52, 116]. The Computational Singular Perturbation (CSP) [80, 19] aims to find even more, the slow IM and, in addition, the geometry of its fast foliation. Invariant manifolds can be calculated by various other methods [53, 55, 116, 74, 77].

Very popular are the methods for computation of “first approximations” to the slow IM. The classical quasi steady-state approximation (QSS) was proposed by [13] and was elaborated into an important tool for analysis of chemical reaction mechanism and kinetics [123, 20, 66]. The classical QSS is based on the relative smallness of concentrations of some of active reagents (radicals, concentration of enzyme and substrate-enzyme complexes, or amount of active centers on the catalyst surface) [6, 122, 148]. The quasi-equilibrium approximation (QE) has two basic formulations : the thermodynamic approach, based on conditional entropy maximum (or free energy conditional minimum), or the kinetic formulation, based on equilibration of fast reversible reactions. The very first use of the entropy maximum dates back to Gibbs [43]. Corrections to QE approximation with applications to physical and chemical kinetics were developed by [54, 53]. An important, still unsolved, problem of these two approximations is the detection of QSS species and QE reactions without application of all machinery of the IM or CSP methods. Indeed, not all reactions with large constants are at quasi-equilibrium, and there are no simple rules to find QSS species if there is no such hints as a small amount of a conserved quantity (like the total concentration of enzyme). The method of Intrinsic Low Dimensional Manifolds (ILDM) [89, 18] provides an approximation of a low dimensional invariant manifold and works as a first step of CSP [73].

Another method allowing to simplify multiscale dynamics is averaging. This idea can be tracked back to Poincaré’s perturbative treatment of the many body problem in celestial mechanics [107], further developed in classical mechanics by other authors [7, 88], and also known as adiabatic or Born-Oppenheimer approximation in quantum mechanics [94]. Rather generally, averaging can be applied when some fine scale variables of the system are rapidly oscillating. Then, the dynamics of slow, coarse scale variables, can be obtained by time averaging the system over a timescale much larger than the period of the fast oscillations. The way to perform averaging, depends on the structure of the system, namely on the definition of the coarse grained and fine variables [14, 8, 3, 121, 2, 47, 127].

Some of these ideas have been implemented in computational biology tools. Systems biology markup language SBML [70] can allocate a “fast” attribute to reaction elements. Fast reaction specification can be taken into account by computational biology softwares such as VirtualCell [129] that implements a QE approximation algorithm [128]. Similarly, the simulation tool COPASI [69] implements the ILDM method [135].

Finally, multiscaleness does not uniquely apply to timescales, but equivalently to abundances of various species in these networks. mRNA copy numbers can change from some units to tens of thousands, and the dynamic concentration range of biological proteins can

reach up to five orders of magnitude. Furthermore, the DNA molecule has only one or a few copies. Low copy numbers lead, directly or indirectly (a species can be stochastic even if present in large copy numbers), to stochastic gene expression. In computational biology, model reduction should thus cope not only with deterministic, but also with stochastic and hybrid models. The need to reduce large scale stochastic models is acute. Indeed, stochastic simulation algorithm (SSA, [44, 45]) can be very expensive in computer time when applied to large unreduced models, precluding model analysis and identification. For this reason, extensive effort has been dedicated to adapting the main ideas used for model reduction of deterministic models, namely exact lumping, invariant manifolds, QSS, QE, and averaging, to the case of stochastic models.

Reduction of stochastic rule-based models, based on a weakened version of the exact lumpability criterion, has been proposed by [38] to define abstract species or stochastic-fragments that can be further used in simplified calculations. More generally, rule-based models allow to overcome combinatorial complexity in stochastic simulations [30]. The performance of rule-based stochastic simulators such as NFSim [130] scales independently of the reaction network size. Yet NFSim still suffers from the size of the population (number of molecules) and the choice of data-structures forbids in this case approximations such as tau-leaping. Approximate reduction of the number of states of the Markov chains describing stochastic networks were proposed in [98].

Multiscaleness of stochastic networks is two-fold, it affects both species and reaction rates. This has been exploited in hybrid stochastic simulation schemes that are, for the most of them, based on a partition of the biochemical reactions in fast and slow reactions [64, 17, 5, 65, 4, 117, 75, 63, 134, 118, 60, 11, 83, 50, 105]. Conversely, mixed partitions, using both reactions and species can exploit both types of multiscaleness and more appropriately unravel a rich variety of stochastic functioning regimes such as piece-wise deterministic, switched diffusions, diffusions with jumps, as well as averaged processes [114, 27, 26] only partially covered by some situations discussed in [91].

Machine learning approaches to parameter identification [49] could profit from Fokker-Planck approximations, also known as diffusion approximations or Langevin approach, of the master equation describing dynamics of stochastic networks. Traditional approaches such as central limit theorem [46, 93], the Ω and the Kramers-Moyal expansions [114, 27] were used to derive diffusion approximations. Alternatively, [36] propose diffusion approximations for slow/fast stochastic networks, in which the drift and diffusion parameters were obtained numerically. More recently, these parameters were derived directly from the master equation of stochastic networks with species in small and large copy numbers [113]. Furthermore, by the ergodic theorem, time averaging of multiscale stochastic models boils down to a QE assumption for the fast variables. This idea has been used in [27] to reduce stochastic networks. A few computational biology tools implement stochastic approximations [118].

With the exception of the parameter independent methods, all the model reduction methods described above need a full parametrization of the model. This is a stringent requirement, and can not be easily bypassed. Indeed, the reduction has a local validity. The elements defining a reduced model such as IM, QSS species, QE species, depend on the model parameters and also on the position in phase space and along trajectories. What one can expect is that model reduction is robust, i.e. a given reduced model provides an accurate approximation of the dynamics of the initial model for a wide range of parameters and variables values. One can show that this property is satisfied by biochemical networks with separated constants, because in this case the simplified networks depend on the order relations among model parameters and not on the precise values of these parameters

[56, 112, 103].

In this chapter we will revisit the fundamental concepts of model reduction in the light of a new framework, that should, in the long term, lead to a new generation of reduction tools satisfying all the specific requirements of computational biology. This framework is based on tropical analysis ideas.

2.2 Deterministic dynamical networks

To construct a dynamic reaction network we need the list of components, $\mathcal{A} = \{A_1, \dots, A_n\}$ and the list of reactions (the reaction mechanism) :

$$\sum_i \alpha_{ji} A_i \rightleftharpoons \sum_k \beta_{jk} A_k, \quad (2.2.1)$$

where $j \in [1, r]$ is the reaction number.

Dynamics of nonlinear networks in homogeneous isochoric systems (fixed volume) is described by a system of differential equations :

$$\frac{dc}{dt} = \mathbf{P}(c) = \sum_{j=1}^r \boldsymbol{\nu}_j (R_j^+(c) - R_j^-(c)). \quad (2.2.2)$$

Here, $c \in \mathbb{R}^n$ is the concentration vector, and $\mathbf{P}(c)$ is a vector field on the space of concentrations. For each reaction j , $\boldsymbol{\nu}_j = \boldsymbol{\beta}_j - \boldsymbol{\alpha}_j$ is the global stoichiometric vector. The reaction rates $R_j^{+/-}(c)$ are non-linear functions of the concentrations. For instance, the mass action law reads $R_j^+(c) = k_j^+ \prod_i c_i^{\alpha_{ji}}$, $R_j^-(c) = k_j^- \prod_i c_i^{\beta_{ji}}$, in which case the component i of the vector field, $P_i(c)$, is a multivariate polynomial on the concentrations c_j .

2.3 Multi-scale reduction of monomolecular reaction networks

Monomolecular reaction networks are the simplest reaction networks. The structure of these networks is completely defined by a digraph, in which vertices correspond to chemical species A_i , edges correspond to reactions $A_i \rightarrow A_j$ with kinetic constants $k_{ji} > 0$.

The kinetic equation is

$$\frac{dc_i}{dt} = \sum_j k_{ij} c_j - \left(\sum_j k_{ji} \right) c_i, \quad i \in [1, n], \quad (2.3.1)$$

or in matrix form : $\dot{c} = \mathbf{K}c$.

The solutions of (2.3.1) can be expressed in terms of left and right eigenvectors of the kinetic matrix \mathbf{K} :

$$c(t) = \sum_{k=0}^{n-1} \mathbf{r}^k < \mathbf{l}^k, c(0) > \exp(-\lambda_k t), \quad (2.3.2)$$

where $\mathbf{K}\mathbf{r}^k = \lambda_k \mathbf{r}^k$, and $\mathbf{l}^k \mathbf{K} = \lambda_k \mathbf{l}^k$. The zero-th eigenvalue $\lambda_0 = 0$ corresponds to the total mass conservation ($\mathbf{l}^0 = (1, 1, \dots, 1)$).

Each eigenvalue λ_k , $k > 0$ is the inverse of a timescale of the network. A reduced network having solutions of the type (2.3.2), with eigenvectors \mathbf{r}^k , \mathbf{l}^k , and eigenvalues

λ_k approximating the eigenvectors and the eigenvalues of the original network is called a *multiscale approximation*.

We say that the network constants are totally separated if for all $(i, j) \neq (i', j')$ one of the relations $k_{ji} << k_{j'i'}$, or $k_{ji} >> k_{j'i'}$ is satisfied.

It was shown in [56, 112, 58] that monomolecular reaction networks with totally separated constants can be reduced to acyclic and deterministic digraphs while preserving the multi-scale dynamics. Let us recall that a deterministic digraph is a digraph without branchings, ie a forest of lassos. An acyclic deterministic digraph is simply a forest. The proof of this property uses the fact that not only rates constants, but also monomials rate constants have to be separated. This is true generically for independent, uniformly distributed random constants (see [56]).

In order to reduce a network with total separation, one needs only qualitative information on the constants. More precisely, each edge of the reaction digraph can be labeled by a positive integer representing the rank of the reaction parameter in the ordered series of parameter values, the largest parameter (the quickest reaction) having the lowest label. These integer labels also indicate the timescales of the processes modeled by the network reactions.

The reduced network is not always a subgraph of the initial graph. It is obtained from this integer labeled digraph by graph re-writing operations, that can be generically described as pruning and pooling. Two types of pruning operations are of primary importance (see also Figure 2.1) :

Rule a) If one has one node from which leave more than one edge, then all the edges are pruned with the exception of the fastest one (lowest integer label). This operation corresponds to keeping the dominant term among the terms $c_i k_{ij}$ consuming a species A_i , and reduces the node outdegree to one. The same principle can not be applied to reduce the indegree, because which production term is dominant among $k_{ij} c_j$, $j \in [1, n]$, depends not only on k_{ij} but also on the concentrations c_j .

Rule b) Cycles with separated constants can be transformed into chains, by elimination of the slowest step. This can be justified intuitively by topology, because any two nodes of a cycle are connected by two paths, one containing the slowest step and the other one not containing the slowest step. The latter shortcuts the former.

However, a combination of rules a) and b) is not allowed to prune slow reactions leaving a cycle and further transform the cycle into a chain by eliminating the limiting step. Indeed, the total mass of such cycles is slowly decaying because of outgoing reactions. Pruning the slow reactions that leave a cycle would keep the total cycle mass constant and produce the wrong long time approximation. In this case, pooling operations are needed :

Rule c) Glue each cycle in the pruned system into a new vertex and transform the network of *all initial reactions* into a new one. The concentration of this new component is the sum of the concentration of the glued vertices. Reactions to the cycles transform into reactions to the correspondent new vertices (with the same constants). To transform the reactions from the cycles, we have to calculate the normalized quasi-stationary distributions inside each cycle (with unit sum of the concentrations in each cycle). Let for the vertex A_i from a cycle this concentration be c_i° . Then the reaction $A_i \rightarrow A_j$ with the constant k_{ji} transforms into the reaction from the new (“cycle”) vertex with the constant $k_{ji} c_i^\circ$. The destination vertex of this reaction is A_j if it does not belong to a cycle of the pruned system, it is the correspondent glued cycle if it includes A_j and does not include A_i and the reaction vanishes if both A_i and A_j belong to the same cycle of the pruned system.

After pooling we have to prune (Rule a) and so on, until we get an acyclic pruned system. Then the way back follows : we have to restore cycles and cut them (Rule b).

In more detail, the graph re-writing operations, are described in the Appendix and illustrated in Figure 2.1. The dynamics of reduced acyclic deterministic digraphs follows from their topology and from the timescale labels. First of all, let us notice that the network has as many timescales as remaining edges in the reduced digraph. The computation of eigenvectors of acyclic deterministic digraphs is straightforward [56, 112, 58]. For networks with total separation, these eigenvectors satisfy, in the first approximation, a 0 – 1 type property, the coordinates of \mathbf{l}^k , \mathbf{r}^k belong to the sets $\{0, 1\}$, and $\{0, 1, -1\}$ respectively. The 0 – 1 property of eigenvectors has a non-trivial consequence. On the timescale $t_k = (\lambda_k)^{-1}$, the reduced digraph behaves as an effective reaction (single step approximation). The effective reaction receives (from reactions acting on smaller timescales) the mass coming from the species with coordinate 1 in \mathbf{l}^k (pool) and transfers it (during a time t_k) to the species with coordinate 1 in \mathbf{r}^k . The successive single step approximations of an acyclic deterministic digraph are illustrated in Figure 2.2.

Monomolecular networks with separation represent instructive examples where reduction and qualitative dynamics result from the network topology and from the orders of magnitude of the kinetic constants. This type of models can be used in computational biology to reduce linear subnetworks or even binary reactions for which one reactant is present in much larger quantities than the other (pseudo-monomolecular approximation).

As argued by a few authors, total separation could be a generic property of biochemical networks [41]. This property can be checked empirically by investigating the distribution of network timescales in logarithmic scale. Whenever one finds distributions with large support in logarithmic scale (a log-uniform distribution is equivalent to the Zipf law, i.e. a power law distribution with exponent -1 , well known in critical systems [41]) total separation is valid and the above reduction method applies.

2.4 Separation, dominance, and tropical geometry

The previously presented algorithm is based on the idea of dominance, which occurs at many levels. For instance, when several reactions compete for the same pool, all can be pruned, excepting the dominant one (Rule a)). This simple idea is widely spread, and corresponds to max-plus algebra : the sum of positive, well separated terms, can be replaced by the maximum term. Max-plus algebra, that found many applications to dynamical systems [23, 143, 9], belong to the new mathematical field of tropical geometry [104]. Tropical geometry offers convenient solutions to finding approximate roots of simultaneous polynomial equations, as well as to simplifying and hybridizing systems of polynomial or rational ordinary differential equations with separated monomials. Tropical geometry concepts can be used to rationalize many model reduction operations and find new ones.

The logarithmic transformation $u_i = \log x_i$, $1 \leq i \leq n$, well known for drawing graphs on logarithmic paper, plays a central role in tropical geometry [144].

Let us consider multivariate monomials $M(\mathbf{x}) = a_\alpha \mathbf{x}^\alpha$, where $\mathbf{x}^\alpha = x_1^{\alpha_1} x_2^{\alpha_2} \dots x_n^{\alpha_n}$. Monomials with positive coefficients $a_\alpha > 0$, become linear functions, $\log M = \log a_\alpha + \langle \alpha, \log(\mathbf{x}) \rangle$, by this transformation.

There is a straightforward way to use the logarithmic transformation from tropical geometry in order to obtain approximations of dynamical networks of the type (2.2.2). Let us suppose that reaction rates are polynomial functions of the concentrations (this is satisfied by mass action law and obviously, also by monomolecular networks), such that $\sum_{j=1}^r \nu_j (R_j^+(\mathbf{c}) - R_j^-(\mathbf{c})) = \sum_{\alpha \in A} a_\alpha \mathbf{c}^\alpha$, $A \subset \mathbb{N}^n$, and $\mathbf{c}^\alpha = c_1^{\alpha_1} \dots c_n^{\alpha_n}$.

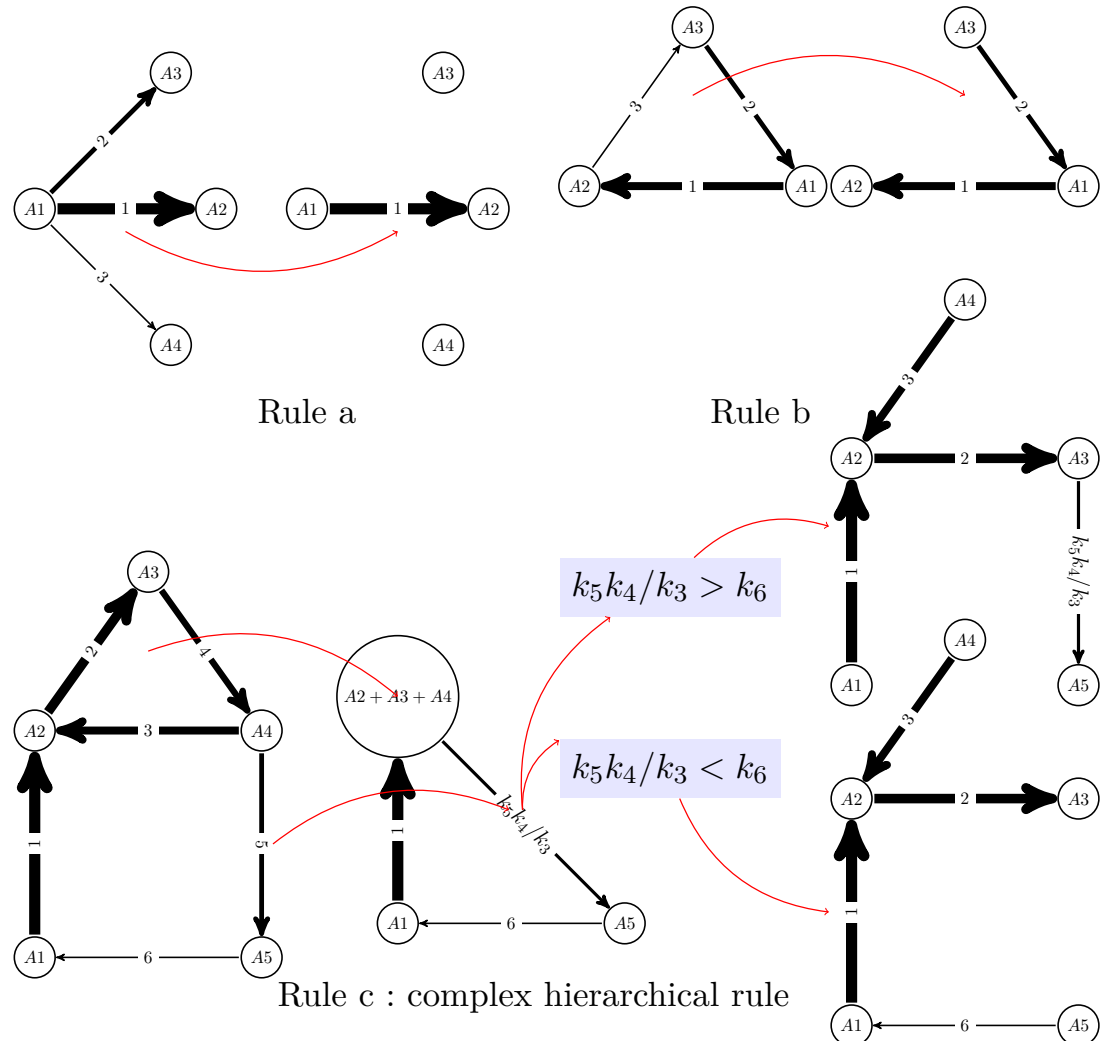


FIGURE 2.1 – A monomolecular network with total separation can be represented as a digraph with integer labels (the quickest reaction has label 1). Two simple rules allow to eliminate competition between reactions (rule a) and transform cycles into chains (rule b). Rule b can not be applied to cycles with outgoing slow reactions, in which case more complex, hierarchical rules should be applied (rule c). In the rule c, first the cycle $A_2 \rightarrow A_3 \rightarrow A_4 \rightarrow A_2$ is “glued” to a new node (pool $A_2 + A_3 + A_4$) and the constant of the slow outgoing reaction renormalized to a monomial $k_5 k_4 / k_3$. Rule b is applied to the resulting network, which is a cycle with no outgoing reactions. The comparison of the constants $k_5 k_4 / k_3$ and k_6 dictates where this cycle is cut. Finally, the glued cycle is restored, with its slowest step removed.

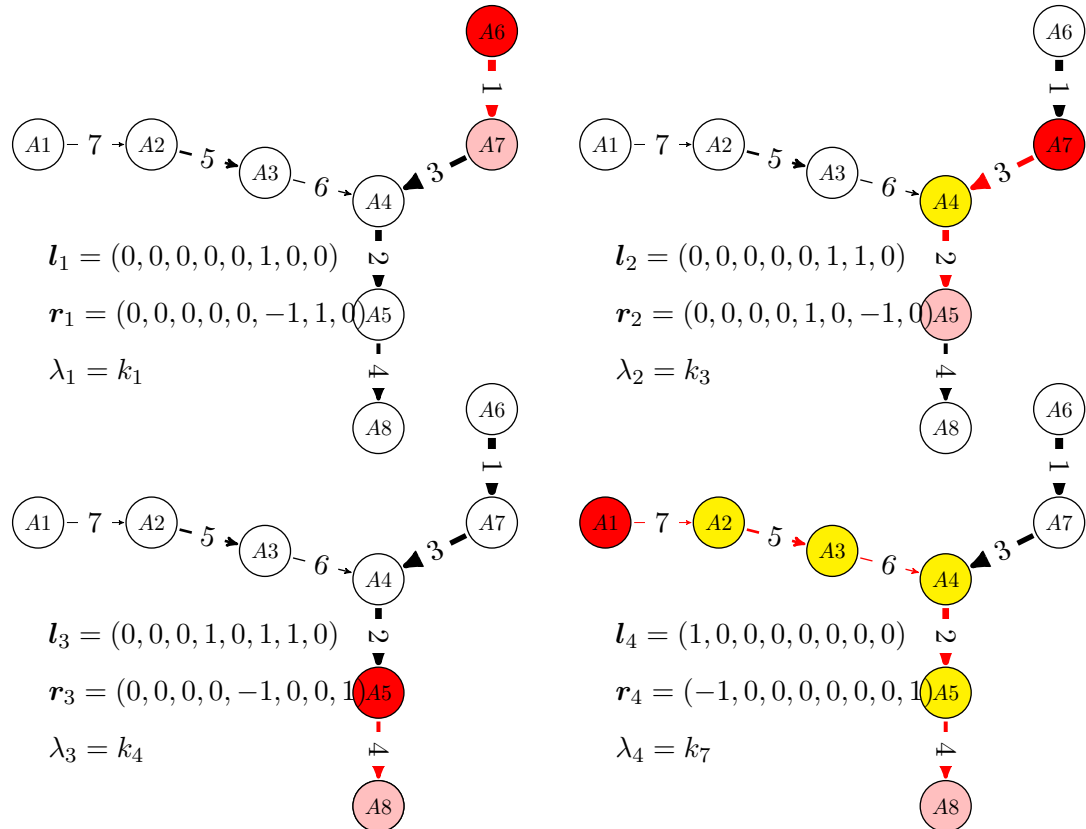


FIGURE 2.2 – For a given timescale, monomolecular networks with total separation behave as a single step : the concentrations of some species (white) are practically constant, some species (yellow) are rapid , low concentration, intermediates, one species (red) is gradually consumed and another (pink) is gradually produced. We have represented the sequence of one step approximations of a reduced, acyclic, deterministic digraph, from the quickest time-scale $t_1 = \lambda_1^{-1}$ to the slowest one $t_4 = \lambda_4^{-1}$. These one step approximations are activated when mass is introduced at $t = 0$ via the “boundary nodes” A_1 and A_6 .

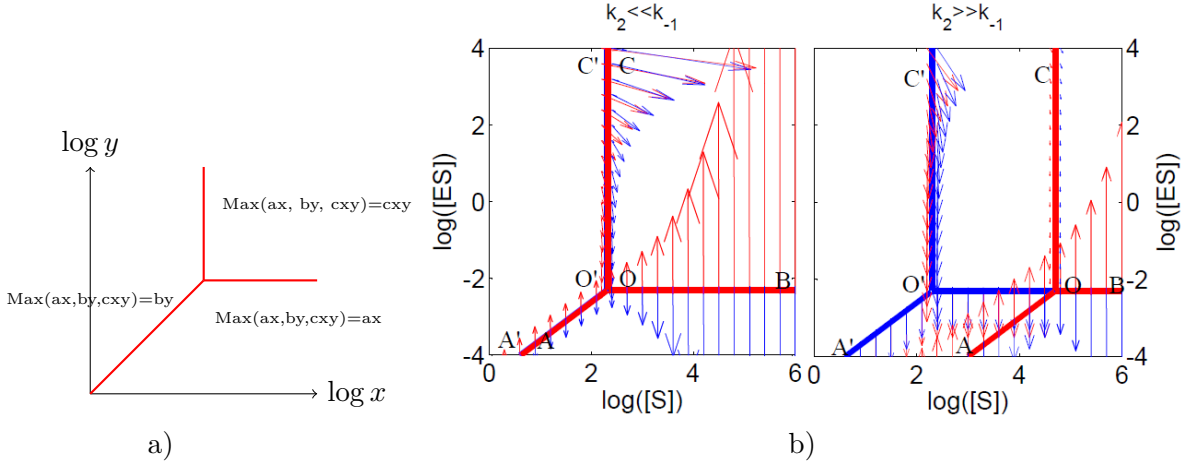


FIGURE 2.3 – a) The tropical manifold of the polynomial $ax + by + cxy$ on “logarithmic paper” is a three lines tripod. b) The tropical manifolds for the species ES (in red) and S (in blue) for the Michaelis-Menten mechanism. The tropicalized flow is also represented on both sides of the tropical manifolds (with arrows, red on one side, blue on the other side). Sliding modes correspond to blue and red arrows pointing in opposite directions.

We call tropicalization of the smooth ODE system (2.2.2) the following piecewise-smooth system :

$$\frac{dc_i}{dt} = s_i(\mathbf{c}) \exp[\max_{\alpha \in A_i} \{\log(|a_{i,\alpha}|) + \langle \log(\mathbf{c}), \boldsymbol{\alpha} \rangle\}], \quad (2.4.1)$$

where $\log(\mathbf{c}) = (\log c_1, \dots, \log c_n)$, $s_i(\mathbf{c}) = \text{sign}(a_{i,\alpha_{\max}(\mathbf{c})})$ and $a_{i,\alpha_{\max}}, \boldsymbol{\alpha}_{\max} \in A_i$ denotes the coefficient of a monomial for which the maximum occurring in (2.4.1) is attained.

The tropicalization associates to a polynomial $\sum_{\alpha \in A} a_{\alpha} \mathbf{c}^{\alpha}$, the max-plus polynomial

$$P^{\tau}(\mathbf{c}) = \exp[\max_{\alpha \in A} \{\log(|a_{\alpha}|) + \langle \log(\mathbf{c}), \boldsymbol{\alpha} \rangle\}].$$

In other words, a polynomial is replaced by a piecewise smooth function, equal to the largest, in absolute value, of its monomials. Thus, (2.4.1) is a piecewise smooth model [101] because the dominating monomials in the max-plus polynomials can change from one domain to another of the concentration space. The singular set where at least two of the monomials are equal, and where the max-plus polynomial $P^{\tau}(\mathbf{c})$ is not smooth is called tropical manifold [95]. On logarithmic paper, the tropical manifolds of various species define polyhedral domains inside which the dynamics is defined by monomial differential equations (Figure 2.3). Tropicalized systems remind of, but are not equivalent to, Savageau’s S-systems [120] that have been used for modeling metabolic networks. S-systems are smooth systems such that the production and consumption terms of each species are multivariate monomials. Tropicalized systems are S-systems locally, within the polyhedral domains defined by the tropical manifolds, and also along some parts of the tropical manifold (that carry sliding modes, see next section).

The tropicalization unravels an important property of multiscale systems, that is to have different behavior on different timescales. We have seen that, on every timescale, monomolecular networks with total separation behave like a single reaction step. This is akin to considering only the dominant processes in the network and implies that the tropicalization is a good approximation for monomolecular networks with total separation.

The tropical geometry framework is particularly interesting for nonlinear networks. In this case, it is less straightforward to define separation rigorously. Very roughly, one can say

that a system (2.2.2) with polynomial rates is separated, if the monomials composing the rates are separated almost all the time on a trajectory, or, equivalently, almost everywhere in phase space (except on the tropical manifolds). Separation of nonlinear models results either from separated kinetic constants, or from separated species concentrations, or both. In the next section, we discuss some examples when the tropicalization provides useful approximations of smooth nonlinear networks.

2.5 Quasi-steady state and Quasi-equilibrium, revisited

Two simple methods are principally useful for model reduction of nonlinear models with multiple timescales : the quasi-equilibrium (QE) and the quasi-steady state (QSS) approximations. As discussed in [58, 59], these two approximations are physically and dynamically distinct. In order to understand these differences let us refer to the simple example of the Michaelis-Menten mechanism,



The QSS approximation, proposed for this system by Briggs and Haldane, considers that the total concentration of enzyme, $E_{tot} = [E] + [ES]$, is much lower than the total concentration of substrate, therefore the complex ES is a *low concentration, fast species*. The complex concentration is slaved by the concentration of S , meaning that the value of $[ES]$ almost instantly relaxes to a value depending on $[S]$. The simplified mechanism correspond to pooling the two reactions of the mechanism into a unique irreversible reaction $S \xrightarrow{R([S], E_{tot})} P$, which means that $\frac{d[P]}{dt} = -\frac{d[S]}{dt} = k_2[ES]_{QSS}$. The QSS value of the complex concentration results from the equation $k_1[S](E_{tot} - [ES]_{QSS}) = (k_{-1} + k_2)[ES]_{QSS}$. From this, it follows that $R([S], E_{tot}) = k_2 E_{tot} [S]/(k_m + [S])$, where $k_m = (k_{-1} + k_2)/k_1$.

The QE approximation considers that the first reaction of the mechanism is a *fast, reversible reaction*. The simplified mechanism corresponds to a pooling of species. Two pools, $S_{tot} = [S] + [ES]$, and $E_{tot} = [E] + [ES]$ are conserved by the fast reversible reaction, but only one, E_{tot} is conserved by the two reactions of the mechanism. The pool S_{tot} is slowly consumed by the second reaction and represents the slow variable of the system.

The single step approximation reads $S_{tot} \xrightarrow{R(S_{tot}, E_{tot})} P$, or equivalently $\frac{d[P]}{dt} = -\frac{dS_{tot}}{dt} = k_2[ES]_{QE}$. The QE value of the complex concentration is the unique positive solution of the quadratic equation $k_1(S_{tot} - [ES]_{QE})(E_{tot} - [ES]_{QE}) = k_{-1}[ES]_{QE}$. From this it follows that $R(S_{tot}, E_{tot}) = 2k_2 E_{tot} S_{tot} (E_{tot} + S_{tot} + k_{-1}/k_1)^{-1} (1 + \sqrt{1 - 4E_{tot} S_{tot} / (E_{tot} + S_{tot} + k_{-1}/k_1)^2})^{-1}$. When the concentration of enzyme is small, $E_{tot} \ll S_{tot}$, we obtain the original equation of Michaelis and Menten, $R(S_{tot}, E_{tot}) \approx k_2 \frac{E_{tot} S_{tot}}{k_{-1}/k_1 + S_{tot}}$.

One of the main difficulties to applying QE or QSS reduction to computational biology models is that QE reactions and QSS species should be specified a priori. For some models, biological information can be used to rank reactions according to their rates. For instance, one knows that metabolic processes and post-transcriptional modifications are more rapid than gene expression. However, this information is rather vague. In detailed gene expression models, some processes can be rapid, while others are much slower. Furthermore, the relative order of these processes can be inverted from one functioning regime to another, for instance the binding and unbinding rates of a repressor to DNA, can be slow or fast depending on various conditions. Even if some numerical approaches such as iterative IM, CSP and ILDM propose criteria for detecting fast and slow processes, at present there is no general direct method to identify QE reactions and QSS species.

Here we present two methods, based, the first one on singular perturbations, and the second on tropical geometry ideas, allowing to detect QE reactions and QSS species.

The first method uses simulation of the trajectories, therefore it can only be applied to a fully parametrized model. However, in systems with separation, the sets of QE reactions and QSS species are robust, ie remain the same for broad ranges of the parameters. One can use imprecise parameters (resulting for instance from crude estimates or fitting) to compute these sets. The method starts by detecting *slaved species*. Given the trajectories $\mathbf{c}(t)$ of all species, the imposed trajectory of the i -th species is a real, positive solution $c_i^*(t)$ of the polynomial equation

$$P_i(c_1(t), \dots, c_{i-1}(t), c_i^*(t), c_{i+1}(t), \dots, c_n(t)) = 0, \quad (2.5.2)$$

where P_i is the i -th component of the rhs of (2.2.2). We say that a species i is slaved if the distance between the trajectory $c_i(t)$ and some imposed trajectory $c_i^*(t)$ is small for some time interval I , $\sup_{t \in I} |\log(c_i(t)) - \log(c_i^*(t))| < \delta$, for some $\delta > 0$ sufficiently small. The remaining species, that are not slaved, are called slow species.

Slaved species are rapid and are constrained by the slow species. The minimum number of variables that we expect for a reduced model is equal to the number of slow species. The slow species can be obtained by direct comparison of the imposed and actual trajectories. This method is illustrated for a model of NF κ B canonical pathway in Figure 2.4.

There are two types of slaved species. Low concentration, slaved species satisfy QSS conditions. Large concentration, slaved species are consumed and produced by fast QE reactions and satisfy QE conditions. Because the reduction schemes are different in the two situations, it is useful to have a method to separate the two cases. Using the values of concentrations can work when concentrations are well separated, but may fail for a continuum of values. A better method is to identify which are the dominant terms in the Eq.(2.5.2). Using again the example of Michaelis-Menten mechanism, the complex ES will be detected as slaved in both QSS and QE conditions. Eq.(2.5.2) reads $k_1[S][E] = (k_{-1} + k_2)[ES]$. For QE condition, the term k_2 will be dominated by k_{-1} . We call pruned version of Eq.(2.5.2) the equation obtained after removing all the dominated monomials, in this case the equation $k_1[S][E] - k_{-1}[ES] = 0$. When the pruned version is a combination of reversible reaction rates set to zero, then the slaved species satisfy QE conditions. Again, the comparison of monomials is possible for a fully parametrized model, however we expect this comparison to be robust for models with separation.

The second method to identify QE and QSS conditions, follows from the calculation of the tropicalization (2.4.1). This can be done formally and do not require simulation of trajectories and numerical knowledge of the parameters. Indeed, it was shown in [101] that there is a relation between sliding modes of the tropicalized system (2.4.1) and the QSS or QE conditions. The system (2.4.1) belongs to the class of ordinary differential equations with discontinuous vector fields [40]. In such systems, the dynamics can follow discontinuity hypersurfaces where the vector field is not defined. This type of motion is called sliding mode. When the discontinuity hypersurfaces are smooth and $n - 1$ dimensional (n is the dimension of the vector field) then the conditions for sliding modes read :

$$\langle \mathbf{n}_+(\mathbf{x}), \mathbf{f}_+(\mathbf{x}) \rangle < 0, \quad \langle \mathbf{n}_-(\mathbf{x}), \mathbf{f}_-(\mathbf{x}) \rangle < 0, \quad \mathbf{x} \in \Sigma, \quad (2.5.3)$$

where $\mathbf{f}_+, \mathbf{f}_-$ are the vector fields on the two sides of Σ and $\mathbf{n}_+ = -\mathbf{n}_-$ are the interior normals.

Let us consider that the smooth system (2.2.2) with polynomial rate functions has quasi-steady state species or quasi-equilibrium reactions. In this case, the fast dynamics

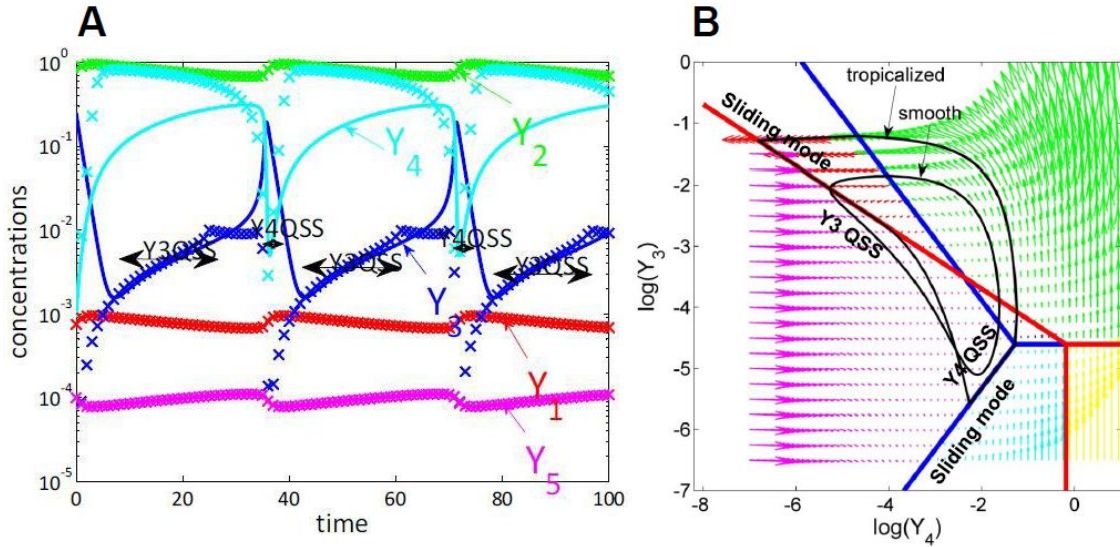


FIGURE 2.4 – Model reduction and tropicalization of a 5 variables cell cycle model defined by the differential equations $y'_1 = k_9y_2 - k_8y_1 + k_6y_3$, $y'_2 = k_8y_1 - k_9y_2 - k_3y_2y_5$, $y'_3 = k'_4y_4 + k_4y_4y_3^2/C^2 - k_6y_3$, $y'_4 = -k'_4y_4 - k_4y_4y_3^2/C^2 + k_3y_2y_5$, $y'_5 = k_1 - k_3y_2y_5$, proposed in [140]. (A) Comparison of trajectories and imposed trajectories show that variables y_1 , y_2 , y_5 are always slaved, meaning that the trajectories are close to the 2 dimensional hyperplane defined by the QE condition $k_8y_1 = k_9y_2$, the QSS condition $k_1 = k_3y_2y_5$ and the conservation law $y_1 + y_2 + y_3 + y_4 = C$. The variables y_3 , y_4 are slaved and the corresponding species are quasi-stationary on intervals. This means that the dimensionality of the dynamics is further reduced to 1, on intervals. (B) Tropicalization on logarithmic paper, in the plane of the variables y_3 , y_4 . The tropical manifold consists of two tripods, represented in blue and red, which divide the logarithmic paper into 6 polygonal sectors. Monomial vector fields defining the tropicalized dynamics change from one polygonal domain to another. The tropicalized (approximated) and the smooth (not reduced) limit cycle dynamics stay within bounded distance one from another. This distance is relatively small on intervals where the variables y_3 or y_4 are quasi-stationary, which correspond to sliding modes of the tropicalization.

reads :

$$\frac{dx_i}{dt} = \frac{1}{\epsilon} \tilde{P}_i(\mathbf{x}) / \tilde{Q}_i(\mathbf{x}), \quad i \text{ fast}, \quad (2.5.4)$$

where $\tilde{P}_i(\mathbf{x})$, $\tilde{Q}_i(\mathbf{x})$ are pruned versions of P_i , Q_i (obtained by keeping only the lowest order terms), and ϵ is the small, singular perturbation parameter.

For sufficiently large times, the fast variables satisfy (to $\mathcal{O}(\epsilon)$) :

$$\tilde{P}_i(\mathbf{x}) = 0, \quad i \text{ fast}. \quad (2.5.5)$$

The pruned polynomial is usually a fewnomial (contains a small number of monomials). In particular, let us consider the case when only two monomials remain after pruning, $\tilde{P}_i(\mathbf{x}) = a_1 \mathbf{x}^{\alpha_1} + a_2 \mathbf{x}^{\alpha_2}$. Then, the equation (2.5.5) defines a hyperplane $S = \{ < \log(\mathbf{x}), \alpha_1 - \alpha_2 > = \log(|a_1|/|a_2|) \}$. This hyperplane belongs to the tropical variety of \tilde{P}_i , because it is the place where the monomial \mathbf{x}^{α_1} switches to \mathbf{x}^{α_2} in the max-plus polynomial defined by \tilde{P}_i . For ϵ small, the QE or QSS conditions guarantee the existence of an invariant manifold \mathcal{M}_ϵ , whose distance to S is $\mathcal{O}(\epsilon)$.

Let n_+, n_- defined as above and let $(f_+)_i = \frac{1}{\tilde{Q}_i(\mathbf{x})} a_1 \mathbf{x}^{\alpha_1}$, $(f_-)_i = \frac{1}{\tilde{Q}_i(\mathbf{x})} a_2 \mathbf{x}^{\alpha_2}$, $f_i = \frac{1}{\epsilon} [(f_+)_i + (f_-)_i]$ for i fast, $(f_+)_j = (f_-)_j = f_j = \frac{\tilde{P}_j}{\tilde{Q}_j}$, for j not fast. Then, the stability conditions for the invariant manifold read $< n_+(x_+), f(x_+) > < 0$, $< n_-(x_-), f(x_-) > < 0$, where x_+, x_- are close to \mathcal{M}_ϵ on the side towards which points n_+ and n_- , respectively. We note that $|f_+(x_+)| > |f_-(x_+)|$. Thus, $< n_+, f > = \frac{1}{\epsilon} (n_+)_i [(f_+)_i + (f_-)_i] + \sum_{j, \text{not fast}} (n_+)_j (f_+)_j$ and $< n_+, f_+ > = \frac{1}{\epsilon} (n_+)_i (f_+)_i + \sum_{j, \text{not fast}} (n_+)_j (f_+)_j$. Thus, if $< n_+, f > < 0$, then for ϵ small enough $(n_+)_i (f_+)_i < 0$ and $< n_+, f_+ > < 0$ because $< n_+, f > > < n_+, f_+ >$. Similarly, we show that $< n_-, f > < 0$ implies $< n_-, f_- > < 0$. This proves the following

Theorem 2.5.1. *If the smooth dynamics obeys QE or QSS conditions and if the pruned polynomial \tilde{P} defining the fast dynamics is a 2-nomial, then the QE or QSS equations define a hyperplane of the tropical variety of \tilde{P} . The stability of the QE or QSS manifold implies the existence of a sliding mode of the tropicalization along this hyperplane.*

This result suggests that checking the sliding mode condition (2.5.3) on the tropical manifold, provides a method of detecting QE reactions and QSS species.

To illustrate this method, let us use again the Michaelis-Menten example. In this case, two conservation laws allow elimination of two variables E and P and the dynamics can be described by two ODEs :

$$\begin{aligned} \frac{d[S]}{dt} &= -k_1 E_{tot}[S] + k_1[S][ES] + k_{-1}[ES] \\ \frac{d[ES]}{dt} &= k_1 E_{tot}[S] - k_1[S][ES] - (k_{-1} + k_2)[ES] \end{aligned} \quad (2.5.6)$$

The tropical manifolds of the two species S and ES are tripods with parallel arms like in Figure 2.3. Indeed, the slopes of the arms of tropical manifold are only given by the powers of different variables of the monomials, and these are the same for the two species. Investigation of the flow field close to the tripod arms identifies sliding modes on an unbounded subset AOB of the tropical manifold of the species ES . This subset is a global attractor of the tropicalized dynamics and represents a tropicalized version of the invariant manifold of the smooth system. If the initial data is not in this set, the tropicalized trajectory converges quickly to it and continues on it as a sliding mode.

When $k_2 \gg k_{-1}$, ES satisfies QSS conditions leading to the Michaelis-Menten equation. The arm AO of the tropical manifold of the species ES carry a sliding mode, has the equation $k_1 E_{tot}[S] = (k_{-1} + k_2)[ES] \gg k_1[S][ES]$, and corresponds to the linear regime of the Michaelis-Menten equation. Similarly, the arm OB of the tropical manifold of ES has the equation $k_1 E_{tot}[S] = k_1[S][ES] \gg (k_{-1} + k_2)[ES]$ and corresponds to the saturated regime of the Michaelis-Menten equation. When $k_2 \ll k_{-1}$, the tropical manifolds of the two species S and ES practically coincide. Both species are rapid and satisfy QE conditions, namely $k_1 E_{tot}[S] = k_{-1}[ES] \gg k_1[S][ES]$ on the arm AO , and $k_1 E_{tot}[S] = k_1[S][ES] \gg k_{-1}[ES]$ on the arm OB .

The tropicalization can thus be used to obtain global reductions of models. Even when global reductions are not possible (sliding modes leave the tropical manifold or simply do not exist), the tropicalization can be used to hybridize smooth models, ie transform them into piecewise simpler models (modes) that change from one time interval to another. These changes occur when the piecewise smooth trajectory of the system meets a hyperplane of the tropical manifold and continues as a sliding mode along this hyperplane or leaves immediately the hyperplane. Hybridization is a particularly interesting approach to modeling cell cycle. Indeed, progression of the cell cycle is a succession of several different regimes (phases). This strategy is illustrated in Figure 2.4 for a simple cell cycle model.

2.6 Graph rewriting for large nonlinear, deterministic, dynamical networks

We have seen in Section 2.3 that model reduction of monomolecular networks with total separation is based on graph rewriting operations.

Similarly, QSS and QE approximations can be used to produce simpler networks from large nonlinear networks. The classical implementation of these approximations leads to differential-algebraic equations. It is however possible to reformulate the simplified model as a new, simpler, reaction network. We showed in the previous section how to do this for the Michaelis-Menten mechanism under different conditions. In general, one has to solve the algebraic equations corresponding to QE or QSS conditions, eliminate (prune) QSS species and QE reactions, pool reactions (for QSS approximation) or species (for QE approximation), and finally calculate the kinetic laws of the new reactions.

By reaction pooling we understand here replacing a set of reactions by a single reaction whose stoichiometry vector ν is the sum of the stoichiometry vectors ν_i of the reactions in the pool, $\nu = \sum_i \gamma_i \nu_i$. If the reactions are reversible then the coefficients γ_i can be arbitrary integers, otherwise they must be positive integers. Reaction pools conserve certain species that were previously consumed or produced by individual reactions in the pools. These species were called intermediates in [112]. The species that are either produced or consumed by the pools were called terminal in [112]. For example, an irreversible chain of reactions $A_1 \rightarrow A_2 \rightarrow A_3$ can be pooled onto a single reaction $A_1 \rightarrow A_3$, which in terms of

stoichiometry vectors reads $\begin{bmatrix} -1 \\ 0 \\ 1 \end{bmatrix} = \begin{bmatrix} -1 \\ 1 \\ 0 \end{bmatrix} + \begin{bmatrix} 0 \\ -1 \\ 1 \end{bmatrix}$. In this example A_1, A_3 are terminal species and A_2 is an intermediate species. Reaction pooling is used with QSS conditions, in which case the intermediates are the QSS species.

By species pooling we understand replacing a set of species concentrations $\{c_i\}$ by a linear combination with positive coefficients of species concentrations, $\sum_i b_i c_i$. Species pooling is used with QE conditions.

In general, the reaction and species pools result from linear algebra. Indeed, let us consider the matrix \mathbf{S}^f that defines the stoichiometry of the rapid subsystem. For the QSS approximation, the matrix \mathbf{S}^f has a number of lines equal to the number of QSS species. The columns of this matrix are the stoichiometries of the reactions in the model, restricted to the QSS species. We exclude zero valued columns, i.e. reactions that do not act on QSS species. For the QE approximation, the number of columns of the matrix \mathbf{S}^f is equal to the number of QE reactions, and the lines of \mathbf{S}^f are the stoichiometries of QE reactions. We exclude zero valued lines corresponding to species that are not affected by QE reactions.

In QE conditions, species pools are defined by vectors in the left kernel of \mathbf{S}^f ,

$$\mathbf{b}^T \mathbf{S}^f = 0 \quad (2.6.1)$$

The vectors \mathbf{b} , that are conservation laws of the fast subsystem, define linear combinations of species concentrations that are the new slow variables of the system. Of course, one could eliminate from these combinations, the conservation laws of the full reaction network, that will be constant (see Appendix).

In QSS conditions, reaction pools (also called routes) are defined by vectors in the right kernel of \mathbf{S}^f ,

$$\mathbf{S}^f \boldsymbol{\gamma} = 0 \quad (2.6.2)$$

According to the definition (2.6.2), a reaction pool does not consume or produce QSS species (these are intermediates). One can impose, like in [112], a minimality condition for choosing the reaction pools. A reaction pool is minimal if there is no other reaction pool with less nonzero stoichiometry coefficients. This is equivalent to choosing reaction pools as elementary modes [145] of the fast subsystem.

After pooling, QE and QSS algebraic conditions must be solved and the rates of the new reactions calculated. The new rates should be chosen such that the remaining species and pools of species satisfy the simplified ODEs. The choice of the rates is not always unique (some uniqueness conditions are discussed in [112], see also the Appendix). In order to compute the new rates, one has to solve QE and QSS equations. For network with polynomial or rational rates, this implies solving large systems of polynomial equations. The complexity of this task is double exponential on the size of the system [103], therefore one needs approximate solutions. Approximate solutions of polynomial equations can be formally derived when the monomials of these equations are well separated. Some simple recipes were given in [112] and could be improved by the methods of tropical geometry.

These ideas were used in [112] to reduce several models of NF- κ B signalling (Figure 2.5).

The NF- κ B activation pathway is complex at many levels. NF- κ B is sequestered in the cytoplasm by inactivating proteins named I κ B. There are five known members of the NF- κ B family in mammals, Rel (c-rel), RelA (p65), RelB, NF- κ B1 (p50 and its precursor p105) and NF- κ B2 (p52 and its precursor p100). This generates a large combinatorial complexity of dimers, affinities and transcriptional capabilities. I κ B family comprises seven members in mammals (I κ B α , I κ B β , I κ B ϵ , I κ B γ , Bcl-3). All these inhibitors display different affinities for NF- κ B dimers, multiplying the combinatorial complexity. The activation of NF- κ B upon signalling, occurs by phosphorylation by a kinase complex, then ubiquitination, and finally degradation of I κ B molecules. The activation signal is transmitted by several possible pathways most of them activating the kinase IKK that modifies I κ B. In the canonical pathway, one important determinant of IKK dynamics is the protein A20

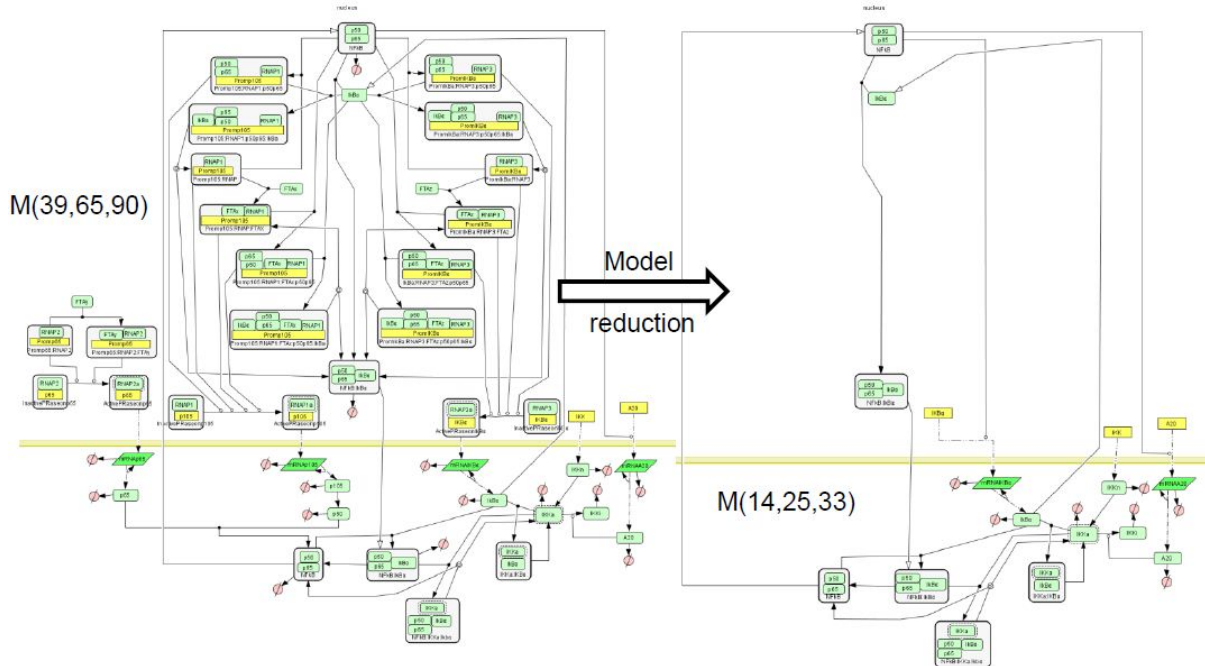


FIGURE 2.5 – Model of NF- κ B signaling (BIOMD0000000227 in Biomodels database [81]), proposing separate production of the subunits p50, p65, the full combinatorics of their interactions as well as with the inhibitor I κ B, the positive self-regulation of p50, and in addition an A20 molecule whose production is enhanced upon NF- κ B stimulation, and which negatively regulates the activity of the stimulus responding kinase IKK [112]. This model, denoted $\mathcal{M}(39, 65, 90)$ contains 39 species, 65 reactions and 90 parameters. We have reduced it to various levels of complexity. Among the reduced model we obtained one, $\mathcal{M}(14, 25, 33)$ that has the same stoichiometry (but different rate functions) as a model published elsewhere by another author [86] and denoted $\mathcal{M}(14, 25, 28)$ (BIOMD0000000226 in Biomodels database). Incidentally, this is also the simplest model in the hierarchy related to $\mathcal{M}(39, 65, 90)$. Comparison (not shown) of the rate functions and of the trajectories of the models $\mathcal{M}(14, 25, 33)$ and $\mathcal{M}(14, 25, 28)$ provided insight into the consequences of various mechanistic modeling choices. The model graphical representation is based on the SBGN standard [82].

that inhibits IKK activation. A20 expression is controlled by NF- κ B. In order to cope with this complexity a model containing 39 species, 65 reactions and 90 parameters was proposed in [112]. Of course, not all reactions and parameters of this complex model are important. In order to determine, in a rational and systematic way, which of the model features are critical, we have used model reduction.

Graph rewriting was performed in a modular way, by applying the pruning and pooling rules to tightly connected submodels of the NF- κ B network. The computation of the reaction pools was performed using Matlab and METATOOL [145]. Using submodel decomposition reduces the complexity of computing elementary modes and of solving large systems of algebraic equations needed for recalculating the reaction rates.

To give an example of modular reduction, let us consider the set of reactions involving

six cytoplasmic located intermediates ($\text{IKK}|\text{active}$, $\text{IKK}|\text{inactive}$, IKK , $\text{IKK}|\text{active} : \text{IkBa}$, $\text{IKK}|\text{active} : \text{IkBa} : \text{p50}$, $\text{p50} : \text{p65@csl}$) and four terminal species (A20 , IkBa@csl , $\text{IkBa} : \text{p50} : \text{p65@csl}$, $\text{p50} : \text{p65@ncl}$). As can be seen from Figure 2.6, the six intermediate species are slaved. The reactions of this submodel form the cytoplasmic part of the signalling mechanism, including 11 kinase transformation reactions, a complex release reaction, a complex formation reaction, and the NF- κ B translocation reaction. The elementary modes of the submodel (computed using METATOOL [145]) are used to define the reactions pools. For this submodel, we find two elementary modes, that can be described as the modulated inhibitor degradation ($\text{IkBa@csl} \rightarrow \emptyset$), and a reaction summarizing the NF- κ B release and translocation ($\text{IkBa} : \text{p50} : \text{p65@csl} \rightarrow \text{p50} : \text{p65@ncl}$), respectively. In order to compute the reaction rates of the two elementary modes as functions of the concentrations of the terminal species, we find approximate solutions of the QSS equations for the intermediate species and equate, for the variation rates of each terminal species, the contributions of elementary modes to the total known variation rate in the unreduced model (see Appendix). The two rates are $k_{21p1}[\text{IkBa@csl}][\text{IkBa} : \text{p50} : \text{p65@csl}] / ((k_{21p2} + [\text{IkBa@csl}](k_{21p3} + [\text{A20}]))$ for the modulated inhibitor degradation, and $k_{15p1}[\text{IkBa} : \text{p50} : \text{p65@csl}] / ((k_{15p2} + [\text{IkBa@csl}](k_{15p3} + [\text{A20}]))$ for the release and translocation reaction.

2.7 Model reduction and model identification

Computational biology models contain mechanistic details that can not all be identified from available experimental data. Determining the parameters of such complex models could lead to overfitting, describing noise, rather than features of data, or can be simply meaningless, when model behavior is not sensitive to the parameters. Furthermore, many model identification methods [49] suffer from the "curse of dimensionality" as it becomes increasingly difficult to cover the parameter space when the number of parameters increases. A rather efficient strategy to bypass these problems is to use model reduction. This method is known in machine learning as backward pruning or post-pruning [147]. It consists in finding a complex model that fits data well and then prune it back to a simpler one that also fits the data well. Far from being redundant, backward pruning can be successfully used in computational biology. Rather often, one starts with a complex model coping with mechanistic details of the network regulation. Then, over-fitting and problems of identifiability of the parameters are avoided by model reduction. By model reduction, the mechanistic model is mapped onto a simpler, phenomenological model. For instance, gene transcription and translation can be represented as one step and one constant in a phenomenological model, but can consist of several steps such as initiation, transcription of mRNA leading region, ribosome binding, translation, folding, maturation, etc. in a complex model. Not all of these steps are important for the network functioning and not all parameters are identifiable from the observed quantities. Following reduction, the inessential steps are pruned and several sensitive parameters are compacted into a few effective parameters that are identifiable.

As discussed in [111, 112, 110, 39], model reduction unravels the important features and the sensitive parameters of the model.

Using model reduction for determining critical features of the model has many advantages relative to numerical sensitivity studies [109, 61, 71]. This approach is less time consuming, brings more insight, and is based on qualitative comparison of the order of the parameters and therefore does not need exhaustive scans of parameter values. In the applications described in [111, 112, 110, 39], the sensitive parameters of the pruned model

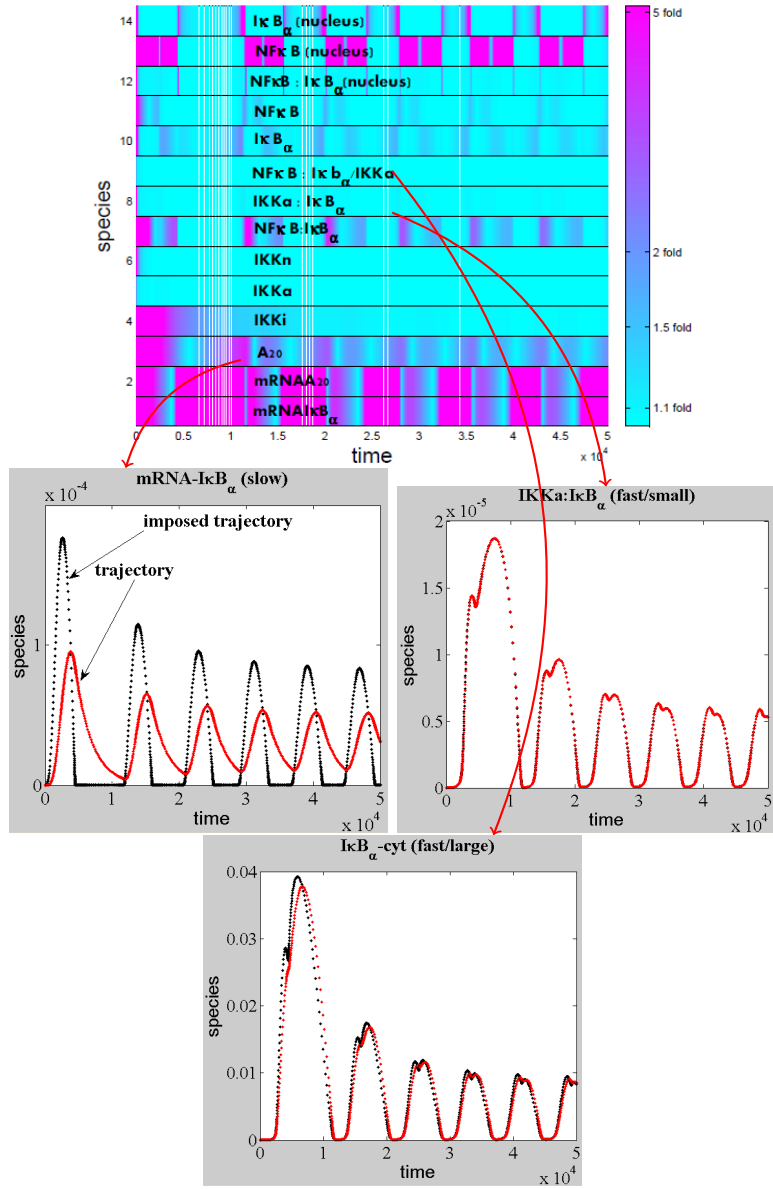


FIGURE 2.6 – The modulus of the log-ratio, $|\log(c_i(t)/c_i^*(t))|$, between actual and imposed trajectories has been calculated as a function of time for each species of the model of $NF\kappa B$ canonical pathway (proposed in [86], model $\mathcal{M}(14, 25, 28)$ from [112]). If the modulus is close to zero (ratio close to one fold from above, or from below) the species is slaved, otherwise the species is slow. Among the slaved species, some have low concentrations and satisfy quasi-steady-state conditions, whereas other have large concentrations and are involved in quasi-equilibrium reactions.

are combinations (most often monomials) of the parameters of the complex models. As only the sensitive combinations can be fitted from data, it is important to have estimates of some individual parameters, allowing to determine the remaining ones.

This methodology has been first proposed in [112]. The model reduction of the NF- κ B model in [112] leads to new, effective parameters that are monomials of the parameters of the complex model. The correspondence between the initial parameters and the effective parameters is shown in Figure 2.7. Although not fully exploited in the theoretical study [112], this mapping can be used for model parameter identification. Effective parameters have increased observability and could be obtained from experimental data. The values of the effective parameters can be used to constrain the parameters of the full model. Some of the parameters of the full model, that are not sensitive or contribute to effective parameters together with other parameters remain arbitrary and could be fixed to generic values.

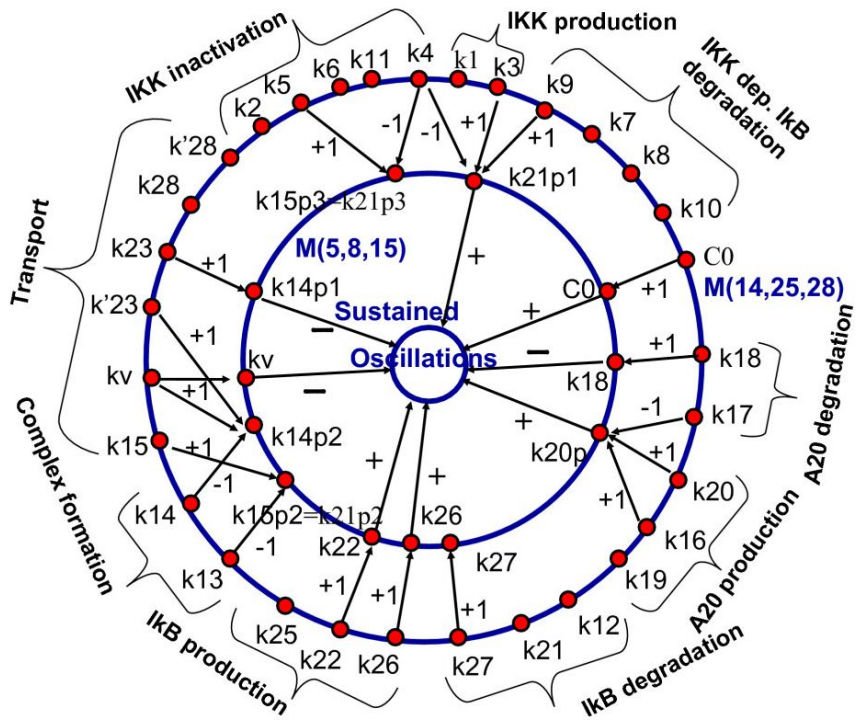


FIGURE 2.7 – The model $\mathcal{M}(14, 25, 28)$ from [112] (first proposed in [86], see also BIOMD0000000226 in Biomodels database) was used to generate a hierarchy of simpler models, the simplest one being $\mathcal{M}(5, 8, 15)$. We show the mapping between the parameters of the models $\mathcal{M}(14, 25, 28)$ and $\mathcal{M}(5, 8, 15)$. Parameters of the first model are gathered into monomials that are parameters of the reduced model. The integers on the arrows connecting parameters represent the corresponding powers of the parameters in the monomial. The innermost circle represents a dynamical property of the model that is influenced positively, negatively, or negligibly by the effective parameters (parameters of the reduced model). From [112].

2.8 Conclusion

The mathematical techniques described in this paper define strategies for the study of large dynamical network models in computational biology. Large networks are needed in order to understand context dependence, specialization, and individuality of the cell behavior. Extensive pathway database accumulation supports somehow the idea that biological cell is a puzzle of networks and pathways, and that once these are put together in a tightly bound, coherent map, the cell physiology should be unraveled by a computer simulation. Actually, confronting biochemical networks with real life is not an easy challenge. Model reduction techniques are needed to bring us one step closer to this objective, as these methods can reveal critical features of complex organizations.

We have proposed that the ideas of limitation and dominance are fundamental for understanding computational biology dynamical models. The essential, critical features of systems with many separated time scales, can be resumed by a dominant, reduced, subsystem. This dominant subsystem depends on the order relations between model parameters or combinations of model parameters. We have shown how to calculate such a dominant subsystem for linear and nonlinear networks. Geometrical interpretation of these concepts in terms of tropicalization provides a powerful framework, allowing to identify invariant manifolds, quasi-steady state species and quasi-equilibrium reactions. We have also discussed how model reduction can be applied to backward pruning parameter learning strategies.

Future efforts are needed to extend these mathematical ideas and model reduction algorithms and implement them into computational biology tools.

2.9 Algorithms

2.9.1 Algorithm 1 : reduction of monomolecular networks with separation

This algorithm consists of three procedures.

I. Constructing of an auxiliary reaction network : pruning.

For each A_i branching node (substrate of several reactions) let us define κ_i as the maximal kinetic constant for reactions $A_i \rightarrow A_j : \kappa_i = \max_j \{k_{ji}\}$. For correspondent j we use the notation $\phi(i) : \phi(i) = \arg \max_j \{k_{ji}\}$.

An auxiliary reaction network \mathcal{V} is the set of reactions obtained by keeping only $A_i \rightarrow A_{\phi(i)}$ with kinetic constants κ_i and discarding the other, slower reactions. Auxiliary networks have no branching, but they can have cycles and confluentes. The correspondent kinetic equation is

$$\dot{c}_i = -\kappa_i c_i + \sum_{\phi(j)=i} \kappa_j c_j, \quad (2.9.1)$$

If the auxiliary network contains no cycles, the algorithm stops here.

II gluing cycles and restoring cycle exit reactions

In general, the auxiliary network \mathcal{V} has several cycles C_1, C_2, \dots with lengths $\tau_1, \tau_2, \dots > 1$.

These cycles will be “glued” into points and all nodes in the cycle C_i , will be replaced by a single vertex A^i . Also, some of the reactions that were pruned in the first part of the algorithm are restored with renormalized rate constants. Indeed, reaction exiting a cycle are needed to render the correct dynamics : without them, the total mass accumulates in the cycle, with them the mass can also slowly leave the cycle. Reactions $A \rightarrow B$ exiting from

cycles ($A \in C_i, B \notin C_i$) are changed into $A^i \rightarrow B$ with the rate constant renormalization : let the cycle C^i be the following sequence of reactions $A_1 \rightarrow A_2 \rightarrow \dots A_{\tau_i} \rightarrow A_1$, and the reaction rate constant for $A_j \rightarrow A_{j+1}$ is k_j (k_{τ_i} for $A_{\tau_i} \rightarrow A_1$). The quasi-stationary normalized distribution in the cycle is :

$$c_j^\circ = \frac{1}{k_j} \left(\sum_{j=1}^{\tau_i} \frac{1}{k_j} \right)^{-1}, \quad j = 1, \dots, \tau_i.$$

The reaction $A_j \rightarrow B$ ($A \in C_i, B \notin C_i$) with the rate constant k is changed into $A^i \rightarrow B$ with the rate constant $c_j^\circ k$.

Let the cycle C_i have the limiting steps that is much slower than other reactions. For the limiting reaction of the cycle C_i we use notation $k_{\lim i}$. In this case, $c_j^\circ = k_{\lim i}/k_j$. If $A = A_j$ and k is the rate constant for $A \rightarrow B$, then the new reaction $A^i \rightarrow B$ has the rate constant $kk_{\lim i}/k_j$. This rate is obtained using quasi-stationary distribution for the cycle.

The new auxiliary network \mathcal{V}^1 is computed for the network with glued cycles. Then we prune it, extract cycles, glue them, iterate until a acyclic network is obtained \mathcal{V}^m , where m is the number of iterations.

III Restoring cycles

The previous procedure gives us the sequence of networks $\mathcal{V}^1, \dots, \mathcal{V}^m$ with the set of vertices $\mathcal{A}^1, \dots, \mathcal{A}^m$ and reaction rate constants defined for each \mathcal{V}^i in the processes of pruning and gluing.

The dynamics of species inside glued cycles is lost after their gluing. A full multi-scale approximation (including relaxation inside cycles) can be obtained by restoration of cycles. This is done starting from the acyclic auxiliary network \mathcal{V}^m back to \mathcal{V}^1 through the hierarchy of cycles. Each cycle is restored according to the following procedure :

- We start the reverse process from the glued network \mathcal{V}^m on \mathcal{A}^m . On a step back, from the set \mathcal{A}^m to \mathcal{A}^{m-1} and so on, some of glued cycles should be restored and cut. On the q th step we build an acyclic reaction network on the set of vertices \mathcal{A}^{m-q} , the final network is defined on the initial vertex set and approximates relaxation of the initial networks.
- To make one step back from \mathcal{V}^m let us select the vertices of \mathcal{A}^m that are glued cycles from \mathcal{V}^{m-1} . Let these vertices be A_1^m, A_2^m, \dots . Each A_i^m corresponds to a glued cycle from \mathcal{V}^{m-1} , $A_{i1}^{m-1} \rightarrow A_{i2}^{m-1} \rightarrow \dots A_{i\tau_i}^{m-1} \rightarrow A_{i1}^{m-1}$, of the length τ_i . We assume that the limiting steps in these cycles are $A_{i\tau_i}^{m-1} \rightarrow A_{i1}^{m-1}$. Let us substitute each vertex A_i^m in \mathcal{V}^m by τ_i vertices $A_{i1}^{m-1}, A_{i2}^{m-1}, \dots A_{i\tau_i}^{m-1}$ and add to \mathcal{V}^m reactions $A_{i1}^{m-1} \rightarrow A_{i2}^{m-1} \rightarrow \dots A_{i\tau_i}^{m-1}$ (that are the cycle reactions without the limiting step) with corresponding constants from \mathcal{V}^{m-1} .
- If there exists an outgoing reaction $A_i^m \rightarrow B$ in \mathcal{V}^m then we substitute it by the reaction $A_{i\tau_i}^{m-1} \rightarrow B$ with the same constant, i.e. outgoing reactions $A_i^m \rightarrow \dots$ are reattached to the heads of the limiting steps. Let us rearrange reactions from \mathcal{V}^m of the form $B \rightarrow A_i^m$. These reactions have prototypes in \mathcal{V}^{m-1} (before the last gluing). We simply restore these reactions. If there exists a reaction $A_i^m \rightarrow A_j^m$ then we find the prototype in \mathcal{V}^{m-1} , $A \rightarrow B$, and substitute the reaction by $A_{i\tau_i}^{m-1} \rightarrow B$ with the same constant, as for $A_i^m \rightarrow A_j^m$.
- After the previous step is performed, the vertices set is \mathcal{A}^{m-1} , but the reaction set differs from the reactions of the network \mathcal{V}^{m-1} : the limiting steps of cycles are excluded and the outgoing reactions of glued cycles are included (reattached to the heads of the limiting steps). To make the next step, we select vertices of \mathcal{A}^{m-1} that are glued cycles from \mathcal{V}^{m-2} , substitute these vertices by vertices of cycles, delete

the limiting steps, attach outgoing reactions to the heads of the limiting steps, and for incoming reactions restore their prototypes from \mathcal{V}^{m-2} , and so on.

After all, we restore all the glued cycles, and construct an acyclic reaction network on the set \mathcal{A} . This acyclic network approximates relaxation of the initial network. We call this system the *dominant system*.

Note that the reduction algorithm does not need precise values of the constants. It is enough to have an initial ordering of the constants. Then, the auxiliary network is obtained only from this ordering. However, after a first iteration, and if the initial network contains cycles, some of the exit constant are renormalized and the new rate constants become monomials of the old ones. In order to prune again, we need to compare these monomials. Monomials of well separated constants are generically well separated [56]. However, a freedom remains on ordering these new monomials, leading to several possible reduced acyclic digraphs, given an initial digraph with ordering of the constants (Figure 4.1 of the main text).

2.9.2 Algorithm 2 : reduction of nonlinear networks with separation

This algorithm consists of the following procedures.

I. Identification of QSS species and QE reactions.

There are two methods of identification, trajectory based, and tropicalization based. Presently we are using the trajectory based method.

Detect slaved species. After generating trajectories $\mathbf{c}(t)$ for $t \in I$, for each species compute the distances $\delta_i = \sup_{t \in I} |\log(c_i(t)) - \log(c_i^*(t))|$. Use k-means clustering to separate species into two groups, slaved (small values of δ) and slow (large values of δ) species.

Prune. For each P_i (polynomial rate) corresponding to slaved species, compute the pruned version \tilde{P}_i by eliminating all monomials that are dominated by other monomials of P_i .

Identify QE reactions and QSS species. Identify, in the structure of \tilde{P}_i the forward and reverse rates of QE reactions. This step can be performed by recipes presented in [131]. The slaved species not involved in QE reactions are QSS.

II. Exploiting QSS conditions, pruning intermediate species, pooling reactions

Define subsets and matrices Given the set of QSS (intermediate) species I , one defines the set \mathcal{R}_I of reactions acting on them. The terminal species T , are the other species, different from I , on which act the reactions from \mathcal{R}_I . Define two stoichiometric matrices \mathbf{S}^f and \mathbf{S}^T . \mathbf{S}^f defines the fast subsystem and has a number of lines equal to the number of QSS species, and a number of columns equal to the number of reactions \mathcal{R}_I . \mathbf{S}^T contains the stoichiometries of the terminal species for the same reactions \mathcal{R}_I . Species I will be pruned, and reactions \mathcal{R}_I will be pooled.

Compute elementary modes (EMs) Compute elementary modes of nonzero terminal stoichiometry as minimal solutions of $\mathbf{S}^f \boldsymbol{\gamma} = 0$, $\mathbf{S}^T \boldsymbol{\gamma} \neq 0$, the minimality being defined with respect to the number of nonzero coefficients. $\mathbf{S}^T \boldsymbol{\gamma} \neq 0$ on the output of elementary modes packages such as METATOOL. If the terminal stoichiometries of the EMs are dependent, restrict to a subset of independent terminal stoichiometries.

Solve QSS equations Find approximate formal solutions for systems of QSS algebraic equations. This step is not yet automatic. It will be automatized in subsequent work by using tropical geometry methods.

Find rates of EMs To each elementary mode γ_i , associate a kinetic law giving the rate of the EM as a function of the terminal species concentrations $R_i^*(\mathbf{c}_T)$. Let $\mathbf{R}(\mathbf{c}_T)$ be the vector of rates of reactions in \mathcal{R}_I . The dependence of these rates on \mathbf{c}_T is direct, or indirect, via \mathbf{c}_I that can be now expressed as function of \mathbf{c}_T . Then, the EM rates $R_i^*(\mathbf{c}_T)$ must satisfy $\mathbf{S}^T \mathbf{R}(\mathbf{c}_T) = \sum R_i^*(\mathbf{c}_T) \mathbf{S}^T \gamma_i$. This equation has an unique solution if the vectors $\mathbf{S}^T \gamma_i$ are independent (this justifies the independence condition for the terminal stoichiometries of EMs).

III. Exploiting QE conditions, pruning QE reactions, pooling species

Define subsets and matrices Given the set of QE reactions Q , one defines the set S of species that are affected by them. The species S are also affected by other reactions that we call terminal, Q_T . Define two stoichiometric matrices \mathbf{S}^f and \mathbf{S}^T . \mathbf{S}^f defines the fast subsystem and has a number of lines equal to the cardinal of E , and a number of columns equal to the cardinal of Q . \mathbf{S}^T contains the stoichiometries of the reactions reactions Q_T for the same species S (it has the same number of lines as \mathbf{S}^f). Reactions Q will be pruned and species E will be pooled.

Compute species pools Species pools are computed as minimal solutions of $\mathbf{b}\mathbf{S}^f = 0$, $\mathbf{b}\mathbf{S}^T \neq 0$ (the second condition stands for looking for conservation laws of the fast subsystem that are not conserved by the entire network; the minimality condition means that we compute elementary modes of the transpose matrix \mathbf{S}^f).

Solve QE equations Same methods as for QSS conditions. Solve the QSS equations together with the conservation of pools and express the concentrations of the species E as functions of the pools $c_i^* = \langle \mathbf{b}_i, \mathbf{c} \rangle$.

Find new rates Re-express (by substitution) the rate of each reaction from Q_T in terms of pools c_i^* .

Chapitre 3

Tropical equilibration principle for chemical kinetics.

3.1 Introduction.

Systems biology develops biochemical dynamic models of various cellular processes such as signalling, metabolism, gene regulation. These models can reproduce complex spatial and temporal dynamic behavior observed in molecular biology experiments. In spite of their complex behavior, currently available dynamical models are relatively small size abstractions, containing only tens of variables. This modest size results from the lack of precise information on kinetic parameters of the biochemical reactions on one hand, and of the limitations of parameter identification methods on the other hand. Further limitations can result from the combinatorial explosion of interactions among molecules with multiple modifications and interaction sites [29]. In middle out modeling strategies small models can be justified by saying that one looks for an optimal level of complexity that captures the salient features of the phenomenon under study. The ability to choose the relevant details and to omit the less important ones is part of the art of the modeler. Beyond modeler's art, the success of simple models relies on an important property of large dynamical systems. The dynamics of multiscale, dissipative, large biochemical models, can be reduced to that of simpler models, that were called dominant subsystems [112, 58, 57]. Simplified, dominant subsystems contain less parameters and are more easy to analyze. The choice of the dominant subsystem depends on the comparison among the time scales of the large model. Among the conditions leading to dominance and allowing to generate reduced models, the most important are quasi-equilibrium (QE) and the quasi-steady state (QSS) approximations [58]. In nonlinear systems, timescales and together with them dominant subsystems can change during the dynamics and undergo more or less sharp transitions. The existence of these transitions suggests that a hybrid, discrete/continuous framework is well adapted for the description of the dynamics of large nonlinear systems with multiple time scales [27, 102, 103].

The notion of dominance can be exploited to obtain simpler models from larger models with multiple separated timescales and to assemble these simpler models into hybrid models. This notion is asymptotic and a natural mathematical framework to capture multiple asymptotic relations is the tropical geometry. Motivated by applications in mathematical physics [87], systems of polynomial equations [133], etc., tropical geometry uses a change of scale to transform nonlinear systems into discontinuous piecewise linear systems. The tropicalization is a robust property of the system, remaining constant for large domains of parameter values ; it can reveal qualitative stable features of the system's dynamics, such

as various types of attractors. Thus, the use of tropicalization to model large systems in molecular biology could be a promising solution to the problem of incomplete or imprecise information on the kinetic parameters.

In this chapter we provide some rigorous mathematical justifications for the idea of tropicalization.

3.2 General settings

In chemical kinetics, the reagent concentrations satisfy ordinary differential equations :

$$\frac{dx_i}{dt} = F_i(\mathbf{x}), \quad 1 \leq i \leq n. \quad (3.2.1)$$

Rather generally, the rates are rational functions of the concentrations and read

$$F_i(\mathbf{x}) = P_i(\mathbf{x})/Q_i(\mathbf{x}), \quad (3.2.2)$$

where $P_i(\mathbf{x}) = \sum_{\alpha \in A_i} a_{i,\alpha} \mathbf{x}^\alpha$, $Q_i(\mathbf{x}) = \sum_{\beta \in B_i} b_{i,\beta} \mathbf{x}^\beta$, are multivariate polynomials. Here $\mathbf{x}^\alpha = x_1^{\alpha_1} x_2^{\alpha_2} \dots x_n^{\alpha_n}$, $\mathbf{x}^\beta = x_1^{\beta_1} x_2^{\beta_2} \dots x_n^{\beta_n}$, $a_{i,\alpha}, b_{i,\beta}$, are nonzero real numbers, and A_i, B_i are finite subsets of \mathbb{N}^n .

The special case of mass action kinetics is represented by

$$F_i(\mathbf{x}) = P_i^+(\mathbf{x}) - P_i^-(\mathbf{x}), \quad (3.2.3)$$

where $P_i^+(\mathbf{x}), P_i^-(\mathbf{x})$ are Laurent polynomials with positive coefficients, $P_i^\pm(\mathbf{x}) = \sum_{\alpha \in A_i^\pm} a_{i,\alpha}^\pm \mathbf{x}^\alpha$, $a_{i,\alpha}^\pm > 0$, A_i^\pm are finite subsets of \mathbb{Z}^n .

In multiscale biochemical systems, the various monomials of the Laurent polynomials have different orders, and at a given time, there is only one or a few dominating terms. Therefore, it could make sense to replace Laurent polynomials with positive real coefficients $\sum_{\alpha \in A} a_\alpha \mathbf{x}^\alpha$, by max-plus polynomials $\exp\{\max_{\alpha \in A} [\log(a_\alpha) + \langle \log(\mathbf{x}), \alpha \rangle]\}$.

This heuristic can be used to associate a piecewise-smooth hybrid model to the system of rational ODEs (3.2.1), in two different ways.

The first method was proposed in [101] and can be applied to any rational ODE system defined by (3.2.1),(3.2.2) :

Definition 3.2.1. We call complete tropicalization of the smooth ODE system (3.2.1),(3.2.2) the following piecewise-smooth system :

$$\frac{dx_i}{dt} = \text{Dom}P_i(\mathbf{x})/\text{Dom}Q_i(\mathbf{x}), \quad (3.2.4)$$

where $\text{Dom}\left(\sum_{\alpha \in A_i} a_{i,\alpha} \mathbf{x}^\alpha\right) = \text{sign}(a_{i,\alpha_{max}}) \exp[\max_{\alpha \in A_i} \{\log(|a_{i,\alpha}|) + \langle \mathbf{u}, \alpha \rangle\}]$. $\mathbf{u} = (\log x_1, \dots, \log x_n)$, and $a_{i,\alpha_{max}}, \alpha_{max} \in A_i$ denote the coefficient of the monomial for which the maximum is attained. In simple words, Dom renders the monomial of largest absolute value, with its sign.

The second method, proposed in [119], applies to the systems (3.2.1),(3.2.3).

Definition 3.2.2. We call two terms tropicalization of the smooth ODE system (3.2.1),(3.2.3) the following piecewise-smooth system :

$$\frac{dx_i}{dt} = \text{Dom}P_i^+(\mathbf{x}) - \text{Dom}P_i^-(\mathbf{x}), \quad (3.2.5)$$

The two-terms tropicalization was used in [119] to analyse the dependence of steady states on the model parameters. The complete tropicalization was used for the study of the model dynamics and for the model reduction [101].

For both tropicalization methods, for each occurrence of the Dom operator, one can introduce a tropical manifold, defined as the subset of \mathbb{R}^n where the maximum in Dom is attained by at least two terms. For instance, for $n = 2$, such tropical manifold is made of points, segments connecting these points, and half-lines. The tropical manifolds in such an arrangement decompose the space into sectors, inside which one monomial dominates all the others in the definition of the reagent rates. The study of this arrangement give hints on the possible steady states and attractors, as well as on their bifurcations.

3.3 Justification of the tropicalization and some estimates

In the general case, the tropicalization heuristic is difficult to justify by rigorous estimates, however, this is possible in some cases. We state here some results in this direction. To simplify, let us consider the class of polynomial systems, corresponding to mass action law chemical kinetics :

$$\frac{dx_i}{dt} = P_i(\mathbf{x}, \epsilon) = \sum_{j=1}^{m_i} M_{ij}(\mathbf{x}, \epsilon), \quad M_{ij}(\mathbf{x}, \epsilon) = P_{ij}(\epsilon) \mathbf{x}^{\alpha_{ij}} \quad (3.3.1)$$

where α_{ij} are multi-indices, and ϵ is a small parameter. So, the right hand side of (3.3.1) is a sum of monomials. We suppose that coefficients P_{ij} have different orders in ϵ :

$$P_{ij}(\epsilon) = \epsilon^{\gamma_{ij}} \bar{P}_{ij}, \quad (3.3.2)$$

where $\gamma_{ij} \neq \gamma_{i'j'}$ for $(i, j) \neq (i', j')$.

We also suppose that the cone $\mathbf{R}_> = \{x : x_i \geq 0\}$ is invariant under dynamics (3.3.1) and initial data are positive :

$$x_i(0) > \delta > 0.$$

The terms (3.3.2) can have different signs, the ones with $\bar{P}_{ij} > 0$ are production terms, and those with $\bar{P}_{ij} < 0$ are degradation terms.

From the biochemical point of view, the choice (3.3.2) is justified by the fact that biochemical processes have many, well separated timescales. Furthermore, we are interested in biochemical circuits that can function in a stable way. More precisely, we use the permanency concept, borrowed from ecology (the Lotka -Volterra model, see for instance [136]).

Definition 3.3.1. *The system (3.3.1) is permanent, if there are two constants $C_- > 0$ and $C_+ > 0$, and a function T_0 , such that*

$$C_- < x_i(t) < C_+, \quad \text{for all } t > T_0(x(0)) \text{ and for every } i. \quad (3.3.3)$$

We assume that C_\pm and T_0 are uniform in (do not depend on) ϵ as $\epsilon \rightarrow 0$.

For permanent systems, we can obtain some results justifying the two procedures of tropicalization.

Proposition 3.3.2. *Assume that system (3.3.1) is permanent. Let x, \hat{x} be the solutions to the Cauchy problem for (3.3.1) and (3.2.4) (or (3.2.5)), respectively, with the same initial data :*

$$x(0) = \hat{x}(0).$$

Then the difference $y(t) = x(t) - \hat{x}(t)$ satisfies the estimate

$$|y(t)| < C_1 \epsilon^\gamma \exp(bt), \quad \gamma > 0, \quad (3.3.4)$$

where the positive constants C_1, b are uniform in ϵ . If the original system (3.3.1) is structurally stable in the domain $\Omega_{C_-, C_+} = \{x : C_- < |x| < C_+\}$, then the corresponding tropical systems (3.2.4) and (3.2.5) are also permanent and there is an orbital topological equivalence $\bar{x} = h_\epsilon(x)$ between the trajectories $x(t)$ and $\bar{x}(t)$ of the corresponding Cauchy problems. The homeomorphism h_ϵ is close to the identity as $\epsilon \rightarrow 0$.

The proof of the estimate (3.3.4) follows immediately by the Gronwall lemma. The second assertion follows directly from the definition of structural stability which means that orbits of the dynamical system are smoothly deformed under small perturbations.

Permanency property is not easy to check. In the case of systems (3.3.1) we can make a renormalization

$$x_i = \epsilon^{a_i} \bar{x}_i \quad (3.3.5)$$

and suppose that (3.3.3) holds for \bar{x}_i with C_i^\pm uniform in ϵ .

We seek for renormalization exponents a_i such that only a few terms dominate all the others, for each i -th equation (3.3.1) as $\epsilon \rightarrow 0$. Let us denote the number of terms with minimum degree in ϵ for i -th equation as m_i . Naturally, $1 \leq m_i \leq M_i$. After renormalization, we remove all small terms that have smaller orders in ϵ as $\epsilon \rightarrow 0$. We can call this procedure *tropical removing*. The system obtained can be named *tropically truncated system*.

Let us denote α_l^{ij} the l^{th} coefficient of the multi-index α_{ij} . If all $m_i = 1$ then we have the following truncated system

$$\frac{d\bar{x}_i}{dt} = \epsilon^{\mu_i} F_i(\bar{x}), \quad F_i(\bar{x}) = P_{ij(i)} \bar{x}^{\alpha^{ij(i)}}, \quad (3.3.6)$$

where

$$\mu_i = \gamma_{ij(i)} + \sum_{l=1}^n \alpha_l^{ij(i)} a_l - a_i \quad (3.3.7)$$

and

$$\mu_i > \gamma_{ij} + \sum_{l=1}^n \alpha_l^{ij} a_l - a_i \quad \text{for all } j \neq j(i). \quad (3.3.8)$$

If all $m_i = 2$, in order to find possible renormalization exponents a_i , it is necessary to resolve a family of linear programming problem. Each problem is defined by a set of pairs $(j(i), k(i))$ such that $j(i) \neq k(i)$. We define μ_i by

$$\mu_i = \gamma_{ij(i)} + \sum_{l=1}^n \alpha_l^{ij(i)} a_l - a_i = \gamma_{ik(i)} + \sum_{l=1}^n \alpha_l^{ik(i)} a_l - a_i \quad (3.3.9)$$

and obtain the system of the following inequalities

$$\mu_i \geq \gamma_{ij} + \sum_{l=1}^n \alpha_l^{ij} a_l - a_i \quad \text{for all } j \neq j(i), k(i). \quad (3.3.10)$$

The following straightforward lemma gives a necessary condition of permanency of the system (3.3.1).

Lemma 3.3.3. *Assume a tropically truncated system is permanent. Then, for each $i \in \{1, \dots, n\}$, the i -th equation of this system contains at least two terms. The terms should have different signs for coefficients p_{ij} , i.e., one term should be a production one, while another term should be a degradation term.*

Démonstration. Let us suppose that $m_i = 1$ for some i , or $m_i > 1$, but all terms have the same sign s . Let us consider this equation. Then one has, for $s = 1$,

$$\frac{dx_i}{dt} > \epsilon^{\mu_i} \delta_i(C^-, C^+) > 0.$$

Therefore, $x_i(t) > \delta t + x_i(0)$ and the system cannot be permanent. If $s = -1$, then

$$\frac{dx_i}{dt} < -\epsilon^{\tilde{\mu}_i} \delta_i(C^-, C^+) < 0.$$

Again it is clear that the system cannot be permanent. \square

We call “tropical equilibration”, the condition in Lemma 3.3.3. This condition means that permanency is acquired only if at least two terms of different signs have the maximal order, for each equation of the system (3.3.1). This idea is not new, and can be traced back to Newton.

The tropical equilibration condition can be used to determine the renormalization exponents, by the following algorithm.

Step 1. For each i let us choose a pair $(j(i), k(i))$ such that $j, k \in \{1, \dots, M_i\}$ and $j < k$. The sign of the corresponding terms should be different.

Step 2. We resolve the linear system of algebraic equations

$$\gamma_{ij(i)} - \gamma_{ik(i)} = - \sum_{l=1}^n \alpha_l^{ij(i)} a_l + \sum_{l=1}^n \alpha_l^{ik(i)} a_l, \quad (3.3.11)$$

for a_l , together with the inequalities (3.3.10).

Notice that although that Step 2 has polynomial complexity, the tropical equilibration problem has a number of choices that is exponential in the number of variables at Step 1.

Assume that, as a result of this procedure, we obtain the system

$$\frac{d\bar{x}_i}{dt} = \epsilon^{\mu_i} (F_i^+(\bar{x}) - F_i^-(\bar{x})), \quad F_i^\pm = P_{ij^\pm} \bar{x}^{\alpha_\pm^{ij}}. \quad (3.3.12)$$

One can expect that, in a “generic” case¹, all μ_i are mutually different, namely

$$0 = \mu_1 < \mu_2 < \dots < \mu_{n-1} < \mu_n. \quad (3.3.13)$$

We can now state a sufficient condition for permanency. Let us consider the first equation (3.3.12) with $i = 1$ and let us denote $y = \bar{x}_1, z = (\bar{x}_2, \dots, \bar{x}_n)^{tr}$. In this notation, the first equation becomes

$$\frac{dy}{dt} = f(y) = b_1(z)y^{\beta_1} - b_2(z)y^{\beta_2}, \quad b_1, b_2 > 0, \quad \beta_i \in \mathbf{R}. \quad (3.3.14)$$

Since $\mu_2 > 0$, one has that $z(t)$ is a slow function of time and thus we can suppose that b_i are constants (this step can be rendered rigorous by using the concept of invariant manifold

1. supposing that multi-indices α_{ij} are chosen uniformly, by generic we understand almost always except for cases of vanishing probability, see also [57]

and methods from [67]). The permanency property can be then checked in an elementary way. All rest points of (3.3.14) are roots of f . If $f > 0$, $y(t)$ is an increasing time function and if $f < 0$, $y(t)$ is a decreasing time function. A single root y_1 of f within $(0, +\infty)$ is given by

$$y_1 = \left(\frac{b_2}{b_1} \right)^d, \quad d = \frac{1}{\beta_1 - \beta_2}. \quad (3.3.15)$$

These properties entail the following result :

Lemma 3.3.4. *Equation 3.3.14 has the permanence property if and only if*

$$\beta_1 < \beta_2.$$

For fixed z , in these cases we have

$$y(t, z) \rightarrow y_0, \quad \text{as } t \rightarrow \infty.$$

Démonstration. Consider the function $f(y) = b_1 y^{\beta_1} - b_2 y^{\beta_2}$. Under the condition $\beta_1 < \beta_2$, f is negative for sufficiently large $y > 0$, and positive for sufficiently small $y > 0$. Moreover, f has a single positive root y_1 on $(0, +\infty)$. Therefore, all the trajectories of $dy/dt = f(y)$ tends to y_* as $t \rightarrow \infty$ and, for any $\delta > 0$, the interval $(y_1 - \delta, y_1 + \delta)$ is a trapping domain. This proves the permanency. \square

Remark. One can easily show that the condition of the Lemma 3.3.4 is weaker than the condition (2.5.3) for having sliding modes on the tropical manifold (see previous chapter). This means that for each sliding mode one has a stable equilibriums.

The generic situation described by the conditions (3.3.13) lead to trivial “chain-like” relaxation towards a point attractor, provided that we have permanency at each step. More precisely, all the variables have separate timescales and dissipative dynamics. The fastest variable relaxes first, then the second fastest one, and so forth, the chain of relaxations leading to a steady state. This result is the nonlinear analogue of the similar result mentioned in the previous chapter, that monomolecular networks with total separation relax as chains and can only have stable point attractors (see also [57]).

The following theorem describes a less trivial situation, when timescales are not totally separated and limit cycles are possible.

Theorem 3.3.5. *Assume $0 = \mu_1 < \mu_2 < \dots < \mu_{n-1} \leq \mu_n$ holds. If the procedure, described above, leads to the permanency property at each step, where $i = 1, 2, \dots, n-2$, and the last two equations have a globally attracting hyperbolic rest point or globally attracting hyperbolic limit cycle, then the tropically truncated system is permanent and has an attractor of the same type. Moreover, for sufficiently small ϵ the initial system also is permanent for initial data from some appropriate domain $W_{\epsilon,a,A}$ and has an analogous attracting hyperbolic rest point (limit cycle) close to the attractor of the truncated system. If the rest point (cycle) is not globally attracting, then we can say nothing on permanency but, for sufficiently small ϵ , the initial system still has an analogous attracting hyperbolic rest point (limit cycle) close to the attractor of truncated system and the same topological structure.*

Démonstration. **i** Suppose that the tropically truncated system (TTS) has a globally attracting compact invariant set \mathcal{A} . Let Π be an open neighborhood of this set. We can choose this neighborhood as a box that contains \mathcal{A} . Then, for all initial data $x(0)$, the

corresponding trajectory $x(t), x(0)$ lies in Π for all $t > T_0(x_0, \Pi)$. Therefore, our TTS is permanent. Here we do not use the fact that the cycle (rest point) is hyperbolic.

ii Permanency of the initial system follows from hyperbolicity of \mathcal{A} . Hyperbolic sets are persistent (structurally stable) (Ruelle 1989). Since this set is globally attracting, all TTS is structurally stable (as a dynamical system). This implies that the initial system has a hyperbolic attractor close to \mathcal{A} , since initial system is a small perturbation of TTC in Π .

iii If the set \mathcal{A} is only locally attracting, the last assertion of Theorem follows from persistency of hyperbolic sets. \square

Finally, let us note that tropical equilibrations with permanency imply the existence of invariant manifolds. This allows to reduce the number of variables of the model while preserving good accuracy in the description of the dynamics. The following Lemma is useful in this aspect.

Lemma 3.3.6. *Consider the system*

$$\frac{dy}{dt} = f(y) = b_1(z)y^{\beta_1} - b_2(z)y^{\beta_2}, \quad b_1, b_2 > \delta_1 > 0, \quad \beta_i \in \mathbf{R}. \quad (3.3.16)$$

$$\frac{dz}{dt} = \lambda F(y, z), \quad (3.3.17)$$

where $z \in \mathbf{R}^m$, $\lambda > 0$ is a parameter and the function F enjoys the following properties. This function lies in an Hölder class

$$F \in C^{1+r}, \quad r > 0,$$

and the corresponding norms are uniformly bounded in $\Omega = (0, +\infty) \times W$, for some open domain $W \subset \mathbf{R}^m$:

$$|F|_{C^{1+r}(\Omega)} < C_2.$$

Assume that the condition of Lemma 3.3.4 holds. We also suppose that b_i are smooth functions of z for all z such that $|z| > \delta_0 > 0$. Assume that $z \in W$ implies $|z| > \delta_0$.

Then, for sufficiently small $\lambda < \lambda_0(C_2, b_1, b_2, \beta_1, \beta_2, \delta)$ equations (3.3.16), (3.3.18) have a locally invariant and locally attracting manifold

$$y = Y(z, \lambda), \quad Y \in C^{1+r}(W), \quad (3.3.18)$$

and Y has the asymptotics

$$Y(z, \lambda) = y_1(z) + \tilde{Y}, \quad \tilde{Y} \in C^{1+r}(W), \quad (3.3.19)$$

where

$$|\tilde{Y}(z, \lambda)|_{C^{1+r}(W)} < C_s \lambda^s, \quad s > 0. \quad (3.3.20)$$

Démonstration. This lemma can be derived from Theorem A of the Appendix to this section (that is a simplified version of Theorem 9.1.1 from [67], Ch. 9). Let us check assumptions of Theorem A.

Definition of the operator $A(z)$ and function G . Let $y_0(z)$ be the unique stable root of equation

$$h(z, y) = b_1(z)y^{\beta_1} - b_2(z)y^{\beta_2} = 0.$$

The operator A is the multiplication operator

$$A(z)y = h_y(z, y)|_{y=y_0(z)}y.$$

Since we assume that b_i are smooth, it is bounded linear operator, thus, it is a sectorial one. We set

$$G = h(z, y) - A(z)y.$$

Definition of the function $Q(z)$ and \tilde{Q} . We define

$$Q = \lambda F(y_0(z), z), \quad \tilde{Q} = \lambda(F - Q).$$

The point (i). Is obvious since all functions are smooth.

The point (ii). We consider a difference of two solutions of equation

$$\frac{dz}{dt} = Q(z).$$

This gives

$$\mu < C\lambda, \quad M_1 = 1.$$

The point (iii). The inequality

$$\|y(t)\| \leq \exp(-\beta t)\|y(0)\|$$

for solution of $dy/dt = A(z)y$ holds for some $\beta > 0$ due to stability of the root $y_0(z)$. Moreover, we notice that β does not depend on λ and thus, $\beta > 2\mu$ for sufficiently small λ .

The point (iv). We take $\theta = 1$. The condition $(1 + \theta)\mu < \beta$ holds for sufficiently small λ (see above).

The point (v). Let us show that constant κ can be estimated as $\kappa < C\lambda$. Let us consider a time interval $(0, c \log(\lambda))$. Within this interval, the solution y of 3.3.16 with $z = z(0)$ enters a $O(\lambda)$ - neighborhood of the point $y_0(z_0)$.

For $t > c \log(\lambda)$, let us make substitution $y = y_0(z) + \tilde{y}$, where \tilde{y} is a new unknown. Then the equation for y takes the following form :

$$\frac{d\tilde{y}}{dt} = A(z)\tilde{y} + g(\tilde{y}) - \lambda y'_0(z)F(y, z).$$

where $|g| < \tilde{y}^2$. This equation implies that

$$|\tilde{y}| < c_1 \lambda$$

for all $t > c \log(\lambda)$. From the last estimate we conclude that κ can be chosen as $O(\lambda)$.

Therefore, all conditions of Theorem A hold and an invariant C^{1+r} smooth manifold exists.

Eq.(3.3.20) results directly from Theorem 9.1.1 from [67], Ch. 9.

□

3.4 Geometry of tropical equilibrations

In this section we provide a geometrical interpretation of tropical equilibrations. We consider networks of biochemical reactions with mass action kinetic laws. This framework has already been introduced in the previous chapter. To simplify notations with respect to (2.2.1), (2.2.2), we consider only one index j per reaction. The reaction rate reads

$$R_j(\mathbf{x}) = k_j \mathbf{x}^{\alpha_j}. \quad (3.4.1)$$

In this notation, reversible reactions will count for two reactions, one for each direction. The network dynamics is described as follows

$$\frac{d\mathbf{x}}{dt} = \sum_j k_j (\beta_j - \alpha_j) \mathbf{x}^{\alpha_j}. \quad (3.4.2)$$

where $\beta_j, \alpha_j \in \mathbb{Z}_+^n$ are stoichiometric vectors (defining the type and numbers of molecules produced and consumed by reaction j , respectively).

After parameters and variables rescaling, $k_j = \bar{k}_j \epsilon^{\gamma_j}$, $\mathbf{x} = \bar{\mathbf{x}} \epsilon^{\mathbf{a}}$ we obtain

$$\frac{d\bar{\mathbf{x}}}{dt} = \left(\sum_j \epsilon^{\mu_j} k_j (\beta_j - \alpha_j) \bar{\mathbf{x}}^{\alpha_j} \right) \epsilon^{-\mathbf{a}}, \quad (3.4.3)$$

where $(\epsilon^{-\mathbf{a}})_i = \epsilon^{-a_i}$, and

$$\mu_j = \gamma_j + \langle \mathbf{a}, \alpha_j \rangle. \quad (3.4.4)$$

Definition 3.4.1. Two reactions j, j' are equilibrated on the species i iff :

- i) $\mu_j = \mu_{j'}$,
- ii) $(\beta_j - \alpha_j)_i (\beta_{j'} - \alpha_{j'})_i < 0$,
- iii) $\mu_k < \mu_j$ for any reaction $k \neq j, j'$, such that $(\beta_k - \alpha_k)_i \neq 0$.

Remark. According to (3.4.4) and Definition 3.4.1, the equilibrations correspond to vectors $\mathbf{a} \in \mathbb{R}^n$ where $\max_j (\gamma_j + \langle \mathbf{a}, \alpha_j \rangle)$ is attained at least twice.

Let us consider the equality $\mu_j = \mu_{j'}$. This represents the equation of a $n-1$ dimensional hyperplane of \mathbb{R}^n , orthogonal to the vector $\alpha_j - \alpha_{j'}$:

$$\gamma_j + \langle \mathbf{a}, \alpha_j \rangle = \gamma_{j'} + \langle \mathbf{a}, \alpha_{j'} \rangle \quad (3.4.5)$$

For each species i , we consider the set of reactions \mathcal{R}_i that act on this species, namely $k \in \mathcal{R}_i$ iff $(\beta_k - \alpha_k)_i \neq 0$. The finite set \mathcal{R}_i can be characterized by the corresponding set of α_k that are vectors with positive integer coefficients in \mathbb{R}^n .

The piecewise affine function $f_i(\mathbf{a}) = \max_j (\gamma_j + \langle \mathbf{a}, \alpha_j \rangle)$ defined from \mathbb{R}^n to \mathbb{R} represents the *Legendre transformation* of the function $\nu_i(\alpha_j) = -\gamma_j$ defined from \mathcal{R}_i to \mathbb{R} .

The set of points of \mathbb{R}^n where at least two reactions equilibrate on the species i corresponds to the places where f_i is not locally affine (the maximum in the definition of f_i is attained at least twice).

For each species, we also define the Newton polytope \mathcal{N}_i , that is the convex hull of the vectors $\alpha_k, k \in \mathcal{R}_i$. The hyperplanes defined by (3.4.5) and corresponding to equilibrations of two reactions on the same species i are orthogonal to edges of the Newton polytope \mathcal{N}_i . \mathcal{N}_i is also the Newton polytope of the polynomial $P_i(\mathbf{x}) = \sum_j k_j (\beta_{ji} - \alpha_{ji}) \mathbf{x}^{\alpha_j}$ that defines the rhs of the ordinary differential equation satisfied by the species i .

We can now state the following

Proposition 3.4.2. *There is a bijection between the locus \mathcal{T}_i of vectors \mathbf{a} where the tropical polynomial $f_i(\mathbf{a})$ is not linear and the tropical manifold of the polynomial $P_i(\mathbf{x})$ that defines the rhs of the ordinary differential equation satisfied by the species i . The reaction equilibrations correspond to vectors \mathbf{a} included in \mathcal{T}_i but satisfying also the condition ii) of Definition 3.4.1.*

Remarks. This property can be used to put into correspondence reaction equilibrations and slow invariant manifolds. Indeed, if a reaction equilibration exists, this leads to a slow manifold that (on logarithmic paper) is close to some parts of the tropical manifold of $P_i(\mathbf{x})$. For instance, a reaction equilibration described by (3.4.5) will correspond to an invariant manifold close to a hyperplane orthogonal to $\alpha_j - \alpha_{j'}$. The condition ii) of Definition 3.4.1 is needed for equilibrium (the equilibrated reactions have to have opposite effects on the species i , one has to produce and the other has to consume the species). Without this condition, the dynamics would simply cross the tropical manifold with no deviation. However, the condition ii) is not sufficient for stability of the equilibration. A sufficient stability condition is the one given by Lemma 3.3.4 or the sliding mode condition (2.5.3) introduced in the previous chapter.

3.5 Tropical approach to the permanency problem

We have shown in the previous sections that tropical ideas can be used to simplify complex systems, by tropical removing. During this procedure, permanency has to be checked at intermediate steps on tropically truncated systems. Lemma 3.3.4 allows to check permanency for toric systems with separation. We provide here a more general approach to permanency. We consider only upper estimates. The lower estimates can be found in a similar way.

For permanent systems we obtain some rigorous results for the two procedures of tropicalization. The complete tropicalization of the system (3.3.1) reads

$$\frac{d\bar{x}_i}{dt} = Dom_R(F_i(\bar{x})), \quad (3.5.1)$$

where $Dom_R(F_i) = F_{ik(i)}(\mathbf{x}, \epsilon)$, $|F_{ik(i)}(\mathbf{x}, \epsilon)| > |F_{ij}(\mathbf{x}, \epsilon)|$, $j \neq k_i$ is the dominant term.

Let us first formulate a Lemma.

Lemma 3.5.1. *Assume that non-tropicalized system (3.3.1) has a smooth Lyapunov function $V(\mathbf{x})$ defined on the cone $\mathbf{R}_{>}^n$ such that*

$$dV(x(t))/dt \leq 0 \quad (3.5.2)$$

on trajectories $\mathbf{x}(t) = (x_1(t), \dots, x_n(t))$ of (3.3.1) and

$$V(\mathbf{x}) \rightarrow \infty \text{ as } |\mathbf{x}| \rightarrow \infty. \quad (3.5.3)$$

Then, if $x \in \Pi$ there is a constant $C_0(C, \delta')$ such that

$$|x(t)| < C_0, \quad t > 0. \quad (3.5.4)$$

Démonstration. Indeed, if $|x(t)|$ are unbounded as $t \rightarrow +\infty$, one has $\sup_{t>0} V(x(t)) = +\infty$, but (3.5.2) entails $V(x(t)) \leq V(x(0))$. \square

Let us consider the tropical version (3.5.1) of (3.3.1). Assume that the tropicalization has a "strong" Lyapunov function $V^{tr}(x)$. For a vector field F this function satisfies

$$dV^{tr}(x(t))/dt \leq -\kappa |\nabla V^{tr}(x(t))| |F(x(t))|, \quad \kappa > 0 \quad (3.5.5)$$

on trajectories $\mathbf{x}(t) = (x_1(t), \dots, x_n(t))$ of (3.3.1) and

$$V^{tr}(\mathbf{x}) \rightarrow \infty \quad \text{as} \quad |\mathbf{x}| \rightarrow \infty. \quad (3.5.6)$$

Here $x \in \mathbf{R}_{>}^n$.

Such a function can be found for some tropical versions of two component systems. For example, if

$$dx/dt = k_1 x^a y^b, \quad (3.5.7)$$

$$dy/dt = -k_2 x^a y^b, \quad (3.5.8)$$

where $a, b > 0$ and $k_1, k_2 > 0$, we can define V^{tr} by

$$V = x + \beta y, \quad (3.5.9)$$

where $\beta k_2 > k_1$. Then $\nabla V = (1, \beta)$, and (3.5.5), (3.5.6) hold.

Lemma 3.5.2. Assume tropicalized system (3.5.1) has a smooth Lyapunov function $V^{tr}(\mathbf{x})$ defined on the cone $\mathbf{R}_{>}^n$ such that (3.5.5), (3.5.6) hold.

Then, if $x \in \Pi$ there is a constant $C_0(C, \delta')$ such that solutions of non-tropicalized system (3.3.1)

$$|x(t)| < C_0, \quad t > 0. \quad (3.5.10)$$

Démonstration. Let us compute the derivative dV^{tr}/dt on trajectories of the initial (non-tropicalized) system. We have the relation

$$dV^{tr}(x(t))/dt = \nabla V^{tr}(x(t)) \cdot F^{tr}(x(t)) + \nabla V^{tr}(x(t)) \cdot \tilde{F}(x(t)), \quad (3.5.11)$$

where $\tilde{F} = F - F^{tr}$, and F^{tr} denotes the tropical part of the vector field F , \tilde{F} contains, thus, all the rest terms.

Using the definition of strong Lyapunov functions, from (3.5.11) one has

$$dV^{tr}(x(t))/dt \leq |\nabla V^{tr}(x(t))| (-\kappa |F^{tr}(x(t))| + |\tilde{F}(x(t))|). \quad (3.5.12)$$

But for large $|x|$ one has $|\tilde{F}(x)| < \kappa$. Therefore, (3.5.12) gives then

$$dV^{tr}(x(t))/dt \leq 0. \quad (3.5.13)$$

This shows that $|x(t)|$ cannot increase to $+\infty$, and finishes the proof. \square

3.6 Appendix : Theorems on invariant manifolds

Let us formulate two theorems on invariant manifold existence. The first theorem A, is a particular case of Theorem 9.1.1 from [67] that is sufficient for our goals (it applies to the time autonomous case, and considers that the slow dynamics is finite dimensional). The second one is a simplified, time autonomous variant of Theorem 6.1.7 [67].

Let us consider the system

$$z_t = Q(z) + \tilde{Q}(z, y), \quad (3.6.1)$$

$$y_t = A(z)y + G(z, y), \quad (3.6.2)$$

where $z = (z_1, \dots, z_n)$ lies in \mathbf{R}^n and y lies in a Banach space B . Assume the sectorial operator A has the form

$$A(z) = A_0 + \tilde{A}(z).$$

In the system (3.6.1), (3.6.2) the variable z is a slow one whereas y is a fast variable.

Theorem A. *Let B be a Banach space and A_0 be a sectorial operator in B , $z \in \mathbf{R}^n$. Assume $A(z)$ is an operator such that*

$$A(z) - A_0 = \tilde{A} : \mathbf{R}^n \rightarrow \mathcal{L}(B^\alpha, B) \quad (3.6.3)$$

is bounded differentiable with respect to z map, U is a neighborhood of 0 in B^α and

$$G, Q, \tilde{Q} : \mathbf{R}^n \times U \rightarrow B \times \mathbf{R}^n \times \mathbf{R}^n \quad (3.6.4)$$

are bounded and differentiable with respect to y, z maps, Q depends only on z .

Moreover, let us assume that the following conditions are satisfied :

- i** *The maps $\tilde{A}, G, Q, \tilde{Q}$ are C^1 differentiable with respect to z and y ;*
- ii** *There are constants $M_1, \mu > 0$ such that*

$$|z_1(t) - z_2(t)| \leq M_1 \exp(\mu|t|)|z_1(0) - z_2(0)| \quad (3.6.5)$$

if z_1, z_2 satisfy the non-perturbed equation $z_t = Q(z)$;

- iii** *For the operator A we have a trivial exponential dichotomy, i.e., if*

$$y_t = A(z(t))y$$

then

$$\|y(t)\| \leq M \exp(-\beta t) \|y(0)\|, \quad \beta > \mu, \quad (3.6.6)$$

if z satisfies the non-perturbed equation $z_t = Q(z)$;

iv *the maps $\tilde{Q}, \tilde{Q}_z, \tilde{Q}_y, Q_z, \tilde{A}$ and A_z are uniformly bounded in the corresponding norms by the number M_0 and there is a number $\theta \in (0, 1]$ such that*

$$\mu(1 + \theta) < \beta$$

and the map $(y, z) \rightarrow G_y, G_z, \tilde{Q}_y, \tilde{Q}_z, Q_z, A_z$ lies in the Holder class with the exponent θ and the constant M_2 ;

- v** *for some κ one has the estimate*

$$\|G(z, 0)\| < \kappa, \quad \|G_z(z, 0)\| < \kappa, \quad \|\tilde{Q}\| < \kappa. \quad (3.6.7)$$

Then for sufficiently small positive κ and r_0 that depend only on $\beta, A_0, \mu, \theta, \beta - \mu(1 + \theta)$ and M_i there exists an invariant manifold

$$y = Y(z), \quad Y \in C^1$$

which is a maximal invariant subset of the set

$$\|y\|_\alpha < r_0$$

and such that

$$\|Y\|, \|Y_z\| \rightarrow 0 \quad \text{as } \kappa \rightarrow 0. \quad (3.6.8)$$

Theorem B. Let us consider (3.6.1), (3.6.2) where $A(z) = A$ does not depend on z . Assume that for some $\beta > 0$

$$\|exp(At)v\| \leq M\|v\| \exp(-\beta t), \quad \|exp(At)v\|_\alpha \leq M\|v\|t^{-\alpha} \exp(-\beta t), \quad t > 0. \quad (3.6.9)$$

Let us denote $\bar{Q}(z, y) = Q + \tilde{Q}$. Assume (3.6.4) holds, $Q, G \in C^{1+r}$, $r \in (0, 1)$ and in $Y = \mathbf{R}^n \times U$

$$\sup \|G\| < C_G, \quad \|G(z_1, y_1) - G(z_2, y_2)\| \leq \lambda(\|z_1 - z_2\| + \|y_1 - y_2\|). \quad (3.6.10)$$

Let us denote

$$\mu = \sup_{(z,y) \in Y} \|D_z \bar{Q}\|, \quad M_2 = \sup_{(z,y) \in Y} \|D_y\|. \quad (3.6.11)$$

Let us denote

$$\Theta_1(\Delta) = \lambda M \int_0^\infty u^{-\alpha} \exp(-(\beta - \mu_1)u) du, \quad \mu_1 = \mu + \Delta M_2.$$

Suppose that for some Δ and R_0 the following conditions and inequalities holds

$$\{v : \|v\|_\alpha < R_0\} \subset U, \quad MC_G \int_0^\infty u^{-\alpha} \exp(-\beta u) du < R_0, \quad (3.6.12)$$

$$\beta/2 > \mu_1, \quad \Theta_1 < \Delta/(1 + \Delta), \quad (3.6.13)$$

and

$$\Theta_1 \max\{1, \frac{(1 + \Delta)M_2}{\mu_1}\} < 1. \quad (3.6.14)$$

Then there is an invariant manifold

$$y = Y(z), \quad z \in \mathbf{R}^n \quad (3.6.15)$$

such that

$$\|Y(z)\| < R_0, \quad \|Y(z_1) - Y(z_2)\| \leq \Delta|z_1 - z_2|. \quad (3.6.16)$$

Chapitre 4

Two paradigmatic cell cycle models and their tropicalization

4.1 Description of the models

The two paradigmatic cell cycle models date both from the early 90'.

The first one (Model 1) is the cell cycle model proposed by Tyson [140]. This model mimics the interplay between cyclin and cyclin dependent kinase cdc2 (forming the maturation promoting factor MPF complex) during the progression of the cell cycle. The model demonstrates that this biochemical system can function as an oscillator, or converge to a steady state with large MPF concentration, or behave as an excitable switch. The three regimes can be associated to early embryos rapid division, metaphase arrest of unfertilized eggs, and growth controlled division of somatic cells, respectively. This model takes into account autocatalytic activity of MPF (positive feed-back). It can be described as a nonlinear cycle of biochemical reactions and corresponds to the following set of differential equations :

$$\begin{aligned} y'_1 &= \epsilon^{-3}k_9y_2 - \epsilon^{-6}k_8y_1 + k_6y_3, & y'_2 &= \epsilon^{-6}k_8y_1 - \epsilon^{-3}k_9y_2 - \epsilon^{-2}k_3y_2y_5, \\ y'_3 &= \epsilon^2k'_4y_4 + \epsilon^{-2}k_4y_4y_3^2 - k_6y_3, & y'_4 &= -\epsilon^2k'_4y_4 - \epsilon^{-2}k_4y_4y_3^2 + \epsilon^{-2}k_3y_2y_5, \\ y'_5 &= \epsilon^2k_1 - \epsilon^{-2}k_3y_2y_5, \end{aligned} \tag{4.1.1}$$

Here $k_i > 0$ are rate constants, y_i , $i \in [1, 5]$ are concentrations of cdc2, p-cdc2 (phosphorylated kinase), cyclin-p :cdc2 complex (active MPF), cyclin-p :cdc2-p complex (inactive MPF), and cyclin, respectively. With respect to the original model we have introduced a small parameter $\epsilon > 0$ to cope with the order of the rate constants. The values of the constants in the original models are given in the Table 4.1. The renormalized constants k_i are all of order one.

The system (4.1.1) has the conservation law

$$y_1(t) + y_2(t) + y_3(t) + y_4(t) = 1, \tag{4.1.2}$$

where the value 1 (total initial concentration of kinase cdc2) was chosen by convenience.

The second model (Model 2), proposed by Goldbeter [48], also mimics a minimal mitotic oscillator. This oscillator is based on a cascade of post-transcriptional modification that modulates the activity of the kinase cdc2. As cyclin progressively increases, it activates the MPF complex, that triggers cyclin degradation and mitosis. The cyclin degradation is

Constant	Value	γ_i	Renormalized value
k_1	0.015	2	1.5
k_3	200	-2	2
k_4	180	-2	1.8
k'_4	0.018	2	1.8
k_6	1	0	1
k_8	1000000	-6	1
k_9	1000	-3	1

TABLE 4.1 – Parameters of the cell cyle model 1, from [140]. These were renormalized by powers of a small positive parameter ϵ^{γ_i} (here $\epsilon = 0.1$). The powers γ_i where chosen such that all renormalized parameters are of order one. The units of time are minutes, and concentration units are arbitrary.

not triggered directly by MPF, but by an third variable (a cyclin protease), activated by MPF.

In the original model the substrate dependence of post-transcriptional modifications are described by Michaelis-Menten kinetics. Furthermore, to cope with situations when one has large amounts of enzyme, the author represented the dependence of the V_{max} parameter on the enzyme concentration by a second Michaelis-Menten function. The original model is described by the following equations :

$$C' = \nu_i - \nu_d X \frac{C}{K_d + C} - k_d C, \quad (4.1.3)$$

$$M' = V_{M1} \frac{C}{K_c + C} \frac{1 - M}{K_1 + 1 - M} - V_2 \frac{M}{K_2 + M}, \quad (4.1.4)$$

$$X' = V_{M3} M \frac{1 - X}{K_3 + (1 - X)} - V_4 \frac{X}{K_4 + X}. \quad (4.1.5)$$

Here, the variable C represents the cyclin, M the active MPF complex, and X is the active cyclin protease.

Using numerical simulations with the parameters proposed in the original paper we realized that several enzymatic processes such as the degradation of cyclin, the activation of MPF, and the activation of the protease works at substrate saturation. Therefore, we have approximated the corresponding Michaelis-Menten functions by constants, and obtained the following, simpler, equations (Model 2) :

$$y'_1 = k_1 \epsilon - k_2 \epsilon^3 y_3 - k_3 \epsilon^2 y_1, \quad (4.1.6)$$

$$y'_2 = k_4 \epsilon^{-3} \frac{y_1}{1 + y_1} - k_5 \epsilon^{-3} \frac{y_2}{1 + y_2}, \quad (4.1.7)$$

$$y'_3 = k_6 y_2 - \epsilon^{-2} k_7 \frac{y_3}{1 + y_3}. \quad (4.1.8)$$

The renormalized variables are defined as $y_1 = C/K_c$, $y_2 = M/K_2$, and $y_3 = X/K_4$. Like in the case of Tyson's model (model 1) we have introduced a small parameter $\epsilon > 0$ to cope with the order of the rate constants. The values of the constants in the original models are given in the Table 4.2. The renormalized constants k_i are all of order one.

Constant	Value	γ_i	Renormalized value
k_1	0.05	1	0.5
k_2	0.0025	3	2.5
k_3	0.001	2	1
k_4	600	-3	0.6
k_5	300	-2	3
k_6	1	0	1
k_7	100	-2	1

TABLE 4.2 – Parameters of the cell cycle model 2, adapted from [48]. These were renormalized by powers of a small positive parameter ϵ^{γ_i} (here $\epsilon = 0.1$). The powers γ_i were chosen such that all renormalized parameters are of order one. Rescaled concentrations are dimensionless and time units are minutes.

4.2 Tropical equilibrations and model reduction of model 1

Let us apply the tropical equilibration principle. To this aim, we renormalize the variables,

$$y_i = \epsilon^{a_i} \bar{y}_i. \quad (4.2.1)$$

Let us substitute these relations into the system of equations. As a result, we obtain

$$\begin{aligned} \bar{y}'_1 &= \epsilon^{-3+a_2-a_1} k_9 \bar{y}_2 - \epsilon^{-6} k_8 \bar{y}_1 + k_6 \epsilon^{a_3-a_1} \bar{y}_3, & \bar{y}'_2 &= \epsilon^{-6+a_1-a_2} k_8 \bar{y}_1 - \epsilon^{-3} k_9 \bar{y}_2 - \epsilon^{-2+a_5} k_3 \bar{y}_2 \bar{y}_5, \\ \bar{y}'_3 &= \epsilon^{2+a_4-a_3} k'_4 \bar{y}_4 + \epsilon^{-2+a_3+a_4} k_4 \bar{y}_4 \bar{y}_3^2 - k_6 \bar{y}_3, & \bar{y}'_4 &= -\epsilon^2 k'_4 \bar{y}_4 - \epsilon^{-2+2a_3} k_4 \bar{y}_4 \bar{y}_3^2 + \epsilon^{-2+a_2+a_5-a_4} k_3 \bar{y}_2 \bar{y}_5, \\ \bar{y}'_5 &= \epsilon^{2-a_5} k_1 - \epsilon^{-2+a_2} k_3 \bar{y}_2 \bar{y}_5. \end{aligned} \quad (4.2.2)$$

The system (4.2.2) has the conservation law

$$\epsilon^{a_1} \bar{y}_1(t) + \epsilon^{a_2} \bar{y}_2(t) + \epsilon^{a_3} \bar{y}_3(t) + \epsilon^{a_4} \bar{y}_4(t) = 1. \quad (4.2.3)$$

In order to compute the exponents a_i we use tropical equilibrations together with the conservation law (4.2.3). There are 2^4 variants of tropical equilibrations. To our surprise, we found that there is only one solution for the exponents values. We can show that all possible equilibrations of the variables y_3 , y_4 and y_5 uniquely set the values of two exponents, $a_3 = 2$, $a_4 = 0$.

Let us consider the variants with respect to the equilibrations of the variables y_1 and y_2 . Denoting by T_i the i^{th} term in the equation, we have the following situations :

- 1) In eq. for $\bar{y}_1 : T_1 = T_2$, $T_3 \leq T_1$, In eq. for $\bar{y}_2 : T_1 = T_2$, $T_3 \leq T_1$.
- 2) In eq. for $\bar{y}_1 : T_1 = T_2$, $T_3 \leq T_1$, In eq. for $\bar{y}_2 : T_1 = T_3$, $T_2 \leq T_3$.
- 3) In eq. for $\bar{y}_1 : T_2 = T_3$, $T_1 \leq T_2$, In eq. for $\bar{y}_2 : T_1 = T_2$, $T_3 \leq T_1$.
- 4) In eq. for $\bar{y}_1 : T_2 = T_3$, $T_1 \leq T_2$, In eq. for $\bar{y}_2 : T_1 = T_3$, $T_2 \leq T_1$.

In the variant 1 (Case **I**) the tropical equilibrations do not fix the values of the exponent a_5 and we get

$$a_1 = 7 - a_5, \quad a_2 = 4 - a_5, \quad a_3 = 2, \quad a_4 = 0, \quad a_5 \geq -1. \quad (4.2.4)$$

In the variants 2,3,4 (Case **II**) the exponents are uniquely determined from equilibrations and we obtain

$$a_1 = 8, \quad a_2 = 5, \quad a_3 = 2, \quad a_4 = 0, \quad a_5 = -1. \quad (4.2.5)$$

However, (4.2.5) and the conservation law (4.2.3) are incompatible. Indeed, (4.2.5) implies that $\bar{y}_4(t) = O(1)$ for all t , while $\bar{y}_i \rightarrow 0, 1 \leq i \leq 3$, when $\epsilon \rightarrow 0$. The conservation law (4.2.3) can be satisfied only if $\bar{y}_4(t) = 1$, for all t , that is a non-generic situation. Therefore, the case **II** can be rejected. In the case **I** the conservation law takes the form $\epsilon^{7-a_5}\bar{y}_1(t) + \epsilon^{4-a_5}\bar{y}_2(t) + \bar{y}_4(t) = 1 + o(1)$, as $\epsilon \rightarrow 0$. Assuming that $\bar{y}_2(0) = O(1)$ and $\bar{y}_4 \neq 1$ (it is reasonable, since it is a generic case), we obtain $a_5 = 4$. Thus, the only possible situation is variant 1 (Case **I**) and the corresponding set of exponents is :

$$a_1 = 3, \quad a_2 = 0, \quad a_3 = 2, \quad a_4 = 0, \quad a_5 = 4. \quad (4.2.6)$$

Let us note that the terms $T1$ and $T2$ in the equations for the variables y_1, y_2 correspond to direct and reverse rates of a phosphorylation/dephosphorylation cycle transforming y_1 into y_2 and back. Thus, biochemically, (Case **I**) corresponds to the quasi-equilibrium of this cycle. Furthermore, the equilibration of all the variables leads to the exponents (4.2.6). In this case, $2 + a_4 - a_3 = -2 + a_3 + a_4 = 0$, $2 = -2 + 2a_3 = -2 + a_2 + a_5 - a_4$, meaning that the tropical equilibrations of the variables y_3, y_4 are triple (in each equation, all three terms have the same order).

We finally obtain the following renormalized system

$$\begin{aligned} \bar{y}'_1 &= \epsilon^{-6}(k_9\bar{y}_2 - k_8\bar{y}_1) + k_6\epsilon^{-1}\bar{y}_3, & \bar{y}'_2 &= \epsilon^{-3}(k_8\bar{y}_1 - k_9\bar{y}_2) - \epsilon^2 k_3\bar{y}_2\bar{y}_5, \\ \bar{y}'_3 &= k'_4\bar{y}_4 + k_4\bar{y}_4\bar{y}_3^2 - k_6\bar{y}_3, & \bar{y}'_4 &= \epsilon^2(-k'_4\bar{y}_4 - k_4\bar{y}_4\bar{y}_3^2 + k_3\bar{y}_2\bar{y}_5), \\ \bar{y}'_5 &= \epsilon^{-2}(k_1 - k_3\bar{y}_2\bar{y}_5). \end{aligned} \quad (4.2.7)$$

The structure of the system (4.2.7) emphasizes the multiple time scales of the model. The timescales of the variables are given by the dominating orders in the right hand sides of the corresponding differential equations. Thus, the fastest variables are in order y_1 (timescale ϵ^6), then y_2 and y_5 (timescales ϵ^3 and ϵ^2 , respectively). The variables y_3 and y_4 are slower (timescales 1 and ϵ^{-2} respectively).

Assume that

$$\bar{y}_2 > \delta > 0, \quad (4.2.8)$$

This important assumption, or another variant of this, is necessary for existence of an invariant manifold and will be justified, a posteriori. Let us explain why this condition is important. In fact, consider the last equation for \bar{y}_5 in (4.2.7). We can apply Theorem A (Appendix of the previous chapter) to this equation. The important condition of this Theorem is an exponential estimate for the linear operator in the equation for the fast variable.. The exponent β in this estimate depends on the minimum of y_2 . The β should be more than a small parameter κ , which is proportional to ϵ^2 .

Remark. A weaker but yet sufficient condition (see Theorem A from Appendix) :

$$\int_0^t \bar{y}_2(s)ds > \delta t + C_0 > 0. \quad (4.2.9)$$

To obtain an invariant manifold, we use Theorem A from Appendix (one can apply as well Theorem 6.1.7 from [67]). To this end, first we make a time rescaling in (4.2.7) by $\tau = \epsilon^6 t$. We then obtain

$$\begin{aligned} \frac{d\bar{y}_1}{d\tau} &= k_9\bar{y}_2 - k_8\bar{y}_1 + k_6\epsilon^5\bar{y}_3, & \frac{d\bar{y}_2}{d\tau} &= \epsilon^3(k_8\bar{y}_1 - k_9\bar{y}_2) - \epsilon^8 k_3\bar{y}_2\bar{y}_5, \\ \frac{\bar{y}_3}{d\tau} &= \epsilon^6(k'_4\bar{y}_4 + k_4\bar{y}_4\bar{y}_3^2 - k_6\bar{y}_3), & \frac{\bar{y}_4}{d\tau} &= \epsilon^8(-k'_4\bar{y}_4 - k_4\bar{y}_4\bar{y}_3^2 + k_3\bar{y}_2\bar{y}_5), \\ \frac{\bar{y}_5}{d\tau} &= \epsilon^4(k_1 - k_3\bar{y}_2\bar{y}_5). \end{aligned} \quad (4.2.10)$$

We see that this system contains a fast variable \bar{y}_1 and all the rest variables are slow. It is easy to check conditions of Theorem A from Appendix (or Theorem B, or 6.1.7 from [67]).

It is clear that the first approximation to the corresponding invariant manifold is

$$\bar{y}_1 \approx Y_1, \quad Y_1 = (k_9\bar{y}_2 + k_6\epsilon^5\bar{y}_3)k_8^{-1}.$$

Let us describe a standard procedure that allows to obtain corrections to this relation. We present \bar{y}_1 as

$$\bar{y}_1 = Y_1 + \tilde{y}_1,$$

where \tilde{y}_1 is a new unknown. For \tilde{y}_1 one obtains

$$\frac{d\tilde{y}_1}{d\tau} = -k_8\tilde{y}_1 - (Y_1)'_\tau.$$

This implies that a good approximation for \tilde{y}_1 is

$$\tilde{y}_1 = -k_8^{-1}(Y_1)'_\tau.$$

Let us compute $(Y_1)'_\tau$. One has

$$\frac{dY_1}{d\tau} = (k_9(\bar{y}_2)'_\tau + k_6\epsilon^5(\bar{y}_3)'_\tau)k_8^{-1}.$$

To estimate the order of this expression, let us calculate $(\bar{y}_2)'_\tau$ by substituting the expression for \bar{y}_1 in the equation for \bar{y}_2 . We obtain that

$$\frac{d\bar{y}_2}{d\tau} = \epsilon^8 k_6 \bar{y}_3 + \epsilon^3 k_6 \tilde{y}_1 - \epsilon^7 k_3 \bar{y}_2 \bar{y}_5. \quad (4.2.11)$$

Using these relations one can show that

$$\tilde{y}_1 = O(\epsilon^7), \quad \frac{d\bar{y}_2}{d\tau} = O(\epsilon^7). \quad (4.2.12)$$

(under condition that all \bar{y}_i are bounded as $\epsilon \rightarrow 0$).

Using the invariant manifold obtained one can exclude \bar{y}_1 from system (4.2.10). Let us consider the new system. We see that \bar{y}_5 is a fast variable and all the rest variables can be considered as slow.

We repeat now the same procedure for \bar{y}_5 . Then, from the last equation (4.2.10) and Lemma 3.3.6 we obtain the relation

$$\bar{y}_2 \bar{y}_5 = k_1/k_3 + O(\epsilon^2), \quad (4.2.13)$$

which represents an equation of an invariant manifold.

In turn, the relation (4.2.13) leads to the following equations for \bar{y}_3, \bar{y}_4

$$\bar{y}'_3 = k'_4 \bar{y}_4 + k_4 \bar{y}_4 \bar{y}_3^2 - k_6 \bar{y}_3 + O(\epsilon^2), \quad \bar{y}'_4 = \epsilon^2 (-k'_4 \bar{y}_4 - k_4 \bar{y}_4 \bar{y}_3^2 + k_1 + O(\epsilon^2)). \quad (4.2.14)$$

The invariant manifold equation is defined, therefore, by the equation

$$\bar{y}_1 = k_8^{-1}(k_9\bar{y}_2 + k_6\epsilon^5\bar{y}_3) + O(\epsilon^7). \quad (4.2.15)$$

Remind that \bar{y}_3, \bar{y}_4 are slow variables. Then, using (4.2.13), (4.2.15), we obtain, for \bar{y}_2 ,

$$(\bar{y}_2)' = \epsilon^2(k_6\bar{y}_3 - k_1) + O(\epsilon^7). \quad (4.2.16)$$

This estimate for the correction can be obtained as above in the case of \bar{y}_1 . We omit this straightforward calculation.

System (4.2.14) represents a two-dimensional reduced model of the initial five-dimensional system. This result shows that tropical equilibrations can be used for model reduction.

The solutions of (4.2.14) either tend to the stable equilibrium

$$\bar{y}_4 = \frac{k_1}{k'_4 + k_4(k_1/k_6)^2}, \quad \bar{y}_3 = k_1/k_6, \quad (4.2.17)$$

or, if this equilibrium is unstable, to a limit cycle.

Based on the general Theorem 3.3.5 we can assert the following :

Theorem 4.2.1. *Assume (4.2.8) holds with $\delta > 0$. If the shorted system (4.2.14) has a stable hyperbolic limit cycle, then, under above the conditions, for sufficiently small ϵ the five component system (4.1.1) also has a stable limit cycle. If the shorted system (4.2.14) has a stable hyperbolic equilibrium, then, under above the conditions, for sufficiently small ϵ the five component system (4.1.1) also has a stable hyperbolic equilibrium.*

We have studied the system (4.2.14) analytically and numerically. The numerical simulations confirm the criteria of cycle existence both for small ϵ and for $\epsilon = O(1)$. For small epsilon the cycle has a singular structure. The amplitude of \bar{y}_3 and the cycle period increase in ϵ , approximatively, as ϵ^{-2} (the assertion about period is natural since the rate of \bar{y}_4 is $O(\epsilon^2)$).

Hyperbolicity can be straightforwardly checked for the rest point (4.2.17), by computing the eigenvalues of the linearized system. Denote by $Y = (\bar{y}_3, \bar{y}_4)$. When the rest point $Y^0 = (\bar{y}_3^0, \bar{y}_4^0)$ is hyperbolic and stable we have the following estimate

$$|Y(t) - Y^0| < C_1 \exp(-c_1 \epsilon^2 t) \quad (4.2.18)$$

with some $C_1, c_1 > 0$ holds. Integrating (4.2.16) for \bar{y}_2 over interval $[0, \tau]$ gives

$$|\bar{y}_2(\tau) - \bar{y}_2(0)| < \epsilon^2 C_1 c_1^{-1} = o(1) \quad (4.2.19)$$

uniformly in $\tau > 0$ as $\epsilon \rightarrow 0$. This yields that $\bar{y}_2(t) > \delta$ if $\bar{y}_2(0) > 2\delta$ and therefore, $\bar{y}_2(t)$ does not go to zero for large t , justifying the estimate (4.2.8) needed for the existence of an invariant manifold. The case of a limit cycle is discussed in the next subsection.

4.3 A priori estimates and permanency for the two component version of the cell cycle model 1

In the previous section we showed how to reduce the five component model to a two component model. According to the general Theorem 3.3.5, one can use the properties of the attractors of the two component models to draw conclusions on the properties of the five components model. This section develops this strategy.

The two component shorted system can be written as follows :

$$\frac{dx}{dt} = k'_4 y + k_4 y x^2 - k_6 x, \quad (4.3.1)$$

$$\frac{dy}{dt} = -k'_4 y - k_4 y x^2 + k_1. \quad (4.3.2)$$

We consider these equations in the cone $\mathbf{R}_>^2$ and assume that

$$x(0) > 0, y(0) > 0.$$

Next, we obtain some simple estimates.

Lemma 4.3.1. *Let $A = k_1/k'_4$. If $y(0) \in (0, A)$, one has*

$$0 < y(t) \leq A, \quad t > 0. \quad (4.3.3)$$

Démonstration. Clearly, $y > 0$. In fact, if it does not hold, there is a point t_0 such that $dy/dt(t_0) \leq 0$ and $y(t_0) = 0$. This gives a contradiction with (4.3.2).

Similarly, we can prove that $y \leq A$. In fact, if it does not hold, there is a point t_0 such that $dy/dt(t_0) \geq 0$ and $y(t_0) = A$. This gives a contradiction with (4.3.2). \square

Lemma 4.3.2.

$$0 \leq x(t). \quad (4.3.4)$$

Démonstration. If (4.3.4) does not hold, there is a point t_0 such that $dx/dt(t_0) \leq 0$ and $x(t_0) = 0$. This gives a contradiction with (4.3.1). \square

Lemma 4.3.3.

$$x(t) + y(t) \leq B = (k_1 + k_6 A)/k_6. \quad (4.3.5)$$

Démonstration. For $v = x + y$ one obtains

$$\frac{dv}{dt} = -k_6 x + k_1 = -k_6 v + k_1 + k_6 y \leq -k_6 v + B k_6.$$

Therefore, as above, one obtains (4.3.5). Notice that then $x(t) \leq B$. \square

Lemma 4.3.4. For some $\delta_1 > 0$ condition $y(0) > \delta_1$ implies

$$y(t) > \delta_1 > 0, \quad t > 0. \quad (4.3.6)$$

Démonstration. We have the inequality

$$\frac{dy}{dt} \geq -k'_4 y - k_4 y B^2 + k_1. \quad (4.3.7)$$

Let δ_1 satisfy

$$0 < \delta_1 < \frac{k_1}{k'_4 + k_4 B^2}.$$

If (4.3.5) does not hold, there is a point t_1 such that $dy/dt \leq 0$ and $y(t) = \delta_1$ at $t = t_1$. Then (4.3.7) leads to a contradiction. \square

Lemma 4.3.5. For some $\delta_2 > 0$ condition $x(0) > \delta_1$ implies

$$x(t) > \delta_2 > 0, \quad t > 0. \quad (4.3.8)$$

Démonstration. We have the inequality

$$\frac{dx}{dt} \geq k'_4 \delta_1 - k_6 x. \quad (4.3.9)$$

Let δ_2 satisfy

$$0 < \delta_2 < \frac{k'_4 \delta_1}{k_6}.$$

If (4.3.5) does not hold, there is a point t_1 such that $dx/dt \leq 0$ and $x(t) = \delta_2$ at $t = t_1$. Then (4.3.9) leads to a contradiction. \square

We can provide now a qualitative description of the dynamics of the two component system.

Due to permanency, and the estimates, obtained above, the two component system has a globally attractive domain. According to Poincaré-Bendixon theory, this domains contains stable equilibria and/or limit cycles.

It is clear that the system (4.3.1),(4.3.2) has a unique equilibrium defined by

$$y_3 = k_1/k_6, \quad y_4 = k_1(k'_4 + k_4(k_1/k_6)^2).$$

We can check the stability of this equilibrium in an elementary way by computing the Jacobian matrix. As a result, we obtain the corresponding eigenvalues are given by the relation

$$\lambda_{\pm} = \frac{1}{2}(-b + k_6 - a) \pm \sqrt{(-b + k_6 - a)^2 - 4k_6 b}, \quad (4.3.10)$$

where

$$b = k'_4 + k_4(k_1/k_6)^2, \quad a = 2k_4(k_1/k_6)k_1(k'_4 + k_4(k_1/k_6)^2).$$

We have a stable equilibrium, if

$$\theta = -b + k_6 - a < 0.$$

For $\theta > 0$ the equilibrium is a repeller, therefore, at least one limit cycle exists. Numerical simulations show that this cycle is unique. The bifurcation at $\theta = 0$ is a supercritical Andronov-Hopf bifurcation. Actually, this is somehow the simplest two component chemical system with a Hopf bifurcation. As shown by [62], a two-component mass action law chemical system can not have limit cycle oscillations if it has only monomolecular or bimolecular reactions (i.e. monomial rates of degree of most two). The two-component model (4.3.1),(4.3.2) contains an autocatalytic reaction of rate x^2y , all other reactions being monomolecular. The same model has been used by Selkov to model the self-sustained oscillations of glycolysis [132]. Some other minimal chemical oscillators are discussed in [146].

4.4 Singular limit cycle and hybrid dynamics of model 1

Up to this point, the tropical ideas were used for reducing the dynamics of the model. In this section we show that the tropicalization heuristic is well adapted for decomposing the limit cycle into slow and fast modes, providing a hybrid description of the dynamics.

Let us note that in a hybrid, excitable system, it is possible that not all variables are equilibrated. Also, the system can have more than two different equilibrations and associated invariant manifolds, and jump from one invariant manifold to another during

the dynamics. Let us consider that the variables y_1, y_2, y_5 are equilibrated as above, but now, only one among the variables y_3 or y_4 are equilibrated. We have four situations :

- 1) In eq. for $\bar{y}_3 : T_1 = T_3, T_2 \leq T_1$,
- 2) In eq. for $\bar{y}_3 : T_2 = T_3, T_1 \leq T_2$,
- 3) In eq. for $\bar{y}_4 : T_1 = T_3, T_2 \leq T_1$,
- 4) In eq. for $\bar{y}_4 : T_2 = T_3, T_1 \leq T_2$.

Combined with the conservation law condition (4.2.3), variant 1 leads to the same triple tropical equilibration as before (Case **I**) and exponents (4.2.6). We denote the corresponding invariant manifold \mathcal{M}_1 . The renormalized equations are the same as (4.2.14).

Variant 2 can be rejected by the general permanency criterion given by Lemma 3.3.4. Indeed, in this case, the degree of the variable \bar{y}_3 in the dominating positive term of the equation for \bar{y}_3 is greater than the degree of the same variable in the negative dominating term of this equation, generating non-permanency.

Variant 4 has two solutions satisfying the permanency criterion and compatible with the conservation law. One of the solutions is the Case **I**, when all variables are equilibrated. The second solution corresponds to a new (Case **III**) set of tropical orders :

$$a_1 = 3, \quad a_2 = 0, \quad a_3 = 0, \quad a_4 = 4, \quad a_5 = 4. \quad (4.4.1)$$

This corresponds to a double equilibration (two equal terms) of the variable y_4 , the variable y_3 being not equilibrated. We denote the corresponding invariant manifold \mathcal{M}_2 . The renormalized equations read

$$\begin{aligned} \bar{y}'_1 &= \epsilon^{-6}(k_9\bar{y}_2 - k_8\bar{y}_1) + k_6\epsilon^{-3}\bar{y}_3, & \bar{y}'_2 &= \epsilon^{-3}(k_8\bar{y}_1 - k_9\bar{y}_2) - \epsilon^2 k_3\bar{y}_2\bar{y}_5, \\ \bar{y}'_3 &= \epsilon^6 k'_4\bar{y}_4 + \epsilon^2 k_4\bar{y}_4\bar{y}_3^2 - k_6\bar{y}_3, & \bar{y}'_4 &= -\epsilon^2 k'_4\bar{y}_4 + \epsilon^{-2}(-k_4\bar{y}_4\bar{y}_3^2 + k_3\bar{y}_2\bar{y}_5), \\ \bar{y}'_5 &= \epsilon^{-2}(k_1 - k_3\bar{y}_2\bar{y}_5). \end{aligned} \quad (4.4.2)$$

Variant 3 leads to a solution (Case **IV**) where a_3 is undetermined, namely :

$$a_1 = 3, \quad a_2 = a_4 = 0, \quad a_5 = 4, \quad a_3 \geq 2. \quad (4.4.3)$$

The corresponding renormalized equations read

$$\begin{aligned} \bar{y}'_1 &= \epsilon^{-6}(k_9\bar{y}_2 - k_8\bar{y}_1) + k_6\epsilon^{-3+a_3}\bar{y}_3, & \bar{y}'_2 &= \epsilon^{-3}(k_8\bar{y}_1 - k_9\bar{y}_2) - \epsilon^2 k_3\bar{y}_2\bar{y}_5, \\ \bar{y}'_3 &= \epsilon^{2-a_3} k'_4\bar{y}_4 + \epsilon^{-2+a_3} k_4\bar{y}_4\bar{y}_3^2 - k_6\bar{y}_3, & \bar{y}'_4 &= \epsilon^2(k_3\bar{y}_2\bar{y}_5 - k'_4\bar{y}_4) - \epsilon^{-2+2a_3} k_4\bar{y}_4\bar{y}_3^2, \\ \bar{y}'_5 &= \epsilon^{-2}(k_1 - k_3\bar{y}_2\bar{y}_5). \end{aligned} \quad (4.4.4)$$

Notice that (Case **I**) is a particular case of (Case **IV**), when $a_3 = 2$ and all variables are equilibrated.

We can provide a hybrid description of the cell cycle, by decomposing the periodic orbit into three modes (Fig.4.1). The first mode is the slowest and has the longest duration. It consists in the dynamics on the slow invariant manifold \mathcal{M}_1 at low values of y_3 , and can be described by the algebraic-differential system $\bar{y}'_3 = k_1 - k_6\bar{y}_3, k'_4\bar{y}_2 + k_4\bar{y}'_4\bar{y}_3^2 - k_1 = 0$ (part between O_1 and O of the orbit in Fig4.1c)). The exit from the invariant manifold \mathcal{M}_1 occurs at a critical point (point O in Fig4.1c)).

The next slowest mode corresponds to the decrease of y_3 (part between O_2 and O_1 of the orbit in Fig4.1c)) and can be described by two terms truncated system $\tilde{y}'_4 = \epsilon^{-2}(k_1 - k_4\tilde{y}_4\tilde{y}_3^2), \tilde{y}'_3 = -k_6\tilde{y}_3$. Finally, there is a fast mode, corresponding to the fast increase of \tilde{y}_3 (part between O and O_2 of the orbit in Fig4.1c)) and described by the truncated system $\tilde{y}'_4 = -\epsilon^2 k_4\tilde{y}_4\tilde{y}_3^2, \tilde{y}'_3 = \epsilon^{-2} k_4\tilde{y}_4\tilde{y}_3^2$. One can notice (Fig4.1c)) that this hybrid approximation is very accurate for small ϵ . At a distance from the tropical manifold, the hybrid orbit coincides with the one generated by the two terms or by the complete tropicalization.

However, close to the tropical manifold, the two term and the complete tropicalization are less accurate than the hybrid approximation described above.

Below we state rigorous estimates describing the slow movement on \mathcal{M}_1 and the fast jump towards \mathcal{M}_2 . The two terms description of the dynamics on \mathcal{M}_2 is a direct consequence of the Proposition 3.3.2 and Lemmas 3.3.4,3.3.6.

The slow movement on \mathcal{M}_1 corresponds to the Case I of tropical equilibrations and leads to (4.2.7),(4.2.14),(4.2.15).

To simplify notation, we rewrite the system (4.2.14) for y_3, y_4 as

$$x' = y + yx^2 - k_0x, \quad (4.4.5)$$

$$y' = \epsilon^2(-y - yx^2 + k_1). \quad (4.4.6)$$

We can obtain such a presentation by a linear variable change.

Let us define the functions

$$X(y) = \frac{k_0^2 - \sqrt{k_0^2 - 4y^2}}{2y},$$

$$X_+(y) = \frac{k_0^2 + \sqrt{k_0^2 - 4y^2}}{2y},$$

and the points

$$y_0 = k_0/2, \quad x_0 = X(y_0) = 1.$$

Lemma 4.4.1. *Solutions of (4.4.5), (4.4.6) with initial data $x(0), y(0)$ such that*

$$0 < \delta_0 < x(0) < X_+(y_0) - \delta_0, \quad 0 < y(0) < y_0 - \delta_0, \quad (4.4.7)$$

where δ_0 is a small positive number independent on ϵ , satisfy

$$|x(t) - X(y(t))| < C_1(\epsilon + \exp(-c_1\delta_0 t)), \quad t > T_0(x(0), y(0), \epsilon) \quad (4.4.8)$$

this estimate holds while

$$y(t) < y_0 - \delta_2, \quad \delta_2 > 0. \quad (4.4.9)$$

Démonstration. Let us consider the equation

$$x' = y(0) + y(0)x^2 - k_0x = f(x). \quad (4.4.10)$$

One observes that

$$f(x) < -\delta_4 < 0, \quad x \in (X(y(0)) + \delta_0, X_+(y_0) - \delta_0),$$

$$f(x) > \delta_4, \quad x \in (\delta_0, X(y_0) - \delta_0),$$

and

$$f'(x)|_{x=X(y_0)} < -\delta_5 < 0.$$

Therefore, if $0 < x(0) < \frac{k_0^2 + \sqrt{k_0^2 - 4y(0)^2}}{2y(0)} - \delta_0$, then the solution $x(t)$ attains a small δ -neighborhood of $X(y(0))$ within a bounded time interval $T_1(\delta, \delta_0, \delta_4)$:

$$|x(t, x_0, y_0) - X(y(0))| < \delta, \quad t = T_1(\delta, \delta_0, \delta_4).$$

Within a small δ -neighborhood of $X(y(0))$ we set $u = x - X(y(0))$ and then we can rewrite (4.4.10) as follows :

$$u' = -\kappa u + h(u), \quad |h(u)| < C_1 u^2, \quad u(T_1) = \delta. \quad (4.4.11)$$

where $\kappa > 0$ is independent of δ . Then, if δ is small enough, we have that $u(t) < \delta$ for all $t > T_1$ and

$$|u(t)| < C(T_1) \exp(-\kappa t/2), \quad t > T_1.$$

Let us compare now the solution $x(t)$ of (4.4.10) and the corresponding solution $\bar{x}(t, x_0, y_0)$ of (4.4.5) with the same initial data. For $\bar{x}(t) - x(t) = w$ one has, since $y(t) - y(0) < C(T_2)\epsilon^2$ on any bounded interval $t \in [0, T_2]$,

$$w_t < a(t)w + \epsilon^2 g(x, t, w), \quad 0 < t \leq T_2,$$

where T_2 is an arbitrary time such that $T_2 = O(1)$ as $\epsilon \rightarrow 0$, g is a smooth function and $a(t)$ is bounded function. Now the Gronwall inequality implies

$$|w(t)| < C_2(T_2)\epsilon^2, \quad t \in [0, T_2].$$

Therefore, one has

$$|\bar{x}(t, x_0, y_0) - X(y(t))| < \delta + C_2\epsilon^2, \quad t = T_2(\delta, \delta_0, \delta_4).$$

Since the function $X(y)$ defines a smooth, locally attracting (for $y < y_0$) invariant manifold, this proves our assertion.

There exists another, more elementary proof. Let us define $v = \bar{x} - X(y)$. Then

$$v' = -\kappa(t)v + h(v) + O(\epsilon), \quad |h(v)| < C_1 v^2, \quad v(T_1) < \delta, \quad (4.4.12)$$

where $\kappa(t) > \kappa_0$ while $y < y_0 - \delta_0$. Again one has $v(t) < 2\delta$ for $t > T_1$ (while $y < y_0 - \delta_0$). Thus,

$$v' \leq -\frac{\kappa_0}{2}v + O(\epsilon)$$

that entails the need estimate (4.4.8). □

Let us find some estimates of solutions at $y = y_0, x = x_0$. Our goal is to prove that at this point $x(t)$ starts to increase sharply. After this, the terms $\pm yx^2$ play the main role in the equations (4.4.5), (4.4.6), and the other terms can be removed while the x -component is big.

Let us introduce new variables u, v by

$$x - x_0 = v, \quad u = y - y_0.$$

For u, v one obtains

$$v' = \frac{k_0}{2}v^2 + u(1 + (1 + v)^2), \quad (4.4.13)$$

$$u' = \epsilon^2 \left(-\left(\frac{k_0}{2} + u \right)(1 + (1 + v)^2) + k_1 \right) = \epsilon^2 g(u, v). \quad (4.4.14)$$

Let us consider for this system the Cauchy problem with initial data

$$v(0) = v_0, \quad u(0) = u_0. \quad (4.4.15)$$

Lemma 4.4.2. Consider the Cauchy problem (4.4.13), (4.4.14) and (4.4.15) under assumptions that

$$u_0 = \kappa > 0, \quad |v_0| < \delta_5,$$

and

$$k_1 > k_0, \quad (4.4.16)$$

where δ_0, δ_5 are small enough (but independent on ϵ). Let A be a large positive number independent of ϵ . Then within some interval $t \in (\tau_0(\delta_5, k_0, k_1, A), \tau_1(\delta_5, k_0, k_1, A))$ one has

$$u(t) > 0, \quad v(t) \geq A, \quad v(\tau_0) = A. \quad (4.4.17)$$

Démonstration. Let us consider the Cauchy problem

$$w' = \frac{k_0}{2} w^2, \quad w(0) = v_0 = v(0) \quad (4.4.18)$$

It is clear, by the comparison principle, that

$$v(t) \geq w(t)$$

while $u(t) > 0$. Consequently, the assertion $w(\tau_0) = A$ proves the lemma.

Let us prove first that if δ_6 is small enough (but independent on ϵ), for some $t = \tau_1$ we have

$$v(\tau_1) = \delta_6, \quad (4.4.19)$$

where δ_6 is any positive number such that

$$\delta_5 < \delta_6 < \sqrt{\frac{2k_1 - k_0}{k_0}} - 1.$$

The root in the right hand side > 1 since $k_1 > k_0$ (see (4.4.16)). Without loss of generality, we assume that

$$v(t) < \delta_6, \quad 0 < t < \tau_1, \quad v(\tau_1) = \delta_6. \quad (4.4.20)$$

Assume $u(t) \geq 0$ within some time interval $[0, \tau_2]$, and $u(\tau_2) = 0$ for some $\tau_2 < \tau_1$. Since $u(0) = 0$, we have $\tau_2 > 0$. We can suppose without loss of generality that τ_2 is the first moment, where $u(\tau_2) = 0$. Then

$$u'(\tau_2) \leq 0.$$

But then we obtain a contradiction with (4.4.14) at $t = \tau_2$, since the right hand side of this equation is positive at this time moment.

Therefore, $u(t) > 0$ for all t from $[0, \tau_1]$ if $v(t) < \delta_6$ for such t . Then $v(t) \geq w(t)$ on this time interval. The function w can be found, and an easy computation gives

$$w(t) = (w^{-1}(0) - 2k_0^{-1}t)^{-1} = (u_0 - 2k_0^{-1}t). \quad (4.4.21)$$

Assume that $v(t) < \delta_6$ for all t . Then (4.4.21) holds for all t , but $w(\tau_1) > \delta_6$ for some τ_1 . We have obtained a contradiction, thus (4.4.19) is proved.

Let us prove that $v(t) = A$ for some $t > \tau_1$. Consider an interval $[\tau_1, T]$ such that

$$|v(t)| < A, \quad t \in [\tau_1, T], \quad v(\tau_1) = \delta_6. \quad (4.4.22)$$

Then (4.4.14) implies

$$u' \leq \epsilon^2 \left(\left(\frac{k_0}{2} + |u| \right) (1 + (1 + A)^2) + k_1 \right), \quad (4.4.23)$$

that gives, by the Gronwall lemma,

$$u(t) < C_2 u(0) \exp(C_1(A) \epsilon^2 t). \quad (4.4.24)$$

Within interval $(t_1, T]$ one has then

$$u(t) < C_4 \kappa, \quad t \in [0, T], \quad (4.4.25)$$

where

$$C_4 \kappa < \frac{k_0}{8} \delta_6.$$

Therefore,

$$v' \geq \frac{k_0}{2} v^2 - C_4 \kappa, \quad t \in [0, T]. \quad (4.4.26)$$

Then (4.4.26) entails

$$v' \geq \frac{k_0}{4} v, \quad t \in [0, T], \quad (4.4.27)$$

This gives

$$v(t) \geq \delta_6 \exp\left(\frac{k_0}{4}(t - t_1)\right).$$

This leads to a contradiction for T large enough. However, let us remark that the time moment T is uniform in ϵ as $\epsilon \rightarrow 0$. \square

This result can be reinforced. Actually, $x(t)$ attains values of the order $O(\epsilon^{-2})$.

Lemma 4.4.3. *Assume that for some time moment t_1 one has*

$$x(t_1) = A \gg 1, \quad y(t_1) \geq k_0/2. \quad (4.4.28)$$

Then

$$x(t) \geq (A^{-1} - \frac{1}{2}\sigma(t - t_1))^{-1}, \quad (4.4.29)$$

$$y(t) \geq \sigma, \quad (4.4.30)$$

for σ, A such that

$$\sigma > 2k_0 A, \quad \sigma > 2(k_0 + k_1) \exp(-2\sigma^{-1}), \quad (4.4.31)$$

and t such that

$$(A^{-1} - \frac{1}{2}\sigma(t - t_1)) \geq \epsilon^2. \quad (4.4.32)$$

Démonstration. Remark : to satisfy (4.4.31) it suffices to set $\sigma = 3k_0 A$.

Suppose that either the estimate (4.4.29) (case A) or the second estimate (4.4.30) (case B) is violated at some T but the both inequalities hold for all $t_1 \leq t < T$. We can set $t_1 = 0$. Let us consider the case A. Since (4.4.30) hold, one has

$$x' \geq \sigma x^2, \quad x(0) = A, \quad t \in [0, T].$$

This implies

$$x'/x^2 = (-1/x)' \geq \sigma, \quad x(0) = A.$$

Thus,

$$x \geq (A^{-1} - \sigma t)^{-1}.$$

For $t = T$ this result gives a contradiction with (4.4.29).

Let us consider the case B. Since (4.4.29) hold, one has

$$y'(t) \leq -\epsilon^2(y + y(A^{-1} - \sigma't)^{-2} - k_1), \quad y(0) = k_0/2, \quad t \in [0, T],$$

where $\sigma' = \sigma/2$. This implies

$$y(t) \leq \frac{k_0}{2} \exp(-\epsilon^2 \int_0^t (1 + (A^{-1} - \sigma's)^{-2}) ds) + \epsilon^2 k_1 \int_0^t \exp(-\epsilon^2 \int_\tau^t (1 + (A^{-1} - \sigma's)^{-2}) ds) d\tau.$$

for $t \in [0, T]$. Notice

$$\int_\tau^t (1 + (A^{-1} - \sigma's)^{-2}) ds = t - \tau + \sigma'^{-1}((A^{-1} - \sigma't)^{-1} - (A^{-1} - \sigma'\tau)^{-1}).$$

Thus, for sufficiently small ϵ , taking into account (4.4.32) one has

$$y(T) \leq C(k_0 + k_1) \exp(-1/\sigma'), \quad C \in (1, 2)$$

for small ϵ . Under condition (4.4.31) this result gives a contradiction with (4.4.30). \square

4.5 Checking condition (4.2.8)

Let us introduce the quantity

$$S(t) = \epsilon^2 \int_0^t (k_6 \bar{y}_3(s) - k_1) ds. \quad (4.5.1)$$

Let us notice that eqs.(4.2.14) for \bar{y}_3, \bar{y}_4 yield

$$S(t) = \epsilon^2(\bar{y}_3(0) - \bar{y}_3(t)) + (\bar{y}_4(0) - \bar{y}_4(t)). \quad (4.5.2)$$

But the equation (4.2.16) for \bar{y}_2 gives

$$\bar{y}_2(t) - \bar{y}_2(0) = S(t).$$

Therefore,

$$\bar{y}_2(t) - \bar{y}_2(0) = \epsilon^2(\bar{y}_3(0) - \bar{y}_3(t)) + (\bar{y}_4(0) - \bar{y}_4(t)). \quad (4.5.3)$$

Now we can formulate a lemma.

Lemma 4.5.1. *If $\bar{y}_2(0)$ is large enough and $\bar{y}_4(0)$ is small enough, i.e.,*

$$\bar{y}_4(0) < \delta_0, \quad \bar{y}_2(0) > C(\delta_0, k'_4, k_6, k_4, k_1), \quad (4.5.4)$$

then (4.2.8) holds, for some $\delta > 0$ and sufficiently small ϵ , for all t .

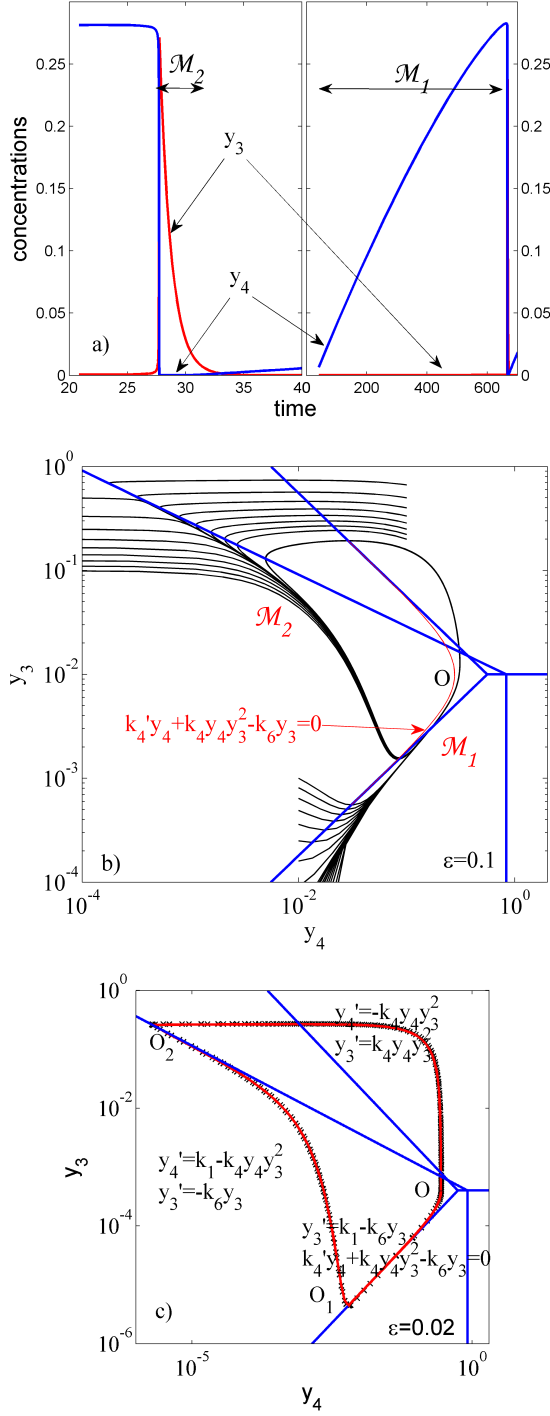


FIGURE 4.1 – Limit cycle behavior of the paradigmatic cell cycle model from [140]. (a) The three main processes during the embryonic cell cycle are, in order of the timescales, fast increase of y_3 (active MPF, triggering mitosis), slower decrease of y_3 and very slow increase of y_4 (inactive MPF). (b) Two invariant manifolds corresponding to the two slow processes are close to the tropical manifolds (blue lines) and result from equilibration of the variables (equilibration of y_4 corresponds to \mathcal{M}_2 and equilibration of y_3 corresponds to \mathcal{M}_1). (c) A three modes hybrid approximation of the cell cycle (in red) compared to the original limit cycle (black crosses).

Démonstration. To prove this lemma, we use our previous results on the cycle form. The condition for $\bar{y}_4(0)$ gives that $\bar{y}_4(t)$ is an increasing function on the time interval up to the point t where $\bar{y}_4(t)$ attains a critical value y_0^* , where the manifold lost stability and a growth of \bar{y}_3 starts. Therefore, using (4.5.3), we remark that for small ϵ on this time interval

$$\bar{y}_2(t) \geq \bar{y}_2(0) + O(\epsilon^2) > \delta_0/2. \quad (4.5.5)$$

On the interval of the growth we have $\bar{y}_3(t) < C_1\epsilon^{-2}$ and $\bar{y}_4 < C_2$, as it was shown above. Let us prove an auxiliary assertion that $\bar{y}_3 < C\epsilon^{-2}$ for some C . If at some time moment $t = t_1$ we have $\bar{y}_3 = C_3\epsilon^{-2}$. Notice that while $k_6\bar{y}_3 > k_1$ we have

$$(\epsilon^2\bar{y}_3 + \bar{y}_4)' < 0.$$

Therefore, y_3 is a time decreasing function that implies $\epsilon^2\bar{y}_3(t) < \epsilon^2\bar{y}_3(t_1) = C_3$. This holds for t such that $\bar{y}_3(t) > k_1/k_6$. For all the rest t one has $\bar{y}_3(t) \leq k_1/k_6$ and our assertion is proved.

Therefore, again (4.5.3) gives

$$\bar{y}_2(t) \geq \bar{y}_2(0) - C_1(k'_4, k_6, k_4, k_1) - C_2 + \delta_0 > \delta_0, \quad (4.5.6)$$

if $C(\delta_0, k'_4, k_6, k_4, k_1) > C_1 + C_2$. \square

4.6 Tropical equilibrations and reduction of model 2

We seek reductions of this system for small ϵ . Notice that y_1, y_3 are slower than y_2 . Therefore one can assume that first we can express y_2 via y_1 . This gives, by (4.1.7) that

$$k_4 \frac{y_1}{1+y_1} = k_5 \frac{y_2}{1+y_2} + o(1), \quad \epsilon \rightarrow 0. \quad (4.6.1)$$

Setting $b = k_5/k_4$, one has

$$y_2 = \frac{y_1}{b + (b-1)y_1} + o(1), \quad \epsilon \rightarrow 0. \quad (4.6.2)$$

This leads to a shorted system

$$y'_1 = k_1\epsilon - k_2\epsilon^3 y_3 - k_3\epsilon^2 y_1, \quad (4.6.3)$$

$$y'_3 = k_6 \frac{y_1}{b + (b-1)y_1} - \epsilon^{-2} \frac{y_3}{1+y_3}. \quad (4.6.4)$$

Here y_3 is a fast mode and y_1 is a slow one. Therefore, we can express y_3 via y_1 , that gives

$$\epsilon^2 k_6 \frac{y_1}{b + (b-1)y_1} = \frac{y_3}{1+y_3}, \quad (4.6.5)$$

and since y_3 is thus small, we obtain

$$y_3 = \epsilon^2 k_6 \frac{y_1}{b + (b-1)y_1} + o(\epsilon^2). \quad (4.6.6)$$

Finally, we have only a single equation

$$y'_1 = k_1\epsilon - k_2\epsilon^5 k_6 \frac{y_1}{b + (b-1)y_1} - k_3\epsilon^2 y_1. \quad (4.6.7)$$

We conclude that for small ϵ the Model 2 does not exhibit oscillations.

The system is excitable for small ϵ , i.e., all the solutions are convergent to an equilibrium given by the asymptotic

$$y_1 = \frac{k_1}{k_3}(\epsilon^{-1} + O(1)). \quad (4.6.8)$$

Here

$$y_3 = O(\epsilon^2)$$

is small. Assume that

$$b \neq 1.$$

Then, by (4.6.2),

$$y_2 = f(y_1) = (b - 1)^{-1} = O(1).$$

If $b = 1$ we have

$$y_2 = b^{-1}y_1 = O(\epsilon^{-1}),$$

we observe a resonance effect.

This heuristic reasoning is rendered rigorous by the following

Theorem 4.6.1. *Let*

$$b > 1.$$

For sufficiently small ϵ all the trajectories of Model 2 with initial data such that

$$0 < y_i(0) < C_1 \quad (4.6.9)$$

converge to the equilibrium given by asymptotics (4.6.8), (4.6.6) and (4.6.2).

Démonstration. It is easy to show, that Model 2 conserve the positivity : if $y_i(0) > 0$ then $y_i(t) > 0$ (see, for example, Smoller 1984). So, we can assume that $y_i(t) > 0$.

We introduce the new variable v by

$$y_2 = v + f(y_1), \quad f(y_1) = \frac{y_1}{b + (b - 1)y_1}.$$

The meaning of this variable is transparent : the v defines a deviation of y_2 from the invariant manifold. Then the Model 2 equations become

$$y'_1 = k_1\epsilon - k_2\epsilon^3y_3 - k_3\epsilon^2y_1, \quad (4.6.10)$$

$$v' = -k_4\epsilon^{-3}\frac{v}{(1 + f(y_1) + v)(1 + f(y_1))} - b(b + (b - 1)y_1)^{-2}(k_1\epsilon - k_2\epsilon^3y_3 - k_3\epsilon^2y_1), \quad (4.6.11)$$

$$y'_3 = k_6\left(\frac{y_1}{b + (b - 1)y_1} + v\right) - \epsilon^{-2}\frac{y_3}{1 + y_3}. \quad (4.6.12)$$

Here

$$v(0) = 0$$

Let us prove an auxiliary lemma.

Lemma 4.6.2. *Solutions of the Cauchy problem (4.6.10)-(4.6.11) satisfy*

$$|v(t)| < C_2\epsilon^4, \quad y_1(t) < C_1\epsilon^{-1}, \quad y_3(t) < C_3\epsilon^2 \quad (4.6.13)$$

for sufficiently small ϵ and some $C_i > 0$.

Démonstration. Assume (4.6.13) hold on $t \in (0, T)$ and, say, $v(T) = C_2\epsilon^4$ (other cases can be considered in a similar way). Then (4.6.11) implies $v'(t) \geq 0$. On other hand, we see that

$$v'(T) < -k_4\epsilon^{-3}c_0C_2\epsilon^4 + c_1(b, C_3, C_1, k_2, k_3)\epsilon < 0$$

that leads to a contradiction. \square

We obtain then

$$y'_1 = k_1\epsilon - k_2\epsilon^3y_3 - k_3\epsilon^3y_1, \quad (4.6.14)$$

$$y'_3 = k_6\left(\frac{y_1}{b + (b - 1)y_1} + \phi(t, \epsilon)\right) - \epsilon^{-2}\frac{y_3}{1 + y_3}. \quad (4.6.15)$$

where $\phi = O(\epsilon^4)$. We repeat the same trick : we introduce w by $y_3 + w = \epsilon^2g(y_1)$, with g defined by

$$g = k_6\frac{y_1}{b + (b - 1)y_1}. \quad (4.6.16)$$

For w , repeating the same procedure as above, we obtain $|w| < C\epsilon^3$. After this we have the trivial equation

$$y'_1 = k_1\epsilon - k_2\epsilon^5g(y_1) - k_3\epsilon^3y_1 + \psi(t, \epsilon), \quad (4.6.17)$$

where $|\psi| = O(\epsilon^6)$. This equation shows that all y_1 trajectories attain a small neighborhood of the point $k_1/k_3\epsilon^{-2}$. So, all the trajectories of Model 2 attain a small neighborhood of the equilibrium. Since this equilibrium is hyperbolic and stable, all the trajectories stay in this neighborhood and approach equilibrium.

The hyperbolicity can be shown as follows. Let us consider the 3×3 matrix of the linear operator L that describes a linearization at the equilibrium found above. The entries of this matrix have the form

$$L_{11} = -\epsilon^2, \quad L_{12} = 0, \quad L_{13} = \epsilon^3$$

$$L_{21} = c_1\epsilon^{-3}y_1(1 + y_1)^2 = O(\epsilon^{-2}), \quad L_{22} = -c_2\epsilon^{-3}y_2(1 + y_2)^2 = O(\epsilon^{-3}), \quad L_{23} = 0,$$

where $c_i > 0$ and

$$L_{33} = -c_3\epsilon^{-2}y_3(1 + y_3)^2 = c_4, \quad L_{31} = 0, \quad L_{32} = 1, \quad c_3, c_4 > 0.$$

The corresponding characteristic equation have the form

$$(\epsilon^2 + \lambda)(c_2\epsilon^{-3} + \lambda)(c_4 + \lambda) = c_5\epsilon.$$

and 3 roots : close to $-\epsilon^2$, $-c_2\epsilon^{-3}$ and $-c_4$ (these roots correspond a slow motion, very fast motion and average speed motion, here we have a spectrum of modes with 3 different rates). Thus, the equilibrium is a hyperbolic attractor. \square

Discussion. This theorem shows that the asymptotic behaviour of the family of models parametrized by ϵ can be qualitatively different from the behaviour of a model with a finite value of ϵ . Indeed, Model 2 has a stable limit cycle for $\epsilon = 0.1$, but (contrary to Model 1) undergoes a Hopf bifurcation when ϵ becomes very small. Another consequence of this difference is the following. The period and amplitude of oscillations of Model 1 diverge when $\epsilon \rightarrow 0$, whereas Model 1 can not produce oscillations with arbitrarily large amplitude and period. If the accumulation time of the cyclin increases too much in Model 2, then it becomes impossible to recover very low values. This shows that having an autocatalytic process (positive self-regulation of MPF) is a much more effective way to obtain excitability and robust oscillations in Model 1.

4.7 Tropical approach for excitable systems. Two component case.

Let us consider a more general class of excitable systems to which we can apply tropical ideas in order to find piecewise approximations of the dynamics. We have shown that Model 1 described by the eqs. (4.1.1) is excitable. Indeed, after a large excursion of amplitude ϵ^{-2} , the variable y_3 returns to very low values of order ϵ^2 , corresponding to the invariant manifold \mathcal{M}_1 . We show now that the similar property is satisfied for more general two component systems of the form

$$x' = y(x^m + P(x, y)) - k_0 x, \quad x(0) = x_0 \quad (4.7.1)$$

$$y' = -\epsilon^2(yx^n + yQ(x, y) - k_1), \quad y(0) = y_0. \quad (4.7.2)$$

where P, Q are polynomials such that

$$\deg_x P < m, \deg_x Q < n, \quad (4.7.3)$$

and $k_1 \geq 0$. Here m, n are positive integers, $n, m \geq 2$. With these equations we associate a tropically truncated system (TTS), namely

$$x' = yx^m, \quad (4.7.4)$$

$$y' = -\epsilon^2 yx^n. \quad (4.7.5)$$

Let us investigate first the TTS. This is a fast/slow system, with x the fast variable and y the slow variable. Starting from $x(0) = x_0$, $y(0) = y_0$, the fast part of the trajectory can be approximated by the equation $x' = y_0 x^m$, that has the solution $x(t) = (x_0^{1-m} - (m-1)y_0 t)^{1/(1-m)}$. Because $1-m < 0$ this means that $x(t)$ increases to large values in a finite time $x_0^{1-m}/((m-1)y_0)$ that does not depend on ϵ .

However, the increase of x is bounded. Indeed, TTS system has a first integral. We can easily check that that

$$V(x, y) = \epsilon^2 x^{n-m+1} + (n-m+1)y = \text{const} \quad (4.7.6)$$

on the trajectories of (4.7.4), (4.7.5). Therefore,

$$x' = (V_0 - \epsilon^2 x^{n-m+1})x^m, \quad x(0) = x_0 > 0. \quad (4.7.7)$$

Thus, the solutions of this Cauchy problem possess the following properties.

i. Under the condition

$$n \geq m \quad (4.7.8)$$

and if $V(x(0), y(0)) = V_0$, then all the solutions converge to

$$x_{eq} = (V_0 \epsilon^{-2})^\beta, \beta = \frac{2}{n-m+1}. \quad (4.7.9)$$

ii The solutions $x(t)$ attain values of the order $O(\epsilon^{-\beta})$ during the time of the order $O(1)$ independent of ϵ . Indeed, from it follows, when $n \geq m$, that $x(t)$ has a maximal value satisfying $V_0 = \epsilon^2 x_{max}^{n-m+1}$, hence $x_{max} = V_0^{\beta/2} \epsilon^{-\beta}$. After reaching this maximum, solutions approach to x_{eq} within a short time interval of the order

$$T_\epsilon = C_0 \epsilon^{\beta(m-1)}.$$

Let us prove that the solutions of the Cauchy problem for the full system (4.7.1), (4.7.2), have similar excitable behavior. We need to show analogues of the key lemmas, obtained in preceding sections for the case $m = n = 2$. These assertions show that, under conditions, the tropical principle is working for initial system (4.7.1), (4.7.2) and the solutions of this system can be approximated by solutions of corresponding TTS.

Lemma 4.7.1. *Assume*

$$x(0) = A \gg 1, \quad y(0) \geq k_0/2, \quad (4.7.10)$$

where $k_0 > 0$. Then the solution of the Cauchy problem (4.7.1), (4.7.2) satisfies

$$x(t) \geq (A^{1-m} - (m-1)\sigma t)^{1/(1-m)}, \quad (4.7.11)$$

$$y(t) \geq \sigma(k_0, A), \quad (4.7.12)$$

for some σ and t such that

$$A^{1-m} - (m-1)\sigma t \geq e^{\beta(m-1)}. \quad (4.7.13)$$

Démonstration. Suppose that either the estimate (4.7.11) (case A) or the second estimate (4.7.12) (case B) is not valid at some T but the both inequalities hold for all $0 \leq t < T$.

Let us consider first the case A. Since (4.7.12) holds, one has

$$x' > \sigma_1 x^m, \quad x(0) = A, \quad t \in [0, T],$$

for some σ_1 satisfying $0 < \sigma_1 < \sigma$. This implies

$$x'/x^m = -((m-1)^{-1} x^{1-m})' > \sigma_1, \quad x(0) = A.$$

Thus, using $1-m > 0$ it follows

$$x < (A^{1-m} - (m-1)\sigma t)^{1/(1-m)}.$$

For $t = T$ this result gives a contradiction with (4.7.11).

Let us consider the case B. Since (4.7.11) holds, one has

$$y'(t) \leq -\epsilon^2 c_1 y(A^{-1} - (m-1)\sigma t)^{-n/(m-1)} + \epsilon^2 k_1, \quad y(0) = k_0/2, \quad t \in [0, T].$$

for some $c_1 > 0$ and small ϵ . Here we have used $\deg_x Q < n$ and majorated Q by a multiple of x^n (this is possible because $x(0) = A \gg 1$). This implies

$$\begin{aligned} y(t) &\leq \frac{k_0}{2} \exp(-\epsilon^2 \int_0^t (A^{-1} - (m-1)\sigma s)^{-n/(m-1)} ds) + \\ &+ \epsilon^2 k_1 \int_0^t \exp(-\epsilon^2 \int_\tau^t (A^{-1} - (m-1)\sigma s)^{-n/(m-1)} ds) d\tau \end{aligned}$$

for $t \in [0, T]$. Notice that

$$\begin{aligned} &\epsilon^2 \left(\int_\tau^t (A^{-1} - (m-1)\sigma s)^{-n/(m-1)} ds \right) \leq \\ &\leq \epsilon^2 c_1 \sigma^{-1} (A^{-1} - (m-1)\sigma t)^{-n/(m-1)+1} - (A^{-1} - (m-1)\sigma \tau)^{-n/(m-1)+1} < \\ &< C_2 \epsilon^{2+\beta(m-1)(1-\frac{n}{m-1})} \leq C_2. \end{aligned}$$

Thus, for sufficiently small ϵ , taking into account (4.7.13) one has

$$y(T) \leq \frac{k_0}{2} \exp(-C_3 \sigma^{-1}).$$

This result gives a contradiction with (4.7.12), and the lemma is proved. \square

Our next goal is to show that solutions of our system return to the domain $A(M)$, the attraction domain of the stable part of our slow manifold, defined now by

$$0 < x^{m-1}y < \text{const}, \quad y < y_0. \quad (4.7.14)$$

The main idea is to compare the solutions of the Cauchy problems for the initial system and tropically truncated on some time interval $[t_3, T]$, where

$$T - t_3 = O(\epsilon^{\beta(m-1)}).$$

We set $t_3 = 0$ to simplify notation. This is possible since all equations are autonomous. The exponent $\beta(m-1)$ can be justified as follows.

The truncated system reduces to the equation

$$x' = (V_0 - \epsilon^2 x^{n-m+1})x^m.$$

If we make a rescaling (as above, for the case $m = 2 = n$)

$$\tau = \epsilon^{-\beta(m-1)}t, \quad x = \epsilon^{-\beta}\bar{x}$$

we obtain an equation that does not involve ϵ at all :

$$\frac{d\bar{x}}{d\tau} = (V_0 - \bar{x}^{n-m+1})\bar{x}^m.$$

Therefore, the characteristic rate for the convergence to the equilibrium of x is $O(\epsilon^{-\beta(m-1)})$, and a natural time interval is $[0, O(\epsilon^{\beta(m-1)})]$.

Let us consider the two Cauchy problems

$$x' = y(x^m + P(x, y)) - k_0x, \quad x(0) = c\epsilon^{-2} \quad (4.7.15)$$

$$y' = \epsilon^2(-yx^n + yQ(x) + k_1), \quad y(0) = \sigma \quad (4.7.16)$$

and

$$\tilde{x}' = \tilde{y}x^m, \quad \tilde{x}(0) = c\epsilon^{-2} \quad (4.7.17)$$

$$\tilde{y}' = -\epsilon^2\tilde{y}\tilde{x}^n, \quad \tilde{y}(0) = \sigma. \quad (4.7.18)$$

Let us set $z = (x, y)^{tr}$ and $\tilde{z} = (\tilde{x}, \tilde{y})^{tr}$. Then for difference $w = \begin{pmatrix} w_1 \\ w_2 \end{pmatrix} = z - \tilde{z}$ one obtains the following matrix evolution equation

$$w' = L(t)w + F(w), \quad (4.7.19)$$

where $L(t)$ is the 2 matrix with entries

$$L_{11} = 2\tilde{y}\tilde{x}^{m-1} = O(\epsilon^{-\beta(m-1)}), \quad L_{12} = \tilde{x}^m = O(\epsilon^{-\beta m})$$

$$L_{21} = -2\epsilon^2\tilde{y}\tilde{x}^{n-1} = O(\epsilon^{2-\beta(n-1)}), \quad L_{12} = -\epsilon^2\tilde{x}^n = O(\epsilon^{2-\beta n}),$$

the vector F has the form

$$F_1 = (\tilde{y} + w_1)(h_1 + P), \quad (4.7.20)$$

and

$$F_2 = -\epsilon^2(\tilde{y} + w_2)(h_2 + Q) + \epsilon^2k_1, \quad (4.7.21)$$

where h_i satisfy estimates

$$|h_1| \leq C(\tilde{x}^{m-2}w_1^2 + \tilde{x}^{m-3}w_1^3 + \dots + w_1^m). \quad (4.7.22)$$

and

$$|h_2| \leq C(\tilde{x}^{n-2}w_2^2 + \tilde{x}^{n-3}w_2^3 + \dots + w_2^n). \quad (4.7.23)$$

Let us observe that the trace of L and $\text{Det}L$ can be estimated as

$$|\text{Tr}(L)| < c\epsilon^{2-\beta n}, \quad |\text{Det}L| < c\epsilon^{4-2\beta n}. \quad (4.7.24)$$

Therefore, for the eigenvalues λ_1, λ_2 of L one obtains

$$\text{Re}\lambda_i < c\epsilon^{2-\beta n}. \quad (4.7.25)$$

We rewrite (4.7.19) as an integral equation (here we observe that $w(0) = 0$ since the initial data is the same in (4.7.15), (4.7.16) and (4.7.17), (4.7.18))

$$w(t) = \int_0^t \exp(L(t-s))F(w(s))ds. \quad (4.7.26)$$

Lemma 4.7.2. *If $\epsilon > 0$ is small enough then within time interval $[0, T]$, where $T = C\epsilon^{\beta(m-1)}$, the solution to (4.7.26) exists and satisfies the estimate*

$$|w_1(t)| < B, \quad |w_2(t)| < \epsilon^\beta B, \quad t \in [0, T], \quad (4.7.27)$$

for some B (which is uniform as $\epsilon \rightarrow 0$). Here w_1 and w_2 are the two components of the vector w .

Démonstration. We apply the Schauder theorem. Let us consider (4.7.26) on the set $D(B)$ of continuous functions such that 4.7.27 holds. Let us prove that a nonlinear map S defined by the right hand side of (4.7.27), maps the domain $D(B)$ into itself.

Notice that, according to estimate (4.7.25),

$$\|\exp(L(t-s))\| < C_0 \exp(-c\epsilon^{2-\beta n})|t-s|.$$

Since $|t-s| \leq T = O(\epsilon^{\beta m})$, one obtains

$$\|\exp(L(t-s))\| \leq C_1, \quad t, s \in [0, T], \quad (4.7.28)$$

Therefore,

$$|Sw(\cdot)| = \left| \int_0^t \exp(L(t-s))F(w(s))ds \right| \leq C_1 \epsilon^{\beta(m-1)} \sup_{w \in D(B)} |F|. \quad (4.7.29)$$

Due to above relations for F, h , and since $\tilde{x} < C\epsilon^{-\beta}$, $\tilde{y} < C$, one obtains by (4.7.22)

$$\sup_{w \in D(B)} |h_1| \leq C_3 \epsilon^{-\beta(m-2)},$$

$$\sup_{w \in D(B)} |h_2| \leq C_4 \epsilon^{2-\beta(n-2)},$$

$$\sup_{w \in D(B)} |P| \leq C_5 \epsilon^{-\beta(m-1)},$$

$$\sup_{w \in D(B)} \epsilon^2 |Q| \leq C_6 \epsilon^{2-\beta(n-1)}.$$

Notice that for some C, C_1 uniform in ϵ one has

$$\begin{aligned} T(\epsilon) \epsilon^{-\beta(m-2)} &< C \epsilon^\beta, \\ T(\epsilon) \epsilon^{2-\beta(n-2)} &< C \epsilon^{2\beta} < C_1, \\ T(\epsilon) \epsilon^{-\beta(m-2)} &< C, \end{aligned}$$

and

$$T(\epsilon) \epsilon^{2-\beta(n-1)} < C \epsilon^\beta < C_1.$$

Therefore, if $B \gg C_3$, our map S fulfills

$$S(D(B)) \subset D(B).$$

The estimate of w_2 can be improved in the same way, that gives

$$|w_2| < c \epsilon^{\beta m}, \quad t \in [0, T]. \quad (4.7.30)$$

For this it suffices to note that estimates for the second components are proportional to ϵ^2 . □

Since the solution $\tilde{x}(t), \tilde{y}(t)$ of the tropically truncated system returns in the domain (4.7.14) and the exact solution, as it is shown, is a small perturbation of this solution, the exact solution also returns in this domain.

4.8 Generalized two component cell cycle model

Let us consider the *generalized* two component cell cycle model inspired from Model 1 :

$$x' = y + k_4 y x^m - k_0 x, \quad x(0) = x_0 \quad (4.8.1)$$

$$y' = -\epsilon^2(y + k_4 y x^n - k_1), \quad y(0) = y_0, \quad (4.8.2)$$

where k_0, k_1, k_4 are parameters.

Estimates obtained in the previous section, show that the condition $n \geq m$ is important for the existence of the cycle. Numerical simulations confirm this conclusion. For $n < m$ the cycle does not exists (see Fig. 4.2). For $n \geq m$ and sufficiently large k_4 there are stable oscillations (Fig. 4.3), whereas for smaller k_4 we can observe that oscillations are damped and the solution converges to an equilibrium (Fig. 4.4).

The behavior of the generalized excitable model in the limit cycle case, can be summarized as follows :

- Most of the time, the system evolves on a slow manifold $x = X(y)$ that is stable up to some $y = y_0$. The speed of movement on this manifold is $O(\epsilon^{-\beta(m-1)})$. The motion on the slow manifold is defined by all the terms.
- The speed of the system leaving the slow manifold is $O(1)$.
- There is also a fast manifold, which defines the return to the slow manifold. The motion on the fast manifold can be described only by the dominant terms (that form the tropically truncated system).
- The approximated equation of the fast manifold is $V_0 = \epsilon^2 x^{n-m+1} + y$.

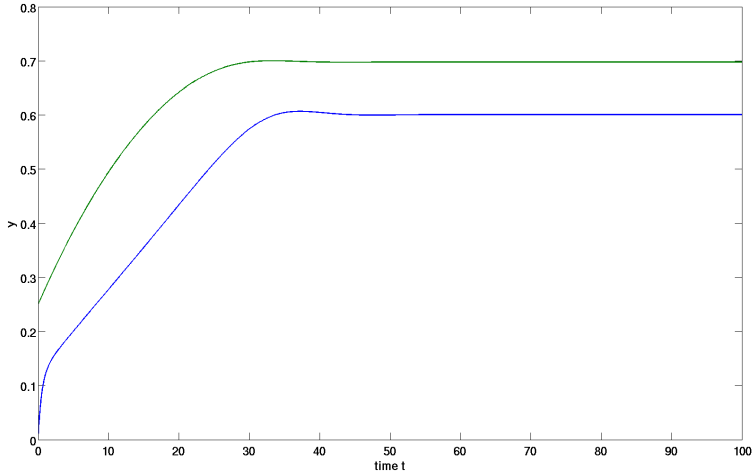


FIGURE 4.2 – Graph of solutions of the system (4.8.1), (4.8.2) for $\epsilon = 0.2$ and $k_4 = 2, k_0 = 2, k_1 = 1$ and $n = 3, m = 2$.

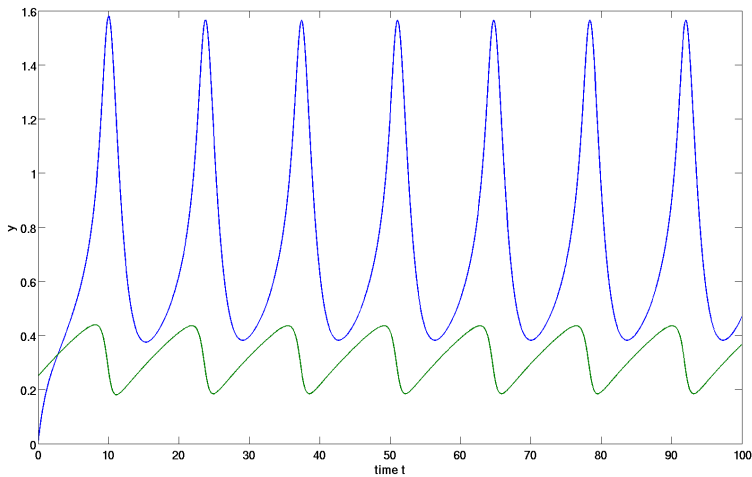


FIGURE 4.3 – Graph of solutions of the system (4.8.1), (4.8.2) for $\epsilon = 0.2$ and $k_4 = 2, k_0 = 1, k_1 = 1$ and $n = 5, m = 2$.

4.9 Conclusion

We showed that tropical ideas can be usefully employed to reduce and hybridize polynomial or rational dynamical systems occurring in modelling the molecular machinery of the cell cycle. The main idea consists in keeping only the dominant monomial terms in the right hand side of the ordinary differential equations. Depending on the position in phase space, one should keep one, two, or more such terms. The places where two or more monomial terms are equal form the so-called tropical manifolds. The one term approximation is valid far from the tropical manifolds, whereas close to tropical manifolds several dominating terms of opposite signs can equilibrate each other. These “tropical equilibra-

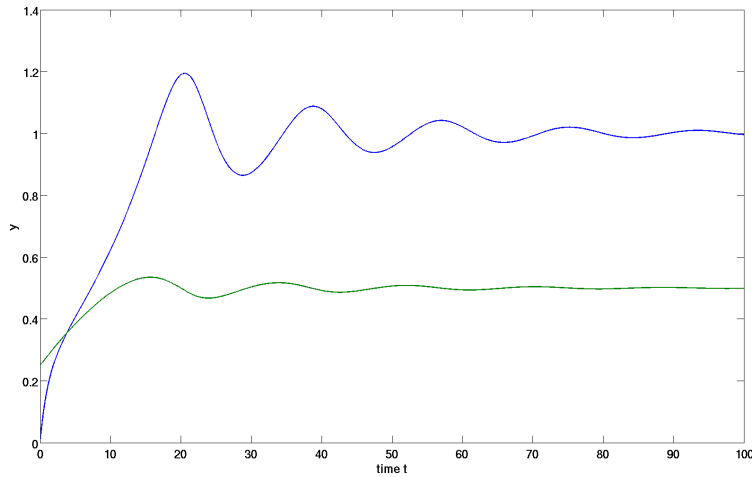


FIGURE 4.4 – Graph of solutions of the system (4.8.1), (4.8.2) for $\epsilon = 0.2$ and $k_4 = 1$, $k_0 = 1$, $k_1 = 1$ and $n = 3$, $m = 2$.

tions” of the dominating terms slow down the dynamics and produce attractive invariant manifolds.

The possible applications of this method are multiple. Generally, the method can be used to obtain simplified models. In the example studied here, we have started with a five variables model, that has been reduced to two variables and hybridized. The modes of the hybrid model have the simple structure of monomial differential or differential-algebraic equations. Two general methods that we called complete and two terms tropicalizations provide description of the modes and of the mode changes. However, these general procedures may lead to inaccurate approximations when the full model does not satisfy permanency globally. In such cases, more thorough analysis is needed. We have shown that the model of embryonic cell cycle has essentially three modes with different timescales, namely slow accumulation of cyclin, rapid activation of MPF and intermediately rapid degradation of cyclin and inactivation of MPF. The fastest mode is described by monomial ODEs, whereas the less fast modes correspond to tropical equilibrations and are described by differential-algebraic equations.

Several improvements and developments are needed in order to apply these methods at a larger scale. The computation of tropical equilibrations suffers from combinatorial explosion. However, for the biochemical network used as working example, the number of solutions seems to be very small compared to the large combinatorics of monomial terms. There is hope, that once formulated in constraint logic programming, the problem of equilibrations could be efficiently computed in practice as a constraint satisfaction problem. Also, effective methods are needed to compute the transitions between modes. The main difficulty here is related to walls (segments of the tropical manifolds) crossing. Near walls, two or more terms are dominant. When these terms are equilibrated, orbits remain close to the walls and are contained in invariant manifolds. The complete or two terms tropicalizations provide general heuristic for mode transitions. These approximations may fail close to walls. For instance, as we showed in [101] (see Chapter 2), the complete tropicalization predicts sliding modes that evolve on the wall and stay thus close to orbits of the full system. However, these sliding modes can be too long, leaving the wall when

the orbits of the full system are already far away. In order to get an accurate description of the behavior near such walls we had to compute invariant manifolds. Although this is generally much simpler than integrating the full set of equations, it could become difficult for tropical equilibrations involving more than two terms. Future work will be dedicated to developing general methods for this problem.

Bibliographie

Bibliographie

- [1] E. H. L. Aarts and P. J. M. Van Laarhoven. Statistical cooling : A general approach to combinatorial optimization problems. *Philips J. Res.*, 40(4) :193–226, 1985.
- [2] A. Acharya. Coarse-graining autonomous ode systems by inducing a separation of scales : practical strategies and mathematical questions. *Mathematics and Mechanics of Solids*, 15(3) :342–352, 2010.
- [3] A. Acharya and A. Sawant. On a computational approach for the approximate dynamics of averaged variables in nonlinear ode systems : Toward the derivation of constitutive laws of the rate type. *Journal of the Mechanics and Physics of Solids*, 54(10) :2183–2213, 2006.
- [4] A. Alfonsi, E. Cancès, G. Turinici, B. Di Ventura, and W. Huisenga. Exact simulation of hybrid stochastic and deterministic models for biochemical systems. Research Report RR-5435, INRIA, 2004.
- [5] A. Alfonsi, E. Cancès, G. Turinici, B. Di Ventura, and W. Huisenga. Adaptive simulation of hybrid stochastic and deterministic models for biochemical systems. In *ESAIM Proceedings*, volume 14, pages 1–13, 2005.
- [6] R. Aris. *Introduction to the analysis of chemical reactors*. Prentice-Hall Englewood Cliffs, New Jersey, 1965.
- [7] V. I. Arnold. *Mathematical methods of classical mechanics*. Springer, New York, 1978.
- [8] Z. Artstein and A. Vigodner. Singularly perturbed ordinary differential equations with dynamic limits. *Proc. Roy. Soc. Edinburgh Sect.A*, 126 :541–569, 1996.
- [9] J. P. Aubin. Macroscopic traffic models : Shifting from densities to "celerities". *Applied Mathematics and Computation*, 217 :963–971, 2010.
- [10] V. Baldazzi, P. T. Monteiro, M. Page, D. Ropers, J. Geiselmann, and H. Jong. Qualitative analysis of genetic regulatory networks in bacteria. *Understanding the Dynamics of Biological Systems*, pages 111–130, 2011.
- [11] K. Ball, T. G. Kurtz, L. Popovic, and G. Rempala. Asymptotic analysis of multiscale approximations to reaction networks. *Ann. Appl. Probab.*, 16 :1925–1961, 2006.
- [12] G. Batt, H. De Jong, M. Page, and J. Geiselmann. Symbolic reachability analysis of genetic regulatory networks using discrete abstractions. *Automatica*, 44(4) :982–989, 2008.
- [13] M. Bodenstein. Eine theorie der photochemischen reaktionsgeschwindigkeiten. *Z. phys. Chem.*, 85 :329–397, 1913.
- [14] N. N. Bogoliubov and Y. A. Mitropolski. *Asymptotic Methods in the Theory of Nonlinear Oscillations*. Gordon and Breach, New York, 1961.

- [15] N. M. Borisov, N. I. Markevich, J. B. Hoek, and B. N. Kholodenko. Signaling through Receptors and Scaffolds : Independent Interactions Reduce Combinatorial Complexity. *Biophys. J.*, 89 :951–966, 2005.
- [16] L. Bortolussi and A. Policriti. (Hybrid) automata and (stochastic) programs. The hybrid automata lattice of a stochastic program. *Journal of Logic and Computation*, 2011.
- [17] K. Burrage, T. Tian, and P. Burrage. A multi-scaled approach for simulating chemical reaction systems. *Progress in Biophysics and Molecular Biology*, 85(2-3) :217–234, 2004.
- [18] V. Bykov, I. Goldfarb, V. Gol'Dshtain, and U. Maas. On a modified version of ildm approach : asymptotic analysis based on integral manifolds. *IMA journal of applied mathematics*, 71(3) :359–382, 2006.
- [19] E. Chiavazzo, A. N. Gorban, and I. V. Karlin. Comparisons of invariant manifolds for model reduction in chemical kinetics. *Comm. Comp. Phys.*, 2 :964–992, 2007.
- [20] J. A. Christiansen. The elucidation of reaction mechanisms by the method of intermediates in quasi-stationary concentrations. *Advances in Catalysis*, 5 :311–353, 1953.
- [21] K. W. Chu, Y. Deng, and J. Reinitz. Parallel simulated annealing by mixing of states. *Journal of Computational Physics*, 148(2) :646–662, 1999.
- [22] K. W. Chu, Y. Deng, and J. Reinitz. Parallel simulated annealing by mixing of states 1. *Journal of Computational Physics*, 148(2) :646–662, 1999.
- [23] G. Cohen, S. Gaubert, and J. P. Quadrat. Max-plus algebra and system theory : where we are and where to go now. *Annual Reviews in Control*, 23 :207–219, 1999.
- [24] S. D. Cohen and A. C. Hindmarsh. Cvode, a stiff/nonstiff ode solver in c. *Computers in physics*, 10(2) :138–143, 1996.
- [25] H. Conzelmann, J. Saez-Rodriguez, T. Sauter, B. N. Kholodenko, and E. D. Gilles. A domain-oriented approach to the reduction of combinatorial complexity in signal transduction networks. *BMC Bioinformatics*, 7 :34, 2006.
- [26] A. Crudu, A. Debussche, A. Muller, and O. Radulescu. Convergence of stochastic gene networks to hybrid piecewise deterministic processes. *Annals of Applied Probability*, to appear, Arxiv preprint arXiv :1101.1431.
- [27] A. Crudu, A. Debussche, and O. Radulescu. Hybrid stochastic simplifications for multiscale gene networks. *BMC Systems Biology*, 3(1) :89, 2009.
- [28] A. Csikász-Nagy, D. Battogtokh, K. C. Chen, B. Novák, and J. J. Tyson. Analysis of a generic model of eukaryotic cell-cycle regulation. *Biophysical Journal*, 90(12) :4361–4379, 2006.
- [29] V. Danos, J. Feret, W. Fontana, R. Harmer, and J. Krivine. Rule-based modelling of cellular signalling. *CONCUR 2007-Concurrency Theory*, pages 17–41, 2007.
- [30] V. Danos, J. Feret, W. Fontana, and J. Krivine. Scalable simulation of cellular signaling networks . In Z. Shao, editor, *Proceedings of the Fifth Asian Symposium on Programming Languages and Systems, APLAS'07, Lecture Notes in Computer Science 4807*, pages 139–157, Berlin, 2007. Springer.
- [31] G. B. Dantzig, A. Orden, and P. Wolfe. The generalized simplex method for minimizing a linear form under linear inequality restraints. *Pacific Journal of Mathematics*, 5(2) :183–195, 1955.

- [32] R. David and H. Alla. Discrete, continuous, and hybrid Petri nets. *IEEE Control Systems*, 28 :81–84, 2008.
- [33] M. Di Bernardo. *Piecewise-smooth dynamical systems : theory and applications*. Springer Verlag, 2008.
- [34] A. Dokoumetzidis and L. Aarons. Proper lumping in systems biology models. *Systems Biology, IET*, 3(1) :40–51, 2009.
- [35] S. Drulhe, G. Ferrari-Trecate, and H. de Jong. The switching threshold reconstruction problem for piecewise-affine models of genetic regulatory networks. *IEEE Transactions on Automatic Control*, 53 :153–165, 2008.
- [36] R. Erban, I. G. Kevrekidis, D. Adalsteinsson, and T. C. Elston. Gene regulatory networks : A coarse-grained, equation-free approach to multiscale computation. *The Journal of chemical physics*, 124 :084106, 2006.
- [37] J. Feret, V. Danos, J. Krivine, R. Harmer, and W. Fontana. Internal coarse-graining of molecular systems. *Proceedings of the National Academy of Sciences*, 106(16) :6453, 2009.
- [38] J. Feret, T. Henzinger, H. Koeppl, and T. Petrov. Lumpability abstractions of rule-based systems . In Z. Shao, editor, *Theoretical Computer Science, special issue MeCBIC 2009-2010*, number 431, pages 137–164, 2012.
- [39] M. L. Ferguson, D. Le Coq, M. Jules, S. Aymerich, O. Radulescu, N. Declerck, and C. A. Royer. Reconciling molecular regulatory mechanisms with noise patterns of bacterial metabolic promoters in induced and repressed states. *Proceedings of the National Academy of Sciences*, 109(1) :155–160, 2012.
- [40] A. F. Filippov. *Differential equations with discontinuous righthand sides*. Springer, 1988.
- [41] C. Furusawa and K. Kaneko. Zipfs law in gene expression. *Physical review letters*, 90(8) :88102, 2003.
- [42] S. Gay, S. Soliman, and F. Fages. A graphical method for reducing and relating models in systems biology. *Bioinformatics*, 26(18) :i575–i581, 2010.
- [43] J. W. Gibbs. *Elementary principles in statistical mechanics : developed with especial reference to the rational foundation of thermodynamics*. Cambridge Univ Pr, 2010.
- [44] D. T. Gillespie. *J.Comput.Phys.*, 22 :403, 1976.
- [45] D. T. Gillespie. Concerning the validity of the stochastic approach to chemical kinetics. *Journal of Statistical Physics*, 16(3) :311–318, 1977.
- [46] D. T. Gillespie. The chemical langevin equation. *J.Chem.Phys*, 113 :297–306, 2000.
- [47] D. Givon, R. Kupferman, and A. Stuart. Extracting macroscopic dynamics : model problems and algorithms. *Nonlinearity*, 17 :R55–R127, 2004.
- [48] A. Goldbeter. A minimal cascade model for the mitotic oscillator involving cyclin and cdc2 kinase. *Proceedings of the National Academy of Sciences of the United States of America*, 88(20) :9107, 1991.
- [49] A. Golightly and D. J. Wilkinson. Bayesian parameter inference for stochastic biochemical network models using particle mcmc. *Interface Focus 1. In press*, 2011.
- [50] C. A. Gómez-Uribe, G. C. Verghese, and A. R. Tzafriri. Enhanced identification and exploitation of time scales for model reduction in stochastic chemical kinetics. *The Journal of chemical physics*, 129 :244112, 2008.

- [51] A. N. Gorban and I. V. Karlin. Method of invariant manifolds and regularization of acoustic spectra. *Transport Theory and Statistical Physics*, (5) :559–632, 1994.
- [52] A. N. Gorban and I. V. Karlin. Method of invariant manifold for chemical kinetics. *Chem. Eng. Sci.*, 58 :4751–4768, 2003.
- [53] A. N. Gorban and I. V. Karlin. *Invariant manifolds for physical and chemical kinetics*, Lect. Notes. Phys. 660. Springer, Berlin, Heidelberg, 2005.
- [54] A. N. Gorban, I. V. Karlin, P. Ilg, and H. C. Öttinger. Corrections and enhancements of quasi-equilibrium states. *Journal of non-newtonian fluid mechanics*, 96(1-2) :203–219, 2001.
- [55] A. N. Gorban, I. V. Karlin, and A. Zinovyev. Invariant grids for reaction kinetics. *Physica A*, 333 :106–154, 2004.
- [56] A. N. Gorban and O. Radulescu. Dynamic and static limitation in multiscale reaction networks, revisited. In G.B. Marin, D.H. West, and G.S. Yablonsky, editors, *Advances in Chemical Engineering : Mathematics and Chemical Engineering and Kinetics*, volume 34, pages 103–173. Academic Press, 2008.
- [57] A. N. Gorban and O. Radulescu. Dynamic and static limitation in reaction networks, revisited . In David West Guy B. Marin and Gregory S. Yablonsky, editors, *Advances in Chemical Engineering - Mathematics in Chemical Kinetics and Engineering*, volume 34 of *Advances in Chemical Engineering*, pages 103–173. Elsevier, 2008.
- [58] A. N. Gorban, O. Radulescu, and A. Y. Zinovyev. Asymptotology of chemical reaction networks. *Chemical Engineering Science*, 65 :2310–2324, 2010.
- [59] A. N. Gorban and M. Shahzad. The Michaelis-Menten-Stueckelberg Theorem. *Entropy*, (13) :966–1019, 2011.
- [60] M. Griffith, T. Courtney, J. Peccoud, and W.H. Sanders. Dynamic partitioning for hybrid simulation of the bistable HIV-1 transactivation network. *Bioinformatics*, 22(22) :2782, 2006.
- [61] R. Gunawan, Y. Cao, L. Petzold, and F. J. Doyle III. Sensitivity analysis of discrete stochastic systems. *Biophysical Journal*, 88(4) :2530–2540, 2005.
- [62] P. Hanusse. De l’existence d’un cycle limite dans l’évolution des systemes chimique ouverts (on the existence of a limit cycle in the evolution of open chemical systems). *Comptes Rendus, Acad. Sci. Paris, (C)*, 274 :1245–1247, 1972.
- [63] L. A. Harris and P. Clancy. A “partitioned leaping” approach for multiscale modeling of chemical reaction dynamics. *The Journal of chemical physics*, 125 :144107, 2006.
- [64] E. L. Haseltine and J. B. Rawlings. Approximate simulation of coupled fast and slow reactions for stochastic chemical kinetics. *J.Chem.Phys.*, 117 :6959–6969, 2002.
- [65] E. L. Haseltine and J. B. Rawlings. On the origins of approximations for stochastic chemical kinetics. *The Journal of chemical physics*, 123 :164115, 2005.
- [66] F. G. Helfferich. Systematic approach to elucidation of multistep reaction networks. *The Journal of Physical Chemistry*, 93(18) :6676–6681, 1989.
- [67] D. Henry. *Geometric theory of semilinear parabolic equations*.
- [68] A. C. Hindmarsh, P. N. Brown, K. E. Grant, S. L. Lee, R. Serban, D. E. Shumaker, and C. S. Woodward. Sundials : Suite of nonlinear and differential/algebraic equation solvers. *ACM Transactions on Mathematical Software (TOMS)*, 31(3) :363–396, 2005.

- [69] S. Hoops, S. Sahle, R. Gauges, C. Lee, J. Pahle, N. Simus, M. Singhal, L. Xu, P. Mendes, and U. Kummer. Copasi—A complex pathway simulator. *Bioinformatics*, 22(24) :3067–3074, 2006.
- [70] M. Hucka, A. Finney, H. M. Sauro, H. Bolouri, J.C. Doyle, H. Kitano, A. P. Arkin, B. J. Bornstein, D. Bray, A. Cornish-Bowden, et al. The systems biology markup language (sbml) : a medium for representation and exchange of biochemical network models. *Bioinformatics*, 19(4) :524–531, 2003.
- [71] A. E. C. Ihekweaba, D. S. Broomhead, R. L. Grimley, N. Benson, and D. B. Kell. Sensitivity analysis of parameters controlling oscillatory signalling in the nf- κ b pathway : the roles of ikk and $i\kappa b\alpha$. *IEE Syst.Biol.*, 1 :93–102, 2004.
- [72] N. Jamshidi and B. Ø. Palsson. Formulating genome-scale kinetic models in the post-genome era. *Molecular Systems Biology*, 4 :171, 2008.
- [73] H. G. Kaper and Kaper T. J. Asymptotic analysis of two reduction methods for systems of chemical reactions. *Physica D*, (165) :66–93, 2002.
- [74] N. Kazantzis and T. Good. Invariant manifolds and the calculation of the long-term asymptotic response of nonlinear processes using singular PDEs. *Computers & Chemical Engineering*, (26) :999–1012, 2002.
- [75] Y. N. Kaznessis. Multi-scale models for gene network engineering. *Chemical engineering science*, 61(3) :940–953, 2006.
- [76] S. Kirkpatrick, C. D. Gelatt Jr, and M. P. Vecchi. Optimization by simulated annealing. *science*, 220(4598) :671–680, 1983.
- [77] B. Krauskopf, H. M. Osinga, E. J. Doedel, M. E. Henderson, J. Guckenheimer, A. Vladimirsky, M. Dellnitz, and O. Junge. A survey of method's for computing (un)stable manifold of vector fields. *International Journal of Bifurcation and Chaos*, 15 :763–791, 2005.
- [78] J. Lam and J. M. Delosme. An efficient simulated annealing schedule : derivation. *Yale University, New Haven, Connecticut, Technical Report*, 8816, 1988.
- [79] J. Lam and J. M. Delosme. An efficient simulated annealing schedule : implementation and evaluation. *Yale University, New Haven, Connecticut, Technical Report*, 8817, 1988.
- [80] S.H. Lam and D.A. Goussis. The csp method for simplifying kinetics. *International Journal of Chemical Kinetics*, 26 :461–486, 1994.
- [81] N. Le Novère, B. Bornstein, A. Broicher, M. Courtot, M. Donizelli, H. Dharuri, L. Li, H. Sauro, M. Schilstra, B. Shapiro, et al. Biomodels database : a free, centralized database of curated, published, quantitative kinetic models of biochemical and cellular systems. *Nucleic acids research*, 34(suppl 1) :D689–D691, 2006.
- [82] N. Le Novère, M. Hucka, H. Mi, S. Moodie, F. Schreiber, A. Sorokin, E. Demir, K. Wegner, M.I. Aladjem, S.M. Wimalaratne, et al. The systems biology graphical notation. *Nature biotechnology*, 27(8) :735–741, 2009.
- [83] H. Li, Y. Cao, L. R. Petzold, and D. T. Gillespie. Algorithms and software for stochastic simulation of biochemical reacting systems. *Biotechnology progress*, 24(1) :56–61, 2008.
- [84] W. Liebermeister, J. Uhendorf, and E. Klipp. Modular rate laws for enzymatic reactions : thermodynamics, elasticities and implementation. *Bioinformatics*, 26(12) :1528, 2010.

- [85] P. Lincoln and A. Tiwari. Symbolic systems biology : Hybrid modeling and analysis of biological networks. *Hybrid Systems : Computation and Control*, pages 147–165, 2004.
- [86] T. Lipniacki, P. Paszek, A. R. Brasier, B. Luxon, and M. Kimmel. Mathematical model of nf- κ b regulatory module. *J.Theor.Biol.*, 228 :195–215, 2004.
- [87] G. L. Litvinov and V. P. Maslov. Idempotent mathematics : a correspondence principle and its applications to computing. *Russian Mathematical Surveys*, 51(6) :1210–1211, 1996.
- [88] P. Lochack and C. Meunier. *Multiphase averaging for classical systems*. Springer, New York, 1988.
- [89] U. Maas and S.B. Pope. Simplifying chemical kinetics : intrinsic low-dimensional manifolds in composition space. *Combust. Flame*, 88 :239–264, 1992.
- [90] W. G. Macready, A. G. Siapas, and S. A. Kauffman. Criticality and parallelism in combinatorial optimization. *Science*, 271(5245) :56–59, 1996.
- [91] E. A. Mastny, E. L. Haseltine, and J. B. Rawlings. Two classes of quasi-steady-state model reductions for stochastic kinetics. *The Journal of Chemical Physics*, 127 :094106, 2007.
- [92] A. S. Matveev and A. V. Savkin. *Qualitative theory of hybrid dynamical systems*. Birkhauser, 2000.
- [93] B. Mélykúti, K. Burrage, and K. C. Zygalakis. Fast stochastic simulation of biochemical reaction systems by alternative formulations of the chemical langevin equation. *The Journal of chemical physics*, 132 :164109, 2010.
- [94] A. Messiah. *Quantum mechanics*. Wiley, New York, 1962.
- [95] G. Mikhalkin. What is a tropical curve. *Notices of the AMS*, 54(4), 2007.
- [96] B. Mishra. Intelligently deciphering unintelligible designs : algorithmic algebraic model checking in systems biology. *Journal of The Royal Society Interface*, 6(36) :575–597, 2009.
- [97] D. Mitra, F. Romeo, and A. Sangiovanni-Vincentelli. Convergence and finite-time behavior of simulated annealing. *Advances in Applied Probability*, pages 747–771, 1986.
- [98] B. Munsky and M. Khammash. The finite state projection algorithm for the solution of the chemical master equation. *The Journal of chemical physics*, (124) :044104, 2006.
- [99] A. Naldi, E. Remy, D. Thieffry, and C. Chaouiya. A reduction of logical regulatory graphs preserving essential dynamical properties. In *Computational Methods in Systems Biology*, pages 266–280. Springer, 2009.
- [100] A. Naldi, E. Remy, D. Thieffry, and C. Chaouiya. Dynamically consistent reduction of logical regulatory graphs. *Theoretical Computer Science*, 412(21) :2207–2218, 2011.
- [101] V. Noel, D. Grigoriev, S. Vakulenko, and O. Radulescu. Tropical geometries and dynamics of biochemical networks. Application to hybrid cell cycle models. *Electronic Notes in Theoretical Computer Science*, 284 :75–91, 2012.
- [102] V. Noel, S. Vakulenko, and O. Radulescu. Piecewise smooth hybrid systems as models for networks in molecular biology. In *Proceedings of JOBIM 2010*. Jobim, Montpellier, 2010.

- [103] V. Noel, S. Vakulenko, and O. Radulescu. Algorithm for identification of piecewise smooth hybrid systems : application to eukaryotic cell cycle regulation. *Lecture Notes in Computer Science*, 6833 :225–236, 2011.
- [104] L. Pachter and B. Sturmfels. Tropical geometry of statistical models. *Proceedings of the National Academy of Sciences of the United States of America*, 101(46) :16132, 2004.
- [105] J. Pahle. Biochemical simulations : stochastic, approximate stochastic and hybrid approaches. *Briefings in bioinformatics*, 10(1) :53–64, 2009.
- [106] J. A. Papin, J. L. Reed, and B. O. Palsson. Hierarchical thinking in network biology : the unbiased modularization of biochemical networks. *Trends in biochemical sciences*, 29(12) :641–647, 2004.
- [107] H. Poincaré. *Les Méthodes Nouvelles de la Mécanique Céleste*. Gauthier-Villars, Paris, 1899.
- [108] R. Porreca, S. Drulhe, H. Jong, and G. Ferrari-Trecate. Structural identification of piecewise-linear models of genetic regulatory networks. *Journal of Computational Biology*, 15(10) :1365–1380, 2008.
- [109] H. Rabitz, M. Kramer, and D. Dacol. Sensitivity analysis in chemical kinetics. *Annual Review of Physical Chemistry*, 34 :419–461, 1983.
- [110] O. Radulescu and A. N. Gorban. Limitation and averaging for deterministic and stochastic biochemical reaction networks. *International Workshop Model Reduction in Reacting Flow, Notre Dame*, 2009.
- [111] O. Radulescu, A. N. Gorban, S. Vakulenko, and A. Zinovyev. Hierarchies and modules in complex biological systems. *Proceedings of ECCS’06*, 2006.
- [112] O. Radulescu, A. N. Gorban, A. Zinovyev, and A. Lilienbaum. Robust simplifications of multiscale biochemical networks. *BMC systems biology*, 2(1) :86, 2008.
- [113] O. Radulescu, G. C. P. Innocentini, and J. E. M. Hornos. Relating network rigidity, time scale hierarchies, and expression noise in gene networks. *Physical Review E*, 85 :041919, 2012.
- [114] O. Radulescu, A. Muller, and A. Crudu. Théorèmes limites pour des processus de markov à sauts. synthèse des résultats et applications en biologie moléculaire. *Technique et Science Informatique*, 26 :443–469, 2007.
- [115] D. Ropers, V. Baldazzi, and H. de Jong. Model reduction using piecewise-linear approximations preserves dynamic properties of the carbon starvation response in Escherichia coli. *IEEE/ACM Transactions on Computational Biology and Bioinformatics*, 8(1) :166–181, 2011.
- [116] M. R. Roussel and S. J. Fraser. On the geometry of transient relaxation. *J. Chem. Phys.*, 94 :7106–7113, 1991.
- [117] H. Salis and Y. Kaznessis. Accurate hybrid stochastic simulation of a system of coupled chemical or biochemical reactions. *The Journal of chemical physics*, 122 :054103, 2005.
- [118] H. Salis, V. Sotiropoulos, and Y.N. Kaznessis. Multiscale Hy3S : hybrid stochastic simulation for supercomputers. *BMC Bioinformatics*, 7(1) :93, 2006.
- [119] M. A. Savageau, P. M. B. M. Coelho, R. A. Fasani, D. A. Tolla, and A. Salvador. Phenotypes and tolerances in the design space of biochemical systems. *Proceedings of the National Academy of Sciences*, 106(16) :6435, 2009.

- [120] M. A. Savageau and E. O. Voit. Recasting nonlinear differential equations as s-systems : a canonical nonlinear form. *Mathematical biosciences*, 87(1) :83–115, 1987.
- [121] A. Sawant and A. Acharya. Model reduction via parametrized locally invariant manifolds : some examples. *Computer methods in applied mechanics and engineering*, 195(44-47) :6287–6311, 2006.
- [122] L. A. Segel and M. Slemrod. The quasi-steady-state assumption : a case study in perturbation. *SIAM Review*, 31(3) :446–477, 1989.
- [123] N. Semenoff. On the kinetics of complex reactions. *The Journal of Chemical Physics*, 7 :683, 1939.
- [124] R. Shorten, F. Wirth, O. Mason, K. Wulff, and C. King. Stability Criteria for Switched and Hybrid Systems. *SIAM Review*, 49(4) :545–592, 2007.
- [125] A. Singh and J. P. Hespanha. Stochastic hybrid systems for studying biochemical processes. *Philosophical Transactions of the Royal Society A : Mathematical, Physical and Engineering Sciences*, 368(1930) :4995–5011, 2010.
- [126] R. Singhania, R. M. Sramkoski, J. W. Jacobberger, and J. J. Tyson. A hybrid model of mammalian cell cycle regulation. *PLoS computational biology*, 7(2) :e1001077, 2011.
- [127] M. Slemrod. Averaging of fast-slow systems. *Coping with Complexity : Model Reduction and Data Analysis*, pages 1–7, 2011.
- [128] B. M. Slepchenko, J. C. Schaff, and Y. S. Choi. Numerical approach to fast reactions in reaction-diffusion systems : application to buffered calcium waves in bistable models. *Journal of Computational Physics*, 162(1) :186–218, 2000.
- [129] B. M. Slepchenko, J. C. Schaff, I. Macara, and L. M. Loew. Quantitative cell biology with the virtual cell. *Trends in cell biology*, 13(11) :570–576, 2003.
- [130] M. W. Sneddon, J. R. Faeder, and T. Emonet. Efficient modeling, simulation and coarse-graining of biological complexity with NFsim. *Nature methods*, (8) :177–183, 2011.
- [131] S. Soliman and M. Heiner. A unique transformation from ordinary differential equations to reaction networks. *PloS one*, 5(12) :e14284, 2010.
- [132] S. Strogatz. Nonlinear dynamics and chaos : with applications to physics, biology, chemistry and engineering. 1994.
- [133] B. Sturmfels. *Solving systems of polynomial equations*. American mathematical society, 2002.
- [134] I. Surovtsova, S. Sahle, J. Pahle, and U. Kummer. Approaches to complexity reduction in a systems biology research environment (SYCAMORE). In *Proceedings of the 37th conference on Winter simulation*, pages 1683–1689. Winter Simulation Conference, 2006.
- [135] I. Surovtsova, N. Simus, T. Lorenz, A. König, S. Sahle, and U. Kummer. Accessible methods for the dynamic time-scale decomposition of biochemical systems. *Bioinformatics*, 25(21) :2816, 2009.
- [136] Y. Takeuchi. *Global dynamical properties of Lotka-Volterra systems*. World Scientific, Singapore, 1996.
- [137] L. Tavernini. Differential automata and their discrete simulators. *Nonlinear Anal. Theory Methods Applic.*, 11(6) :665–683, 1987.

- [138] E. Teller, N. Metropolis, and A. Rosenbluth. Equation of state calculations by fast computing machines. *J. Chem. Phys.*, 21(13) :1087–1092, 1953.
- [139] C. Torrence and G. P. Compo. A practical guide to wavelet analysis. *Bulletin of the American Meteorological society*, 79(1) :61–78, 1998.
- [140] J. J. Tyson. Modeling the cell division cycle : cdc2 and cyclin interactions. *Proceedings of the National Academy of Sciences of the United States of America*, 88(16) :7328, 1991.
- [141] S. Vakulenko. Complexité dynamique des réseaux de Hopfield : Dynamical complexity of the Hopfield networks. *Comptes Rendus Mathematique*, 335(7) :639–642, 2002.
- [142] S. Vakulenko and D. Grigoriev. Complexity of gene circuits, pfaffian functions and the morphogenesis problem. *Comptes Rendus Mathematique*, 337(11) :721–724, 2003.
- [143] T. J. J. van den Boom and B. De Schutter. Modelling and control of discrete event systems using switching max-plus-linear systems. *Control engineering practice*, 14(10) :1199–1211, 2006.
- [144] O. Viro. From the sixteenth hilbert problem to tropical geometry. *Japanese Journal of Mathematics*, 3(2) :185–214, 2008.
- [145] A. Von Kamp and S. Schuster. Metatool 5.0 : fast and flexible elementary modes analysis. *Bioinformatics*, (22) :1930–1931, 2006.
- [146] T. Wilhelm and R. Heinrich. Smallest chemical reaction system with hopf bifurcation. *Journal of mathematical chemistry*, 17(1) :1–14, 1995.
- [147] I. H. Witten and E. Frank. *Data Mining : Practical machine learning tools and techniques*. Morgan Kaufmann, 2005.
- [148] G. S. Yablonskii, V. I. Bykov, A. N. Gorban, and V.I. Elokhin. *Kinetic Models of Catalytic Reactions*. Elsevier, Amsterdam, 1991.
- [149] P. Ye, E. Entcheva, SA Smolka, and R. Grosu. Modelling excitable cells using cycle-linear hybrid automata. *Systems Biology, IET*, 2(1) :24–32, 2008.